Current uncertainties on antimatter and gamma-ray production cross sections.

Mattia Di Mauro e Fiorenza Donato

Istituto Nazionale di Fisica Nucleare

Summary of CS relevant for Astroparticle

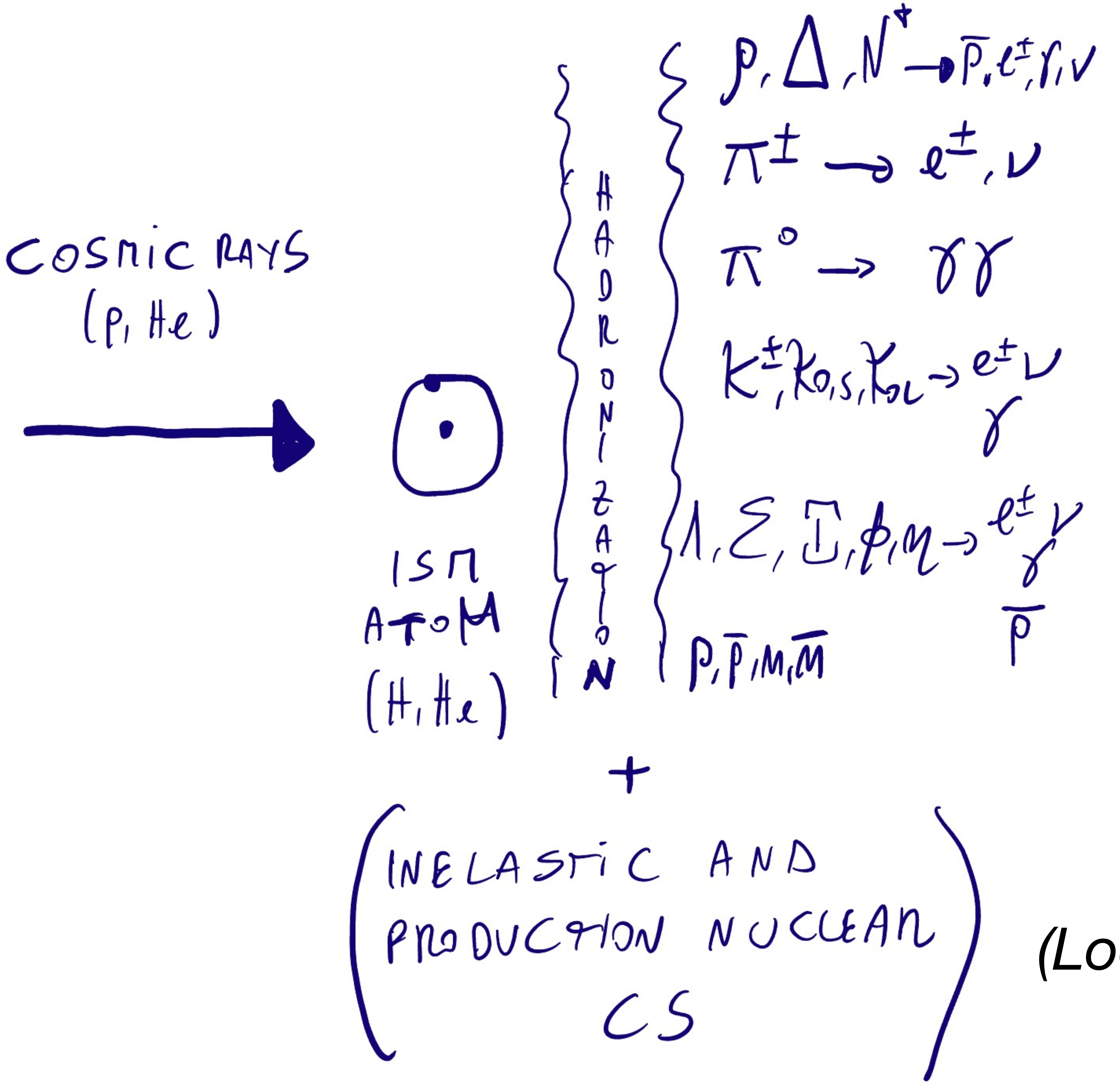

Resonances

Pions

Kaons

Hyperons

Prompt (anti-p)

Mostly O, C —> H, He
(Look Carmelo and Fiorenza's talks)

Antiprotons production CS

Antiprotons data

- The AMS-02 data reach a precision of about 3-6%.
- Errors of cross section data and theoretical models should reach about this precision.
- This is particularly relevant for CR physics and searches for DM signals.

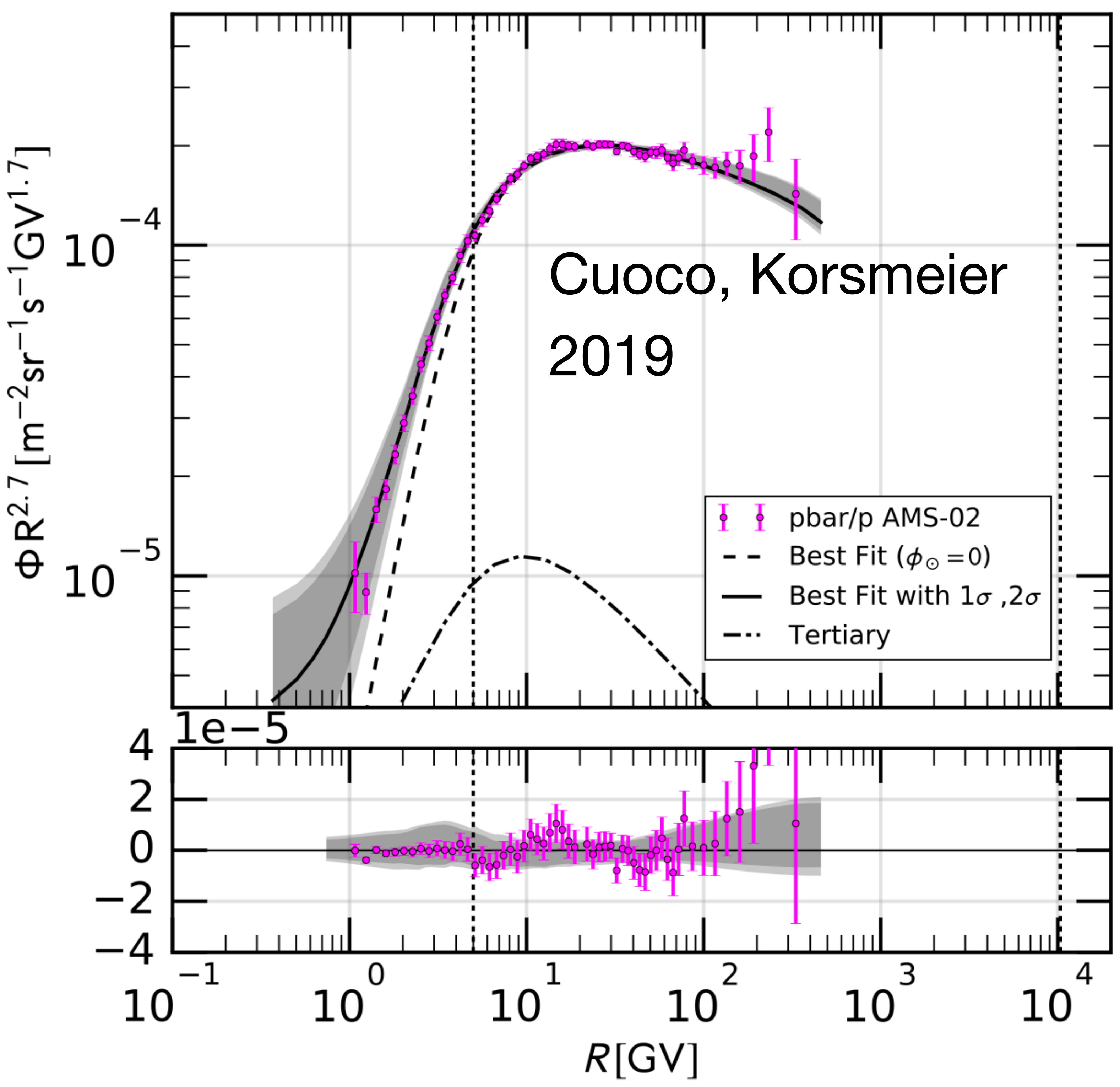

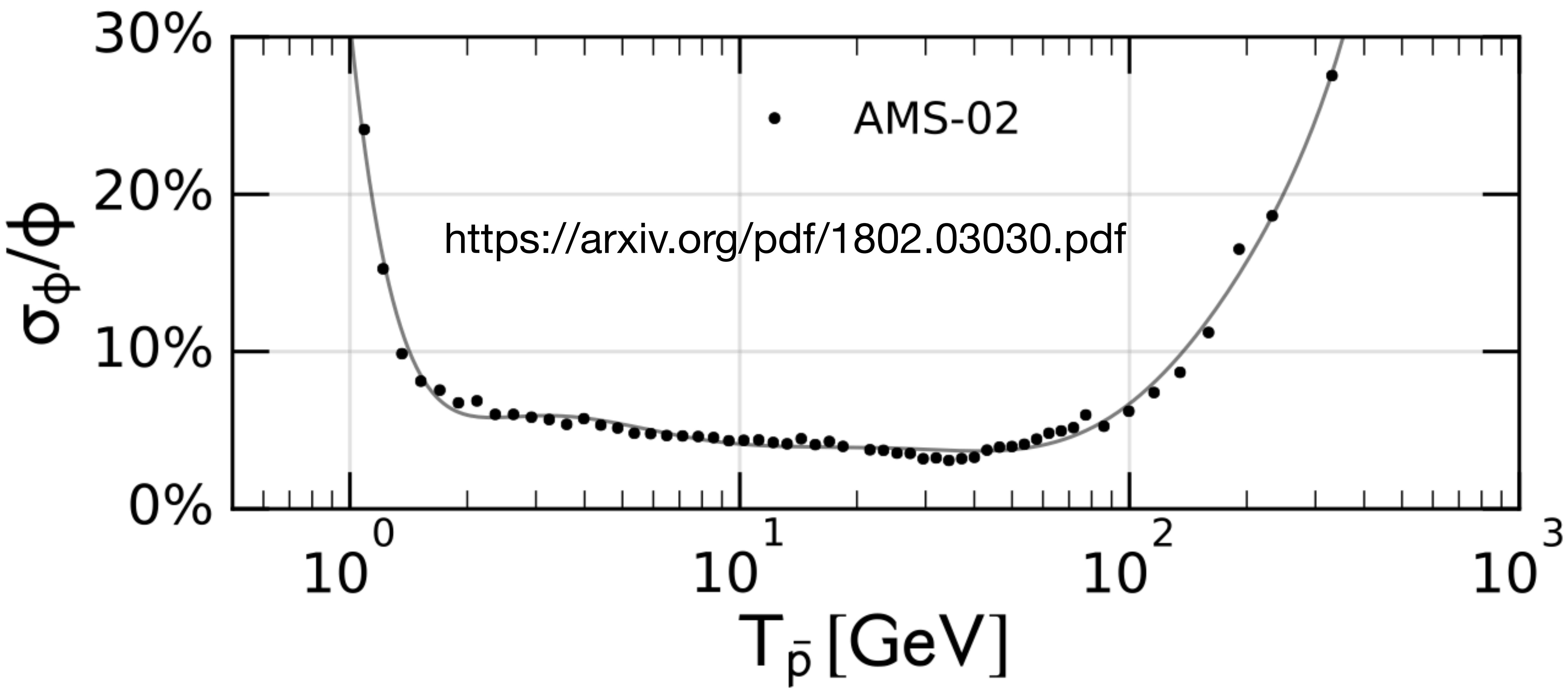

Different channels

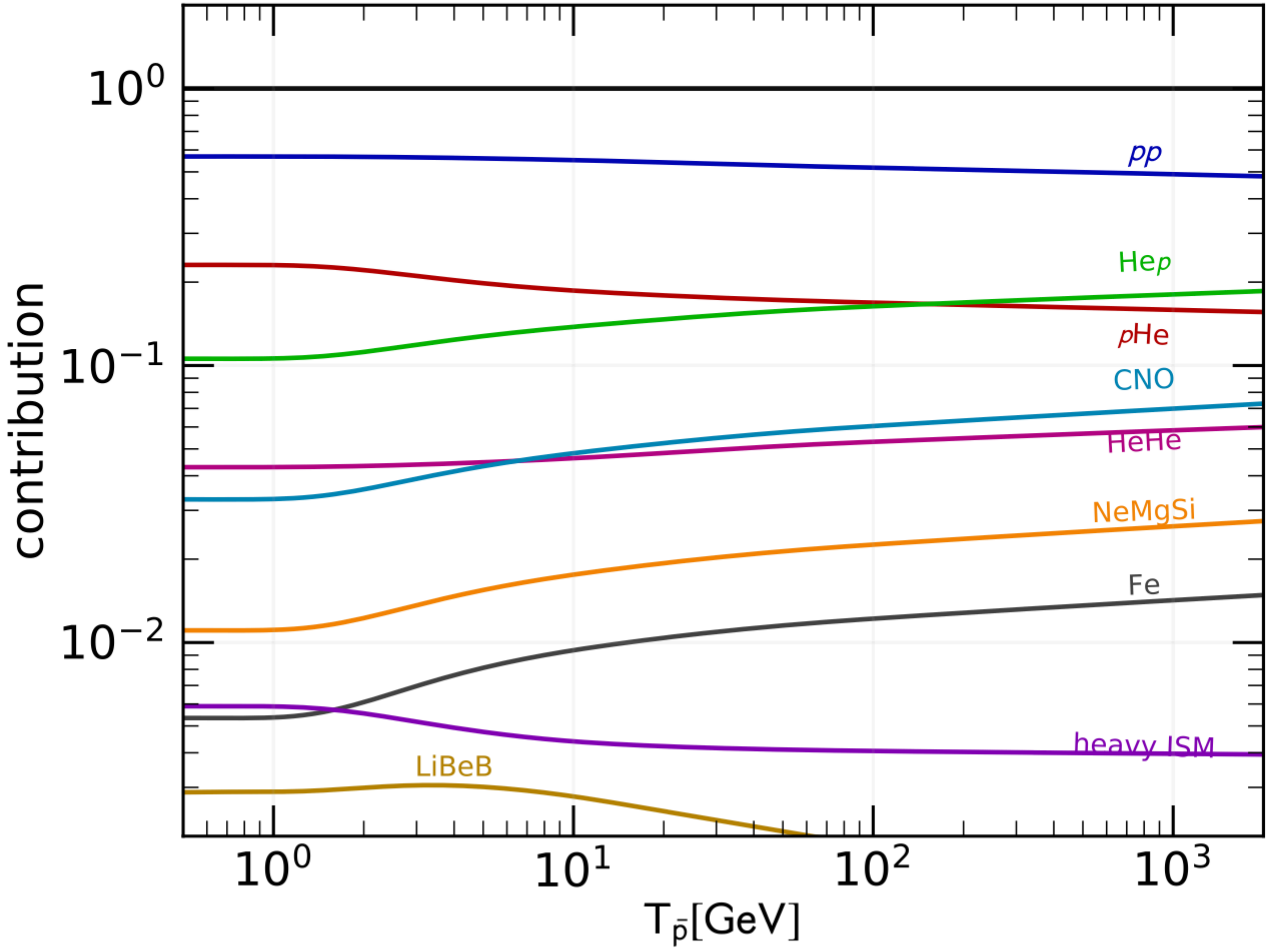

- About 50% from pp and 50% from pHe,Hep,HeHe

Antiproton data from AMS-02 are between 10-1000 GeV —> sqrt(s) = 5-50 GeV

https://arxiv.org/pdf/1802.03030.pdf

Available Data

Experiment	$\sqrt{s}$ (GeV)	p_T (GeV)	x_R
Dekkers *et al*, CERN 1965 [18]	6.1, 6.7	(0., 0.79)	(0.34, 0.65)
Allaby *et al*, CERN 1970 [19]	6.15	(0.05, 0.90)	(0.40, 0.94)
Capiluppi *et al*, CERN 1974 [20]	23.3, 30.6, 44.6, 53.0, 62.7	(0.18, 1.29)	(0.06, 0.43)
Guettler *et al*, CERN 1976 [21]	23.0, 31.0, 45.0, 53.0, 63.0	(0.12, 0.47)	(0.036, 0.092)
Johnson *et al*, FNAL 1978 [22]	13.8, 19.4, 27.4	(0.25, 0.75)	(0.31, 0.55)
Antreasyan *et al*, FNAL 1979 [23]	19.4, 23.8, 27.4	(0.77, 6.15)	(0.08, 0.58)
BRAHMS, BNL 2008 [13]	200	(0.82, 3.97)	(0.11, 0.39)
NA49, CERN 2010 [14]	17.3	(0.10, 1.50)	(0.11, 0.44)

Antiproton data from AMS-02 are between 10-1000 GeV —> sqrt(s) = 5-50 GeV

→ **Feed-down correction applied!**

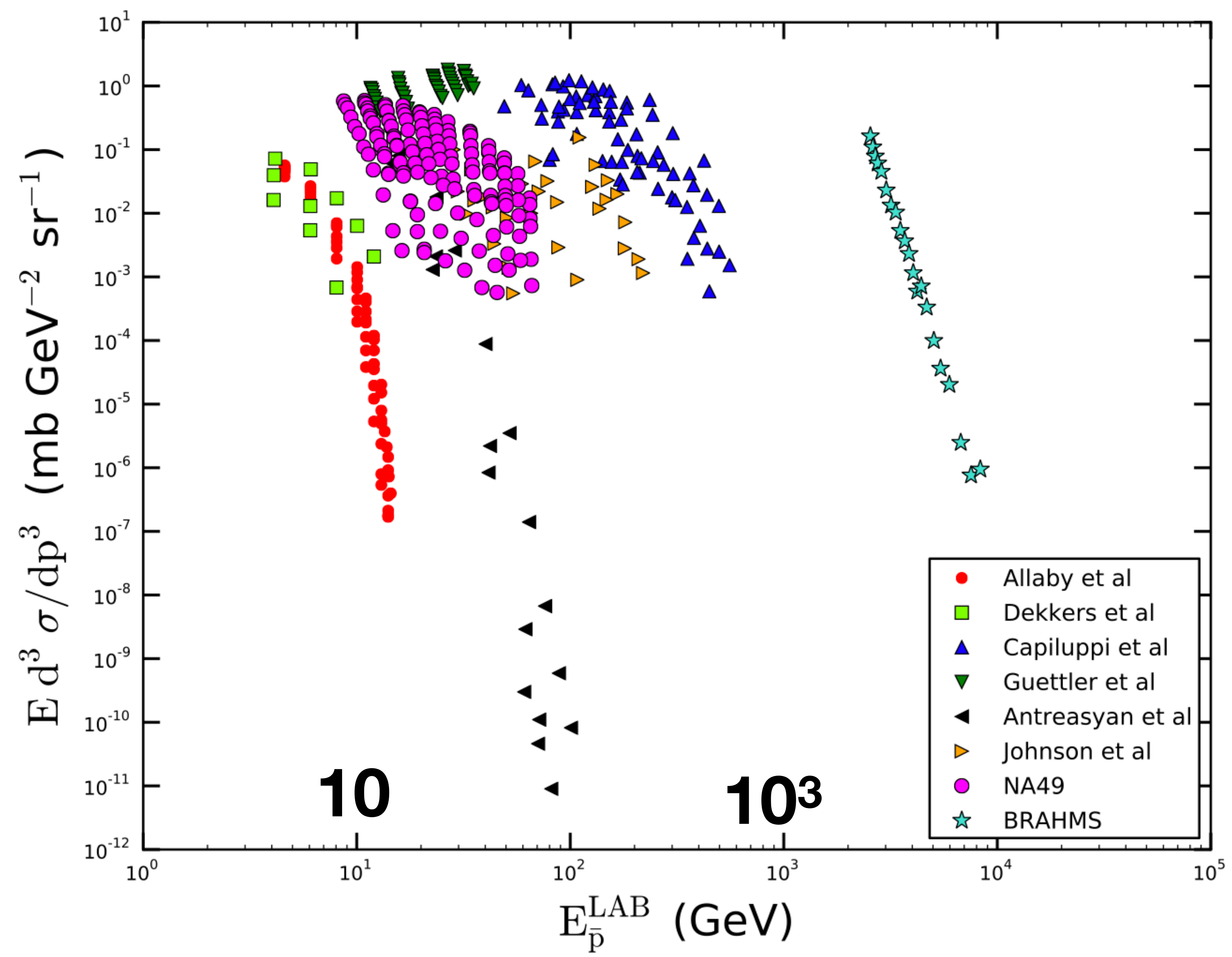

$$f(a+b\to c+X) = E_c\frac{d^3\sigma}{dp_c^3} = \frac{E_c}{\pi}\frac{d^2\sigma}{dp_L dp_T^2} = \frac{d^2\sigma}{\pi dy dp_T^2},$$

$$x_R = \frac{E^*_{\bar{p}}}{E^*_{\bar{p},\max}} \qquad E^*_{\bar{p},\max} = \frac{s-8m_p^2}{2\sqrt{s}} \qquad x_F = \frac{2p_L^*}{\sqrt{s}} \simeq \frac{p_L^*}{p^*_{L,max}}$$

https://arxiv.org/pdf/1408.0288.pdf

Data used in 2018 paper

pp—> anti-p X

Experiment	$\sqrt{s}$ [GeV]	σ_{scale}	I	II	Ref.
NA49	17.3	6.5%	×	×	[26]
NA61	7.7, 8.8, 12.3, 17.3	5%	×	×	[24]
Dekkers *et al.*	6.1, 6.7	10%	×	×	[36]
BRAHMS	200	10%	×		[38]

pA—> anti-p X

	$\sqrt{s}$ [GeV]	σ_{scale}	I-A	I-B	II-A	II-B	Ref.
NA49	17.3	6.5%	×	×	×	×	[35]
LHCb	110	6.0%		×		×	[25]

Ep=6.5 TeV

https://arxiv.org/pdf/1802.03030.pdf

Antiproton production cross section: prompt pp channel

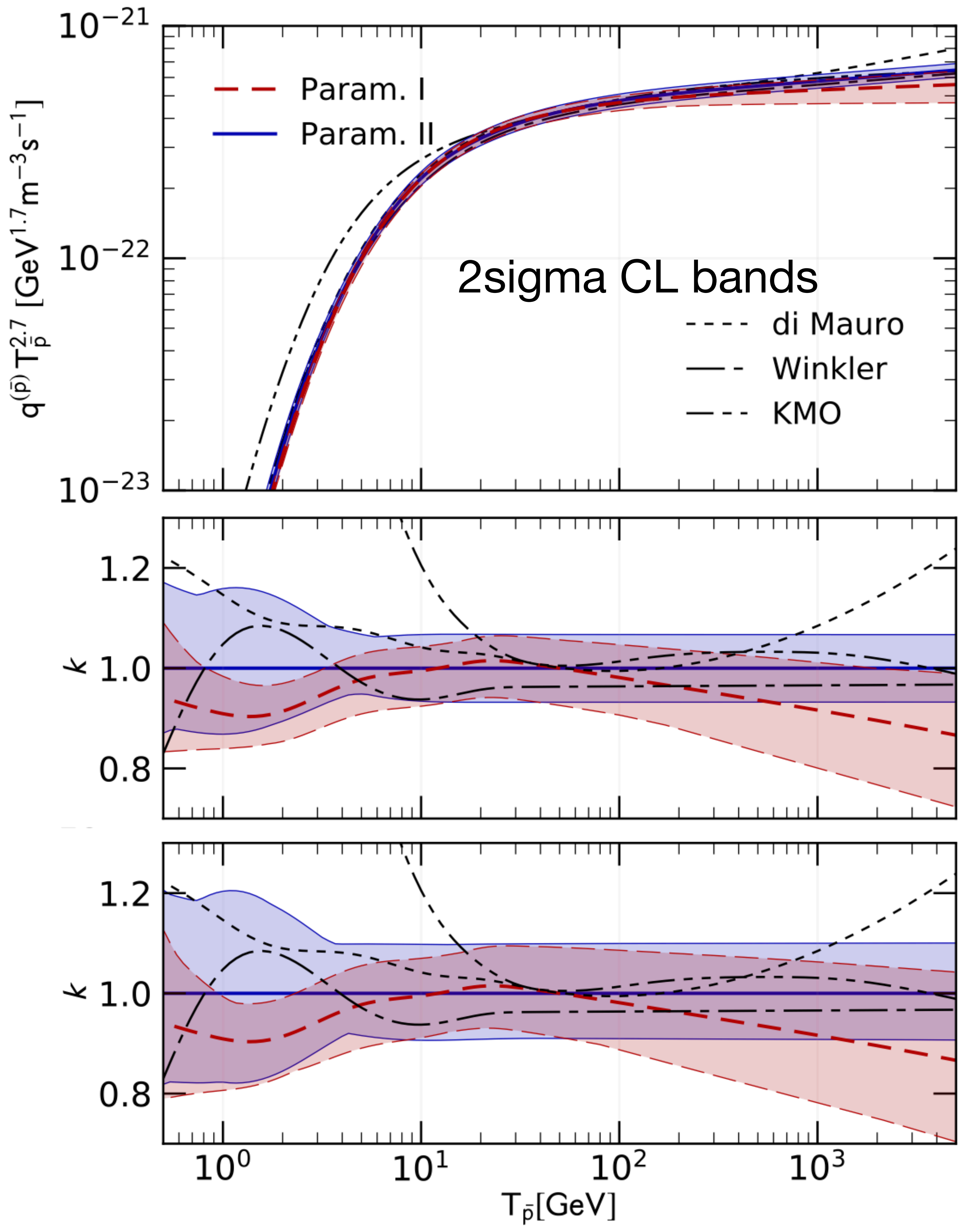

https://arxiv.org/pdf/1802.03030.pdf

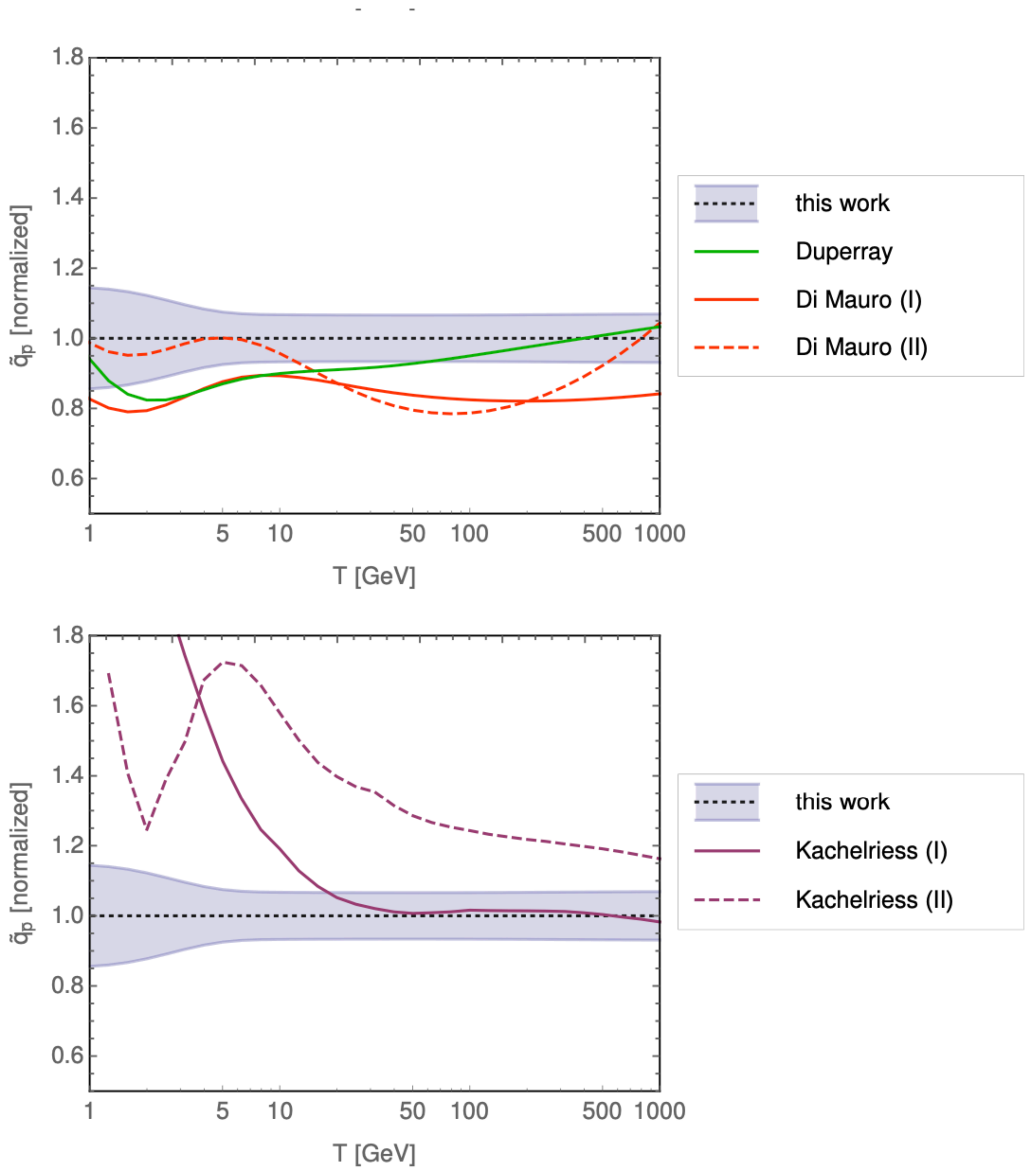

https://arxiv.org/pdf/1701.04866.pdf

Different papers agree on the fact that the prompt pp channel has an uncertainty between 10-15%

Antiproton production cross section: prompt pHe, Hep, HeHe channel

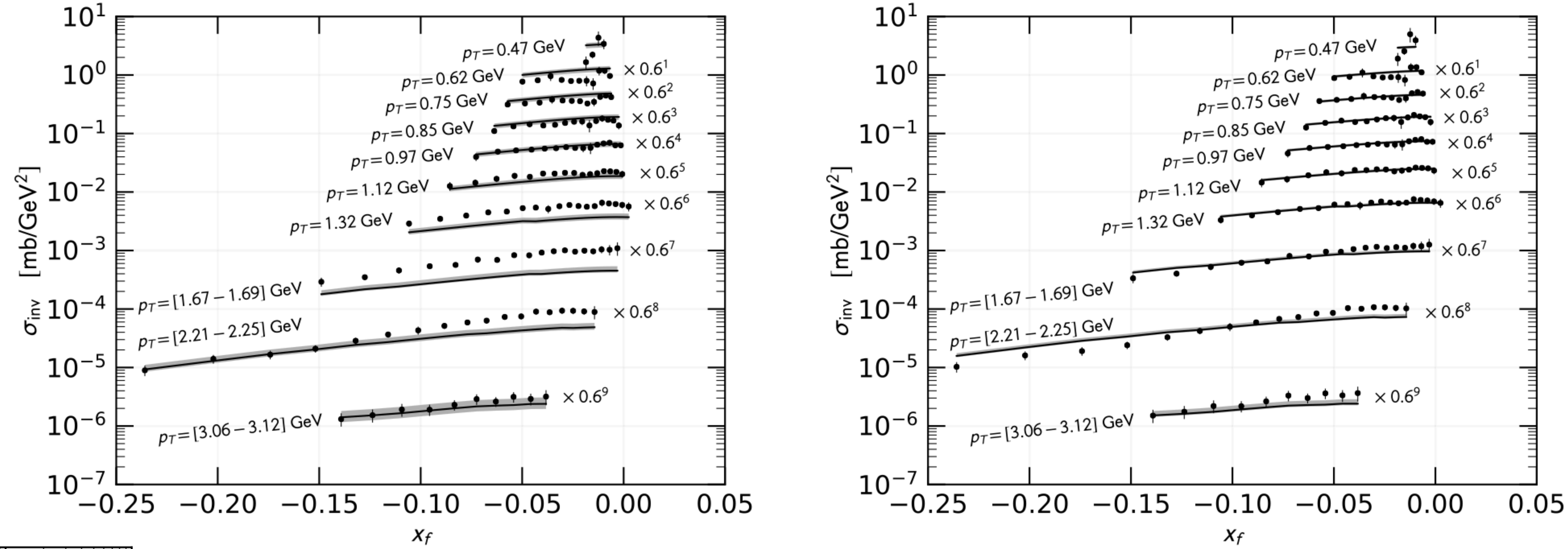

Comparison of LHCb data to the fit with Param. I-B (left) and Param. II-B (right). The grey band corresponds to 2σ uncertainty in the fit. The LHCb data agree better with Param. II and, therefore, they select this model for the high-energy behavior of the Lorentz invariant cross section.

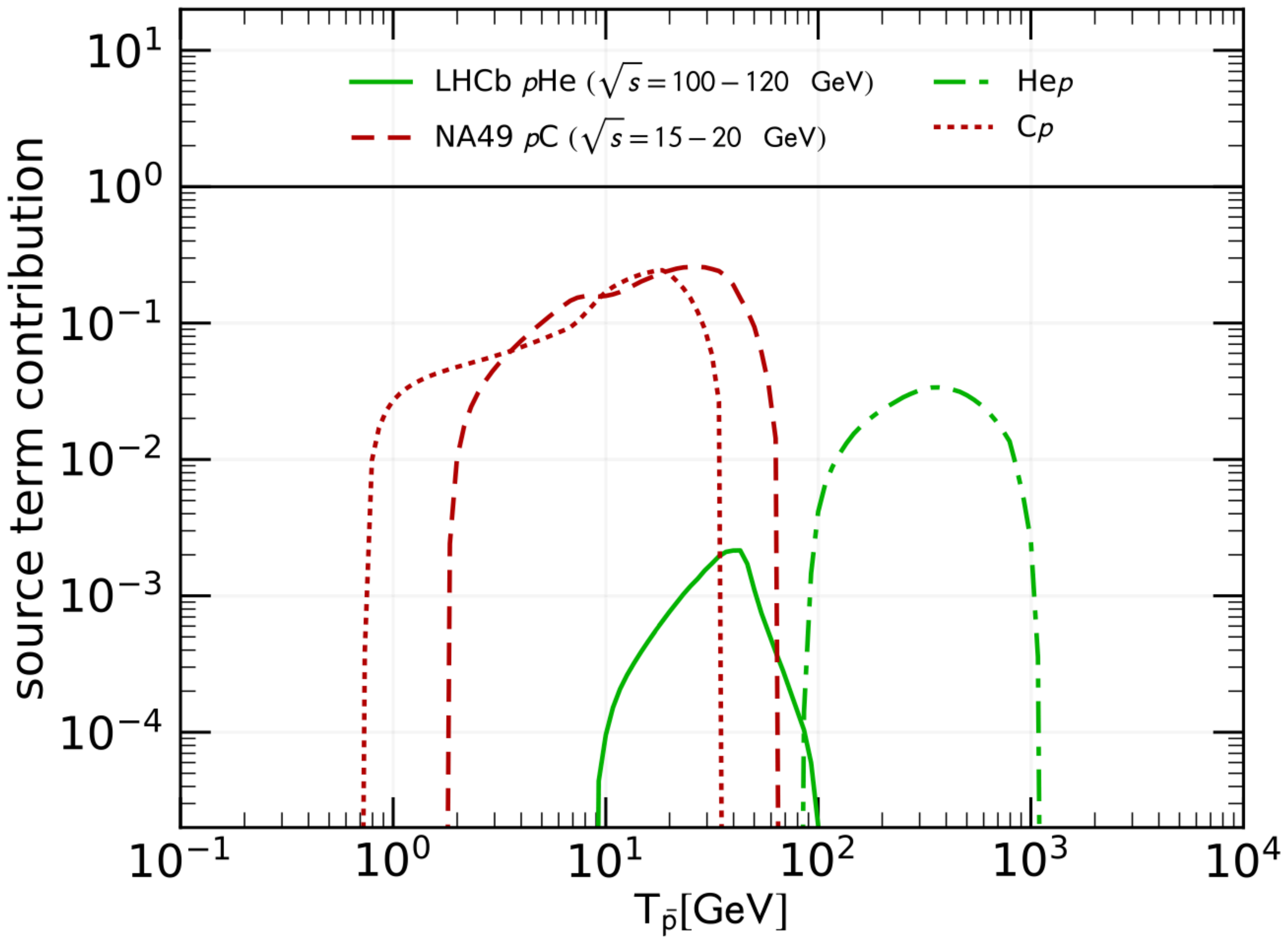

FIG. 3. Similar to Fig. 1, but for the nuclear channel. It shows the fraction of the antiproton source term which is covered by the kinematic parameter space of the cross section measurements by NA49 pC and LHCb pHe. Specifically, we assume a range of $\sqrt{s}$ = 15-20 GeV for NA49 and 100-120 GeV for LHCb. Each contribution is normalized to the total source term of the specific channel.

https://arxiv.org/pdf/1802.03030.pdf

Antiproton production cross section: prompt pHe, Hep, HeHe channel

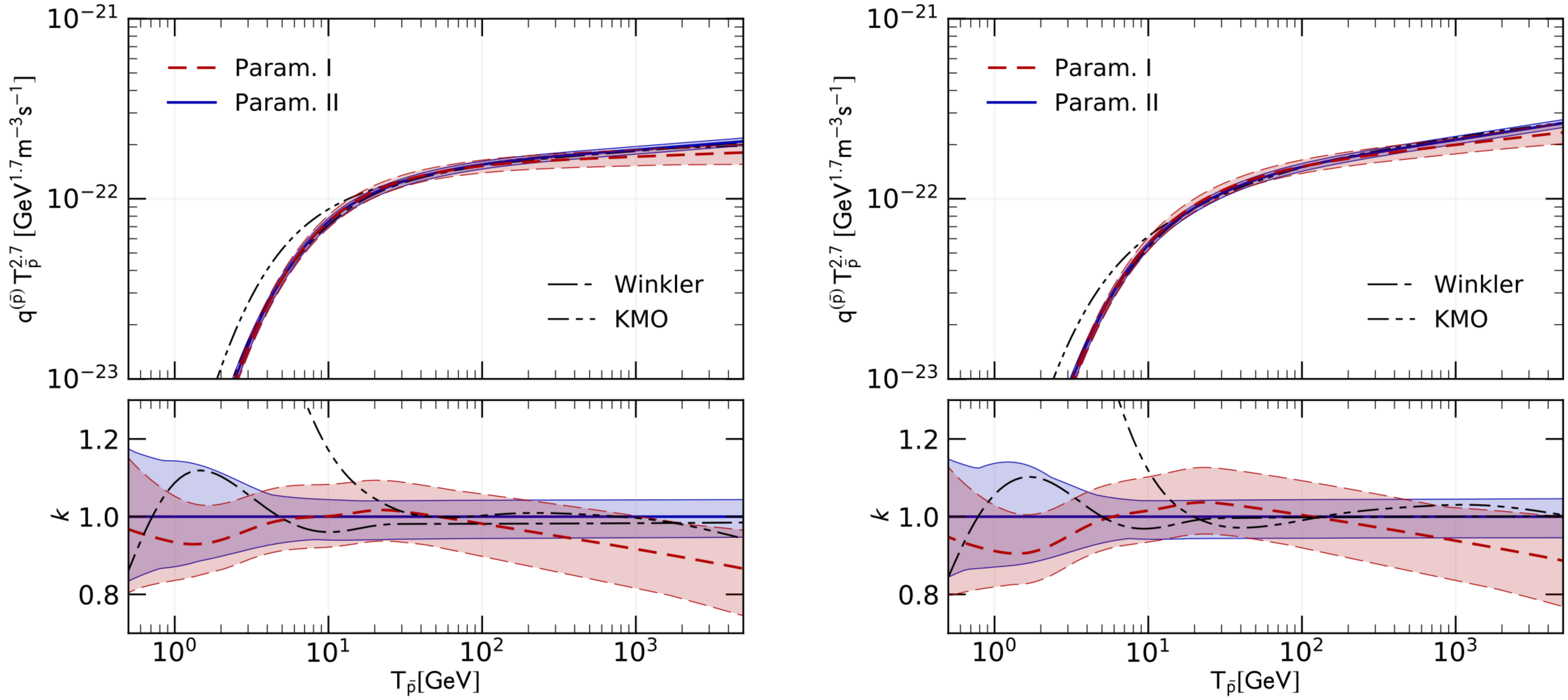

CR pHe (left panel) and Hep (right panel) antiproton source term

The uncertainty for the He part is about 15-20%
However, since this part contribute

https://arxiv.org/pdf/1802.03030.pdf

Uncertainty related to antineutron decay

- ***pp—>anti-n X —>anti-p Y*** usually taken to be the same of pp—>anti X.
- NA49 proceeding found an isospin asymmetry at the level of 20-30% at xf=0.
- **This is the main source of uncertainty in antiproton production cross sections.**
- **What do we expect for the anti-n channel theoretically? Would it be possible to measure this channel experimentally?**

[….] Very recently a small (120 kevents) pilot sample of n + p collisions has been obtained. These are derived from d + p reactions by tagging the spectator proton, where the deuterons in turn are produced by fragmentation of a Pb beam in a C target. [….]

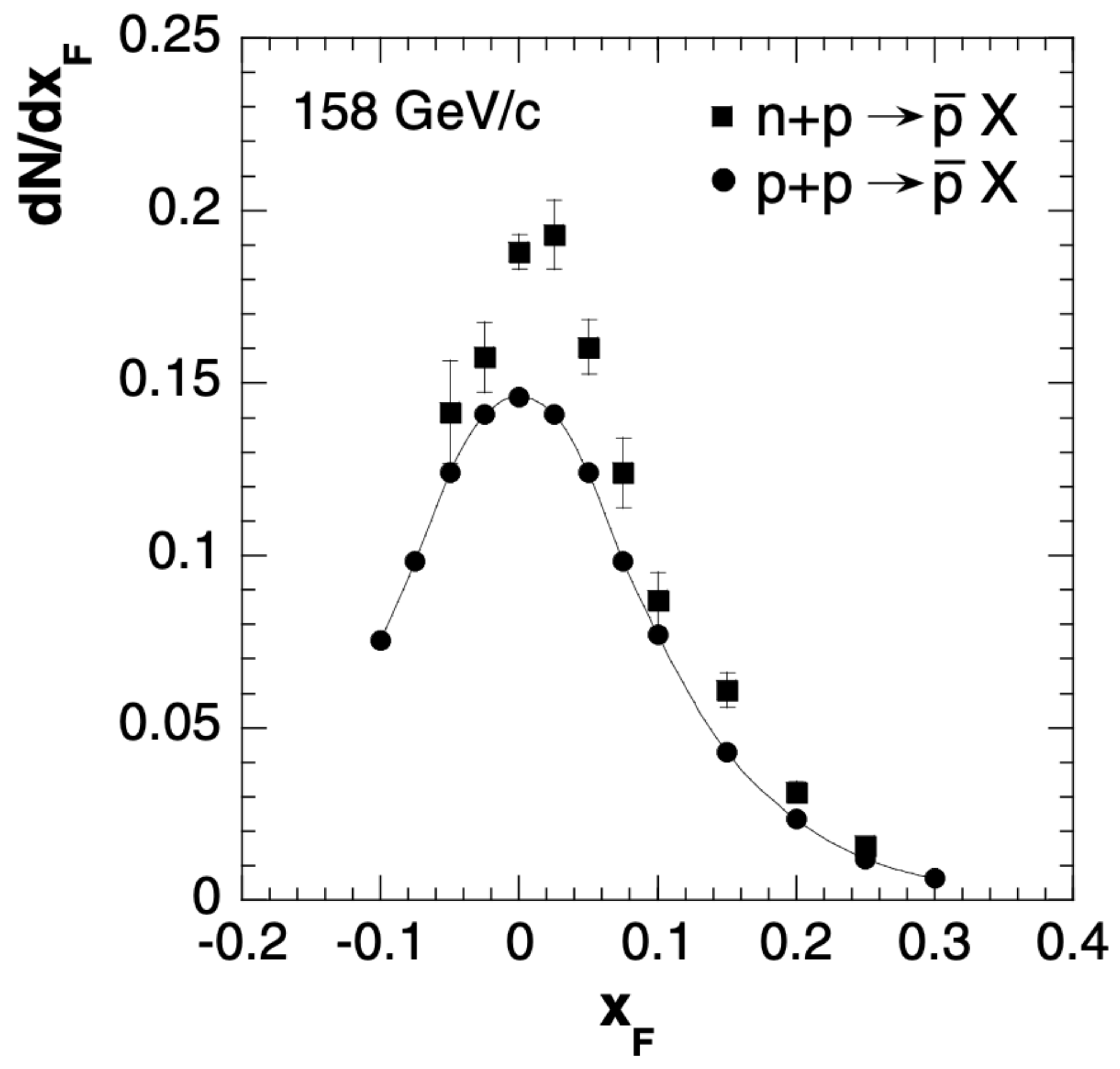

Fig. 3. Anti-proton density distribution as a function of x_F for p + p and n + p interactions

Isospin asymmetry

- It is more relevant at low energy wrt high energies.
- This is the same effect of multiplicity ratio between p-bar and p (n_{pbar}/n_p) and pi- and pi+ (n_{pi-}/n_{pi+}) being small at low s and 1 at high s
- On a Monte Carlo point of view Pythia produce same amount of anti-n and anti-p while others (Herwig) a different amount.

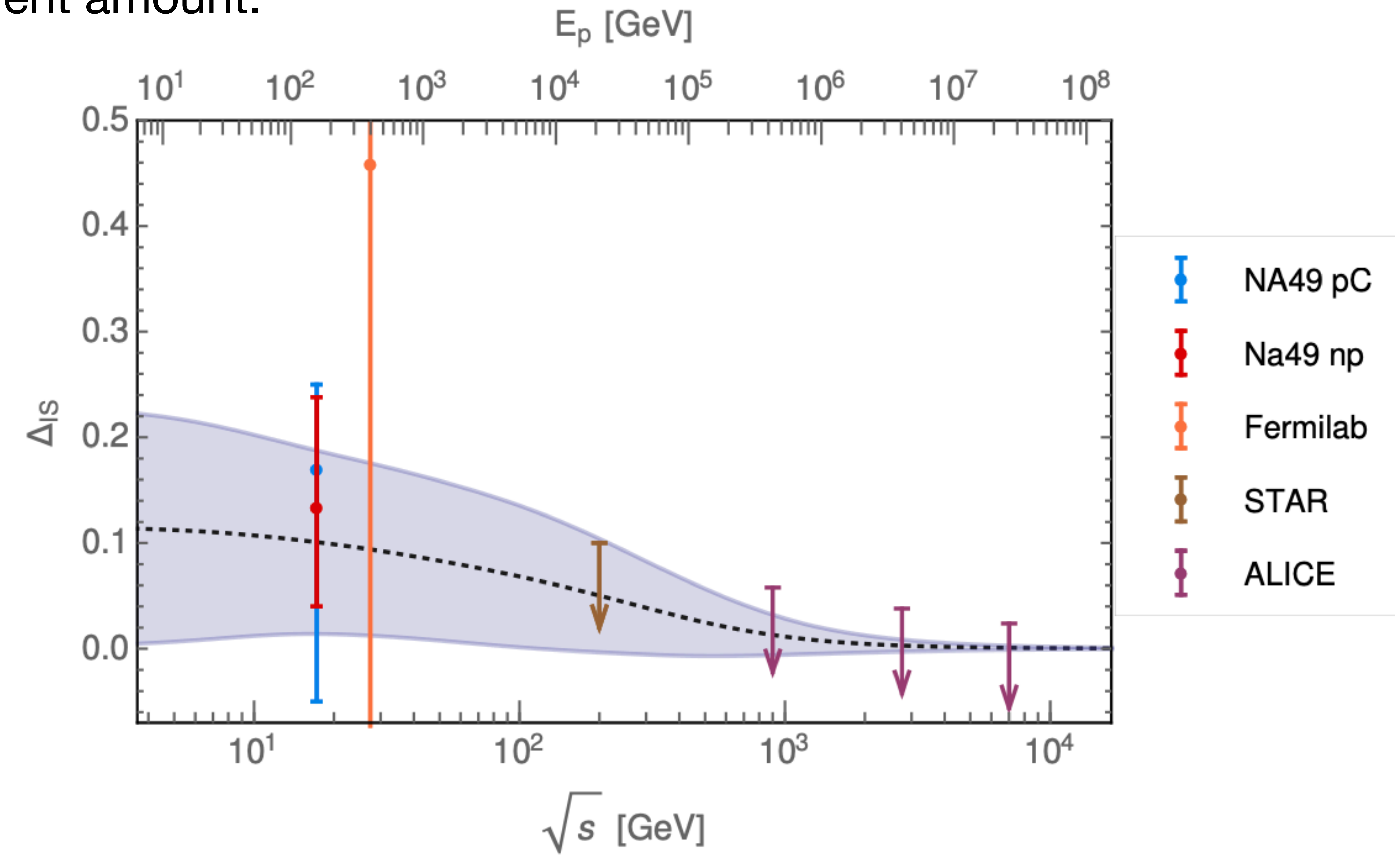

https://arxiv.org/pdf/1701.04866.pdf

Uncertainty related to hyperons

- The contribution of hyperons is usually taken as a rescaling of the pp.
- Hyperons contribute about 30-40% of the prompt pp channel.
- This contribution has an uncertainty of about 20-30%.
- This is probably a subdominant uncertainty of about 5-10%.

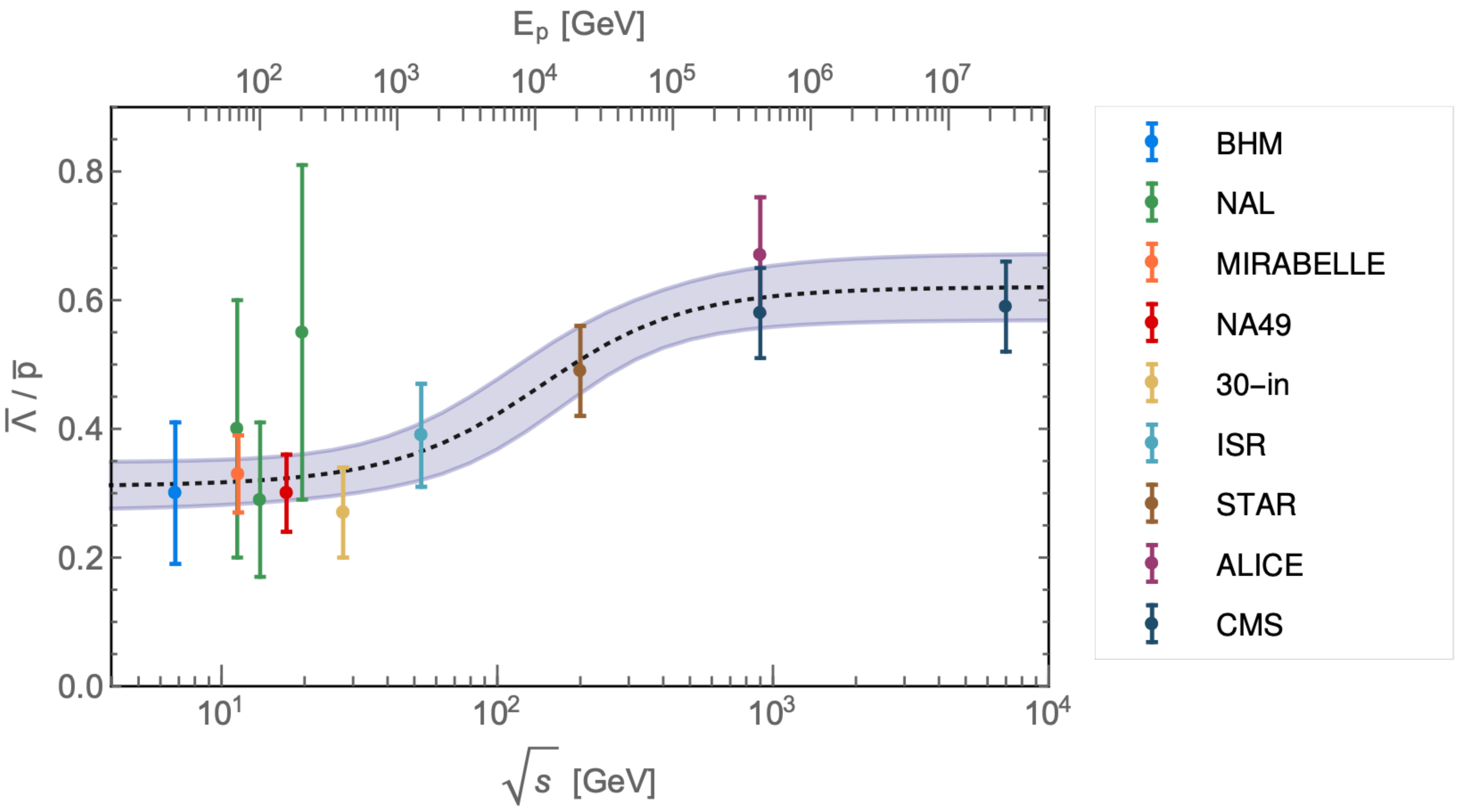

https://arxiv.org/pdf/1701.04866.pdf

Final uncertainty

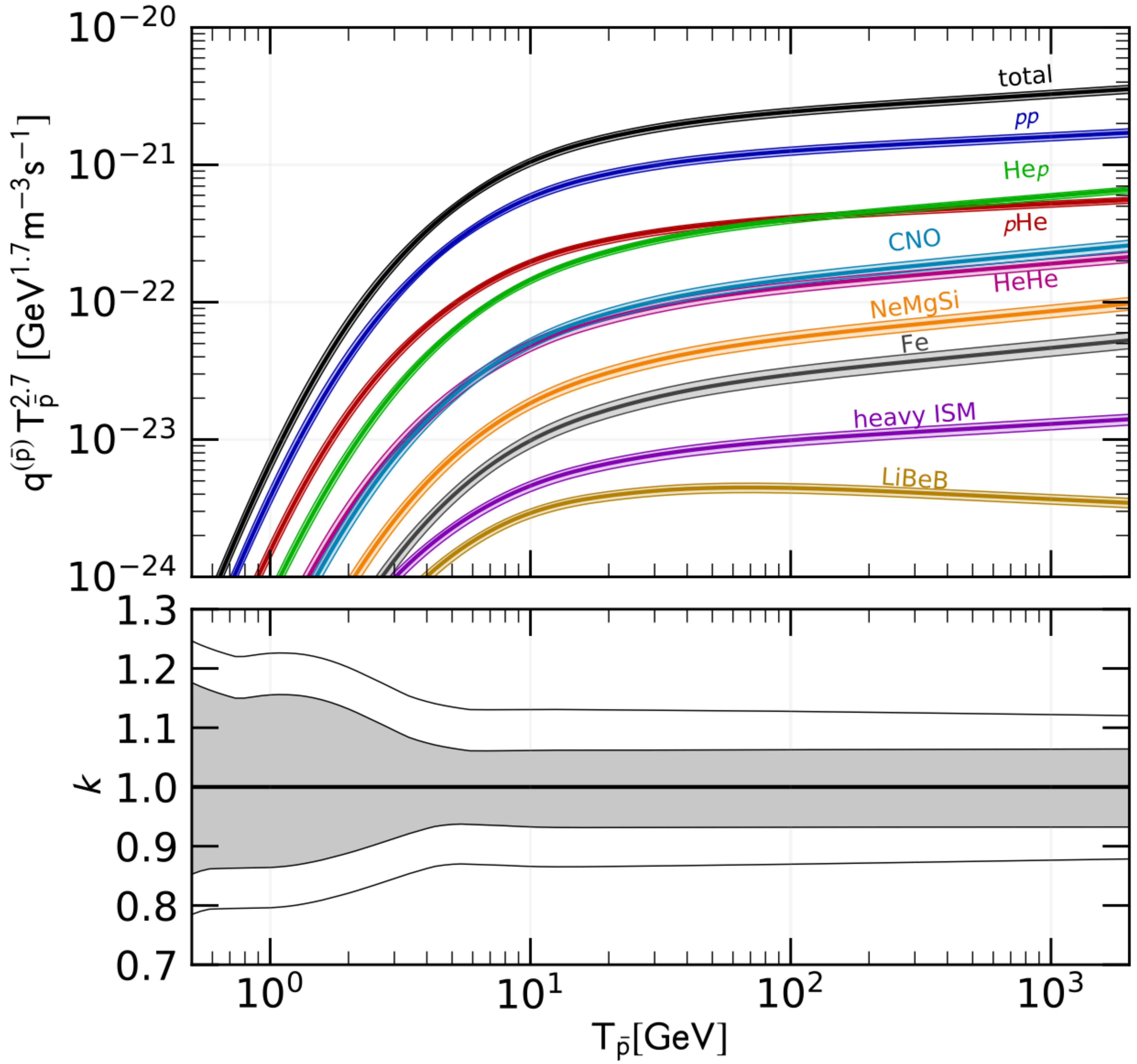

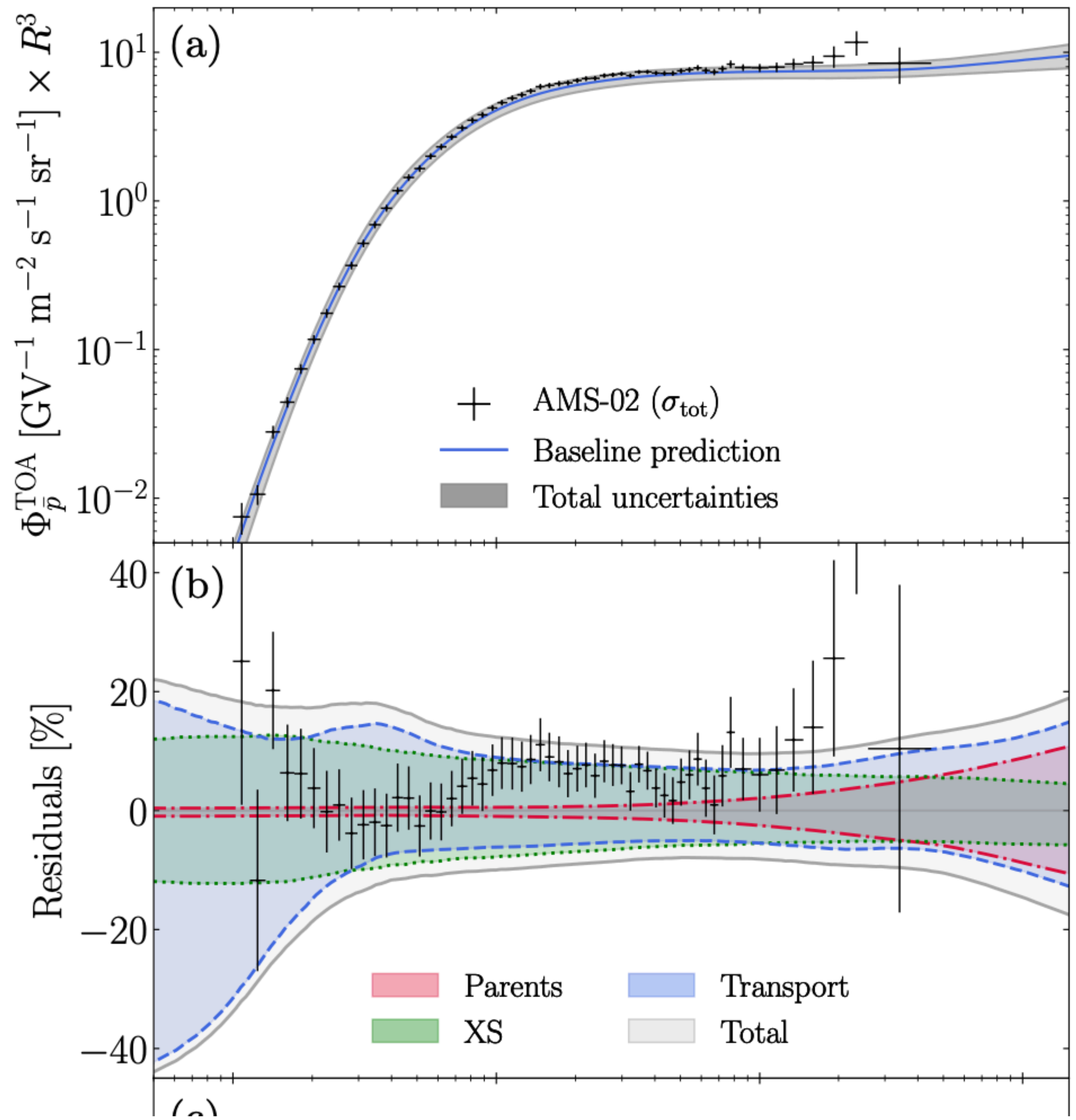

https://arxiv.org/pdf/1802.03030.pdf

https://arxiv.org/abs/2202.03076

P-bar cosmic measurements below 1 GeV

- GAPS will measure with the best sensitivity ever the antiproton cosmic flux below 1 GeV of kinetic energy.
- This energy range is very important for understanding the CR propagation and solar modulation effects.

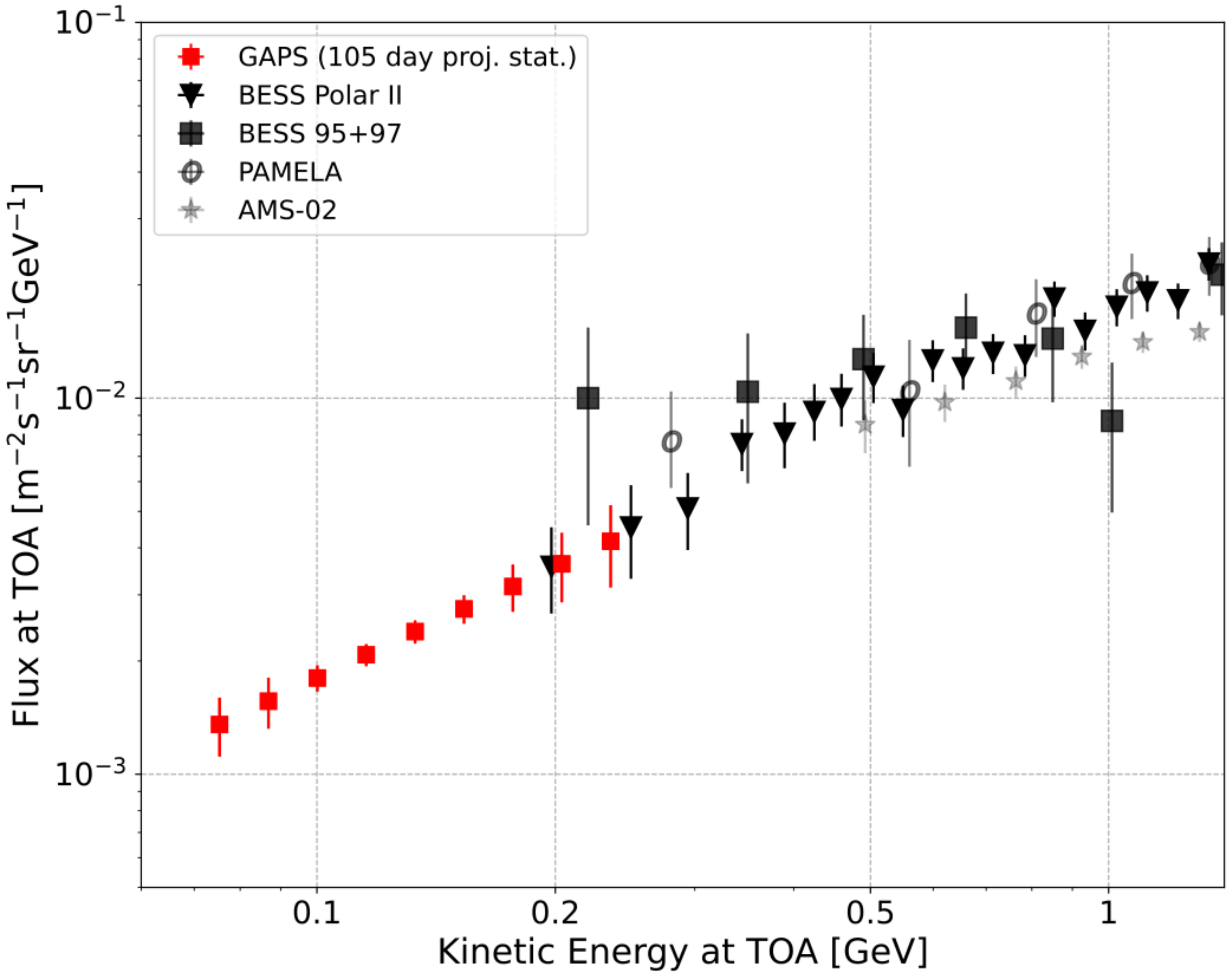

https://arxiv.org/pdf/2206.12991.pdf

Final physics cases for antip

- The first and most important point is a measurement of the anti-n channel.
  - Is there an Isospin asymmetry?
  - Is it possible to calculate it theoretically and/or measure it experimentally?
- We would need to have uncertainties for the prompt pp—> anti-p X and pp—> anti-n X at the level of 5%.
- Also the CS for the Helium part should reach a similar precision.
- The incoming proton energy should be around 10-1000 GeV, the sqrt(s) is 5-50 GeV.

Prescriptions for CS measurements

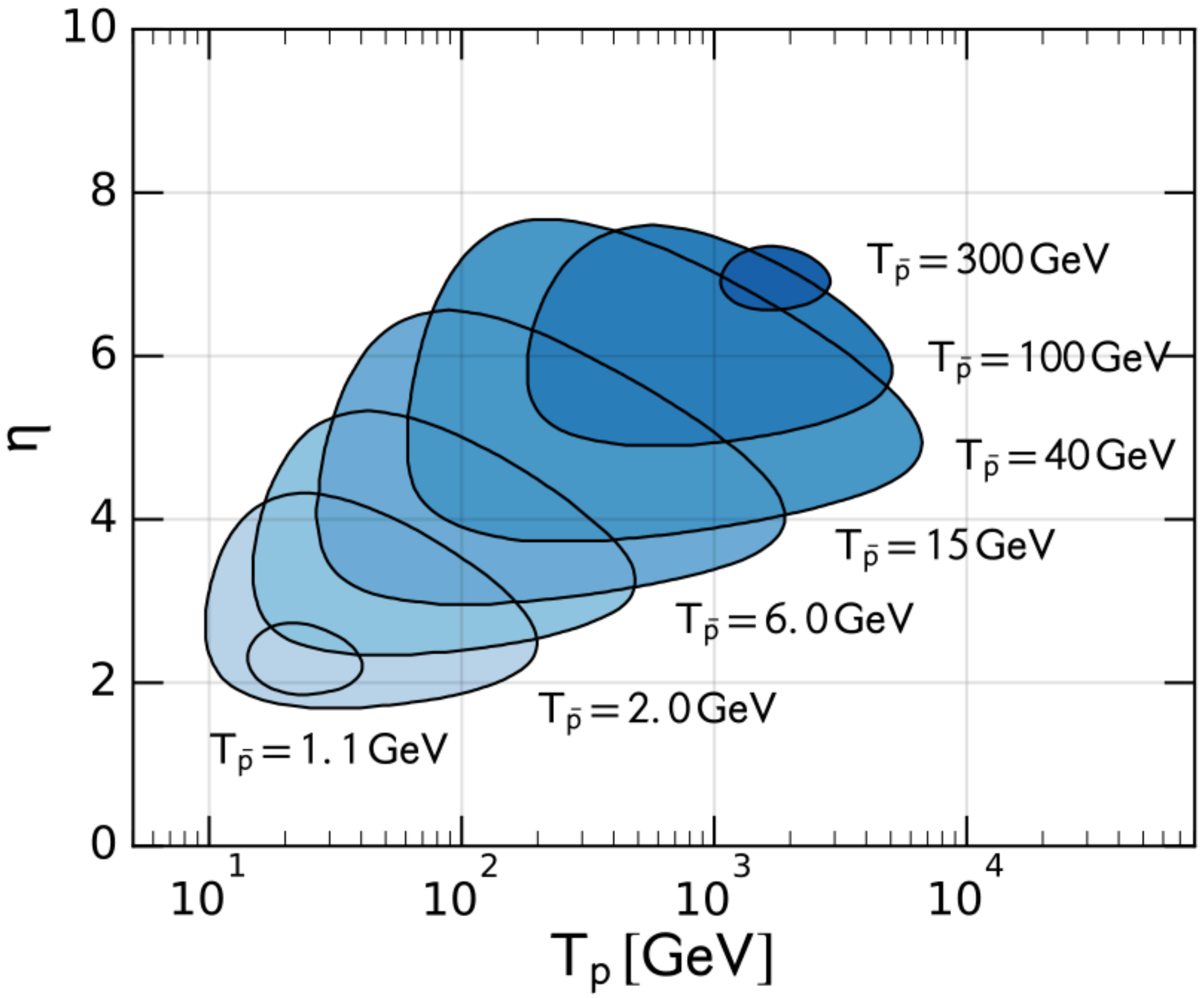

(a) LAB frame

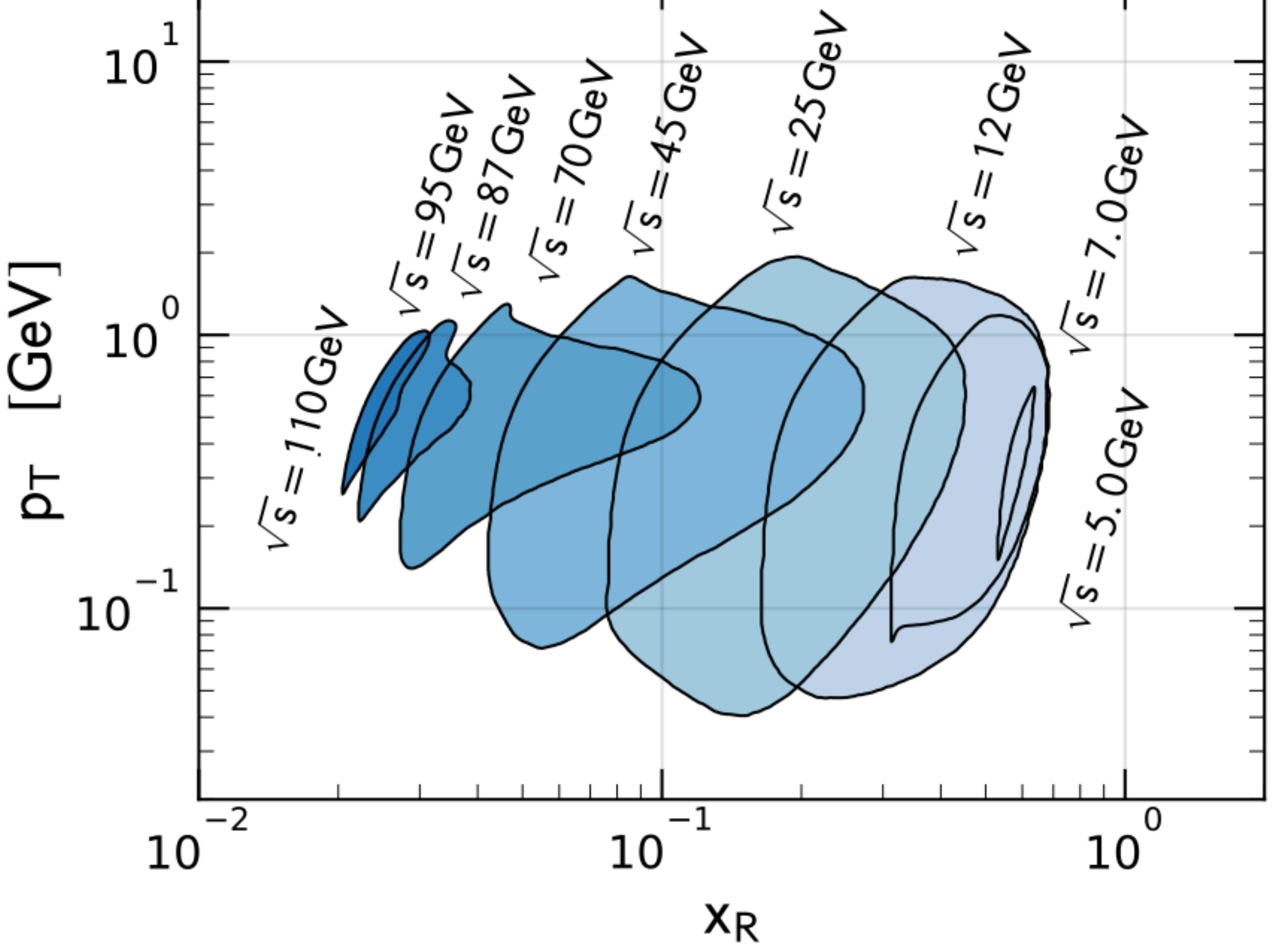

(b) CM frame

FIG. 7. Parameter space of the pp to $\bar{p}$ cross section necessary to determine the antiproton source term with the accuracy reached by recent AMS-02 measurements [12]. Here we require that the cross section has to be known by 3% within the blue shaded regions and by 30% outside the contours. The left (right) panel displays the result for the LAB (CM) reference frame variables.

https://arxiv.org/pdf/1704.03663.pdf

https://arxiv.org/pdf/1704.03663.pdf

Prescriptions for CS measurements

Parameter space that has to be covered in order to guarantee the AMS-02 precision level on the p̄ source term, if the p+p → p̄+X cross section is determined with 3% uncertainty within the blue shaded regions and by 30% outside the contours. The plot is done for the LAB (left panel, a) and CM (right panel, b) reference frame variables. For the LAB frame we show the contours as functions of η and T, for selected values of Tp̄ from 1.1 (the lowest energy below 30% uncertainty in the CR p̄ flux, see Fig. 5) to 300 GeV. As expected the contour size decreases when Tp̄ approaches to 1 GeV, because there the AMS-02 uncertainty on the antiproton flux reaches 30%. A similar explanation holds for large Tp̄. Antiprotons of increasing energy require the coverage of increasing η values. For example, σinv(p+p → p̄+X) at Tp̄=2 GeV is known at 3% level if data were taken with proton beams between 10 and 200 GeV and pseudorapidity from 1.8 to 4. If the whole AMS-02 energy range had to be covered with high precision, one should collect p + p → p̄ + X cross section data with proton beams from 10 GeV to 6 TeV, and η increasing from 2 to nearly 8.

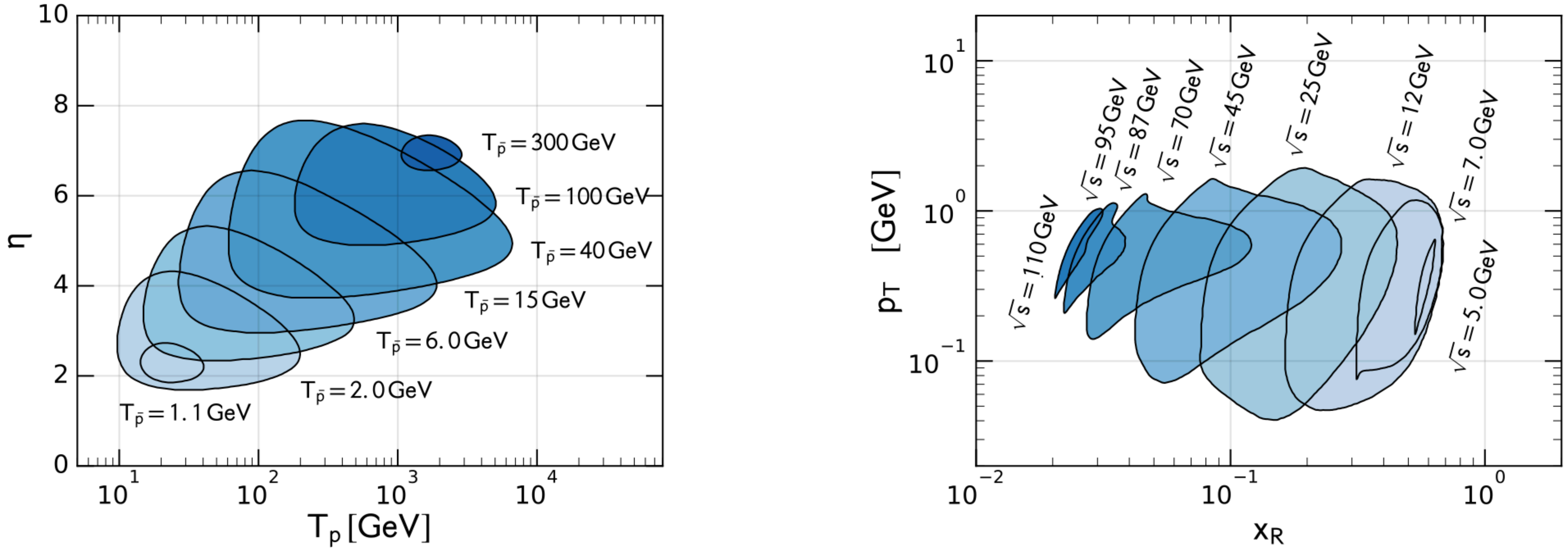

(a) LAB frame   (b) CM frame

FIG. 7. Parameter space of the pp to $\bar p$ cross section necessary to determine the antiproton source term with the accuracy reached by recent AMS-02 measurements [12]. Here we require that the cross section has to be known by 3% within the blue shaded regions and by 30% outside the contours. The left (right) panel displays the result for the LAB (CM) reference frame variables.

PSEUDORAPIDITY $\eta = -\log(\tan(\vartheta/2))$

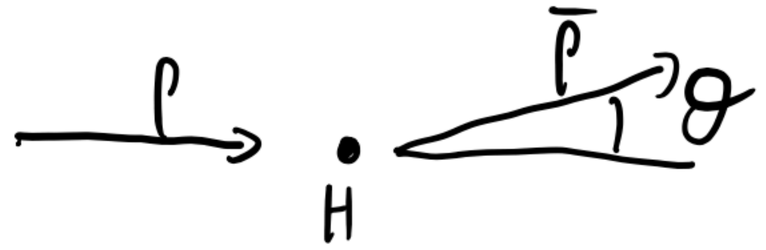

$\eta = \frac{1}{2}\log\left(\frac{|\vec p|+p_L}{|\vec p|-p_L}\right) = \operatorname{arctanh}\left(\frac{p_L}{|\vec p|}\right)$

For relativistic particles $\eta = y$ → rapidity

$\eta \simeq y = \frac{1}{2}\log\left(\frac{E+p_L}{E-p_L}\right)$

For $\vartheta=0$ η very large

η large → θ FORWARD SCATTERING

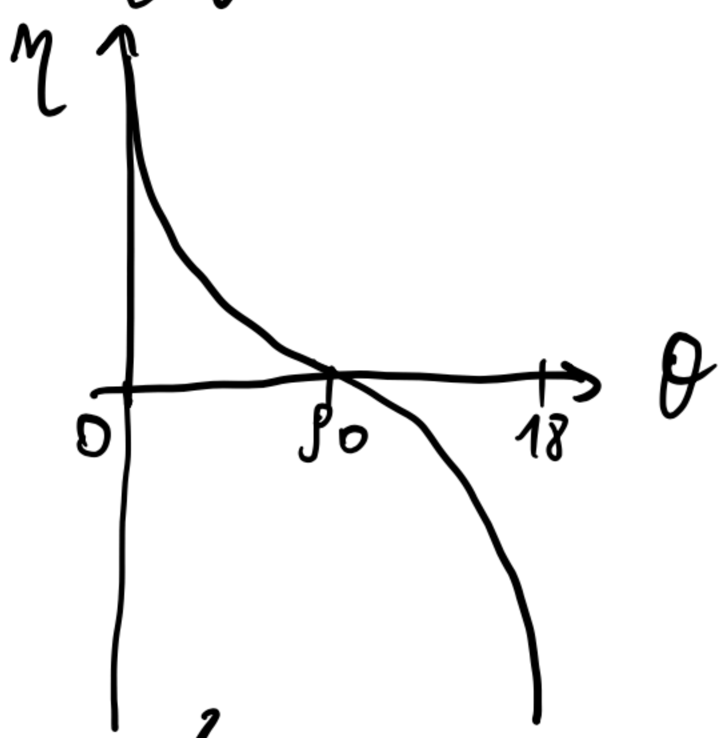

$x_R = \frac{E^*_{\bar p}}{E^*_{\bar p\,max}}$ $E^*_{\bar p\,max} = \frac{s-8m_p^2}{2\sqrt{s}}$ $x_R < 1$

Positrons-electrons production CS

Positrons AMS-02 data and interpretation

- Positrons are measured by AMS-02 from hundreds of MeV to 1 TeV with a precision as low as 3-5%.
- The low-energy part is due mostly to the secondary production while the high-energy part by a primary component (pulsar or dark matter).

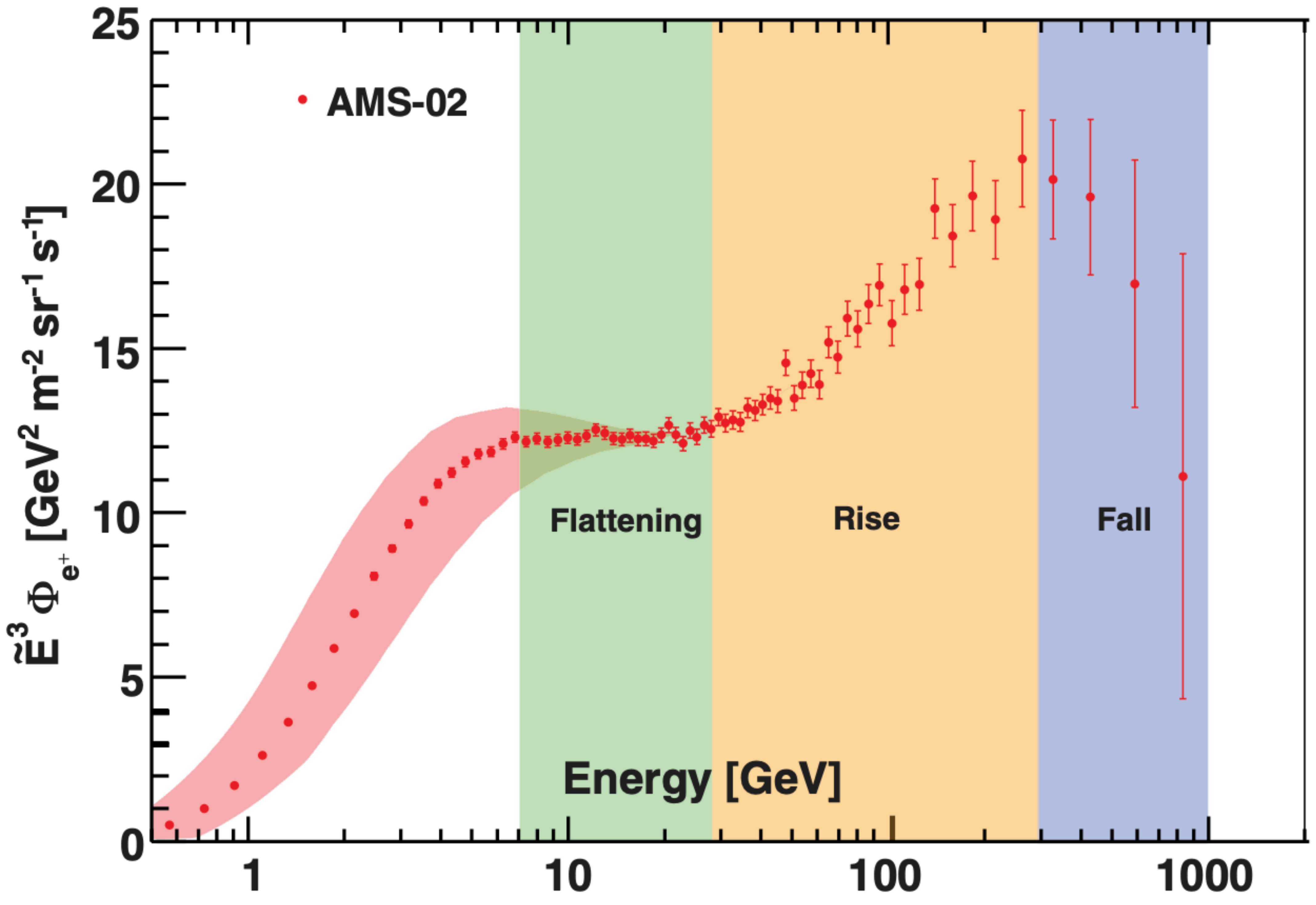

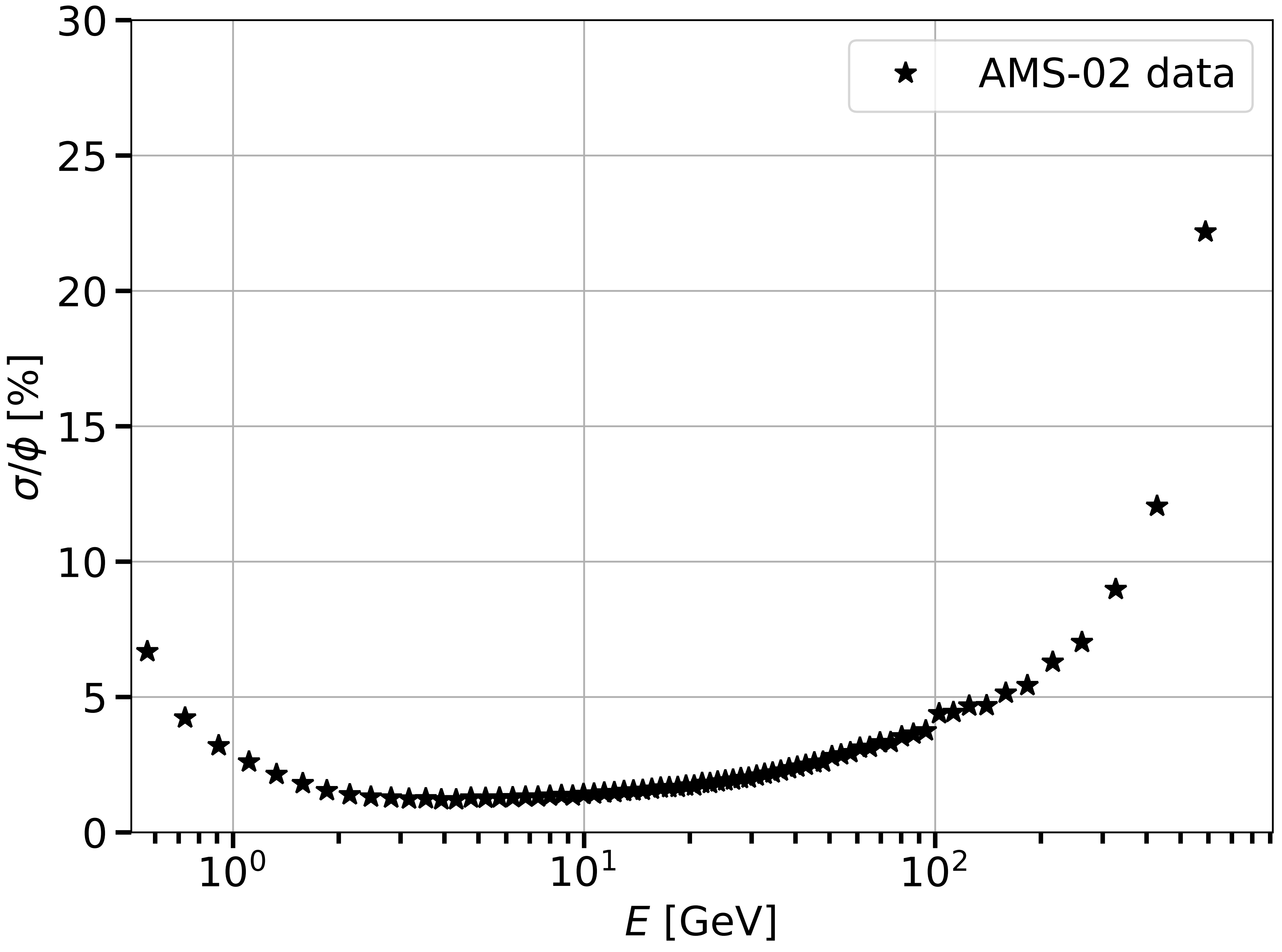

Positrons AMS-02 data and interpretation

- Positrons are measured by AMS-02 from hundreds of MeV to 1 TeV with a precision as low as 3-5%.
- The low-energy part is due mostly to the secondary production while the high-energy part by a primary component (pulsar or dark matter).

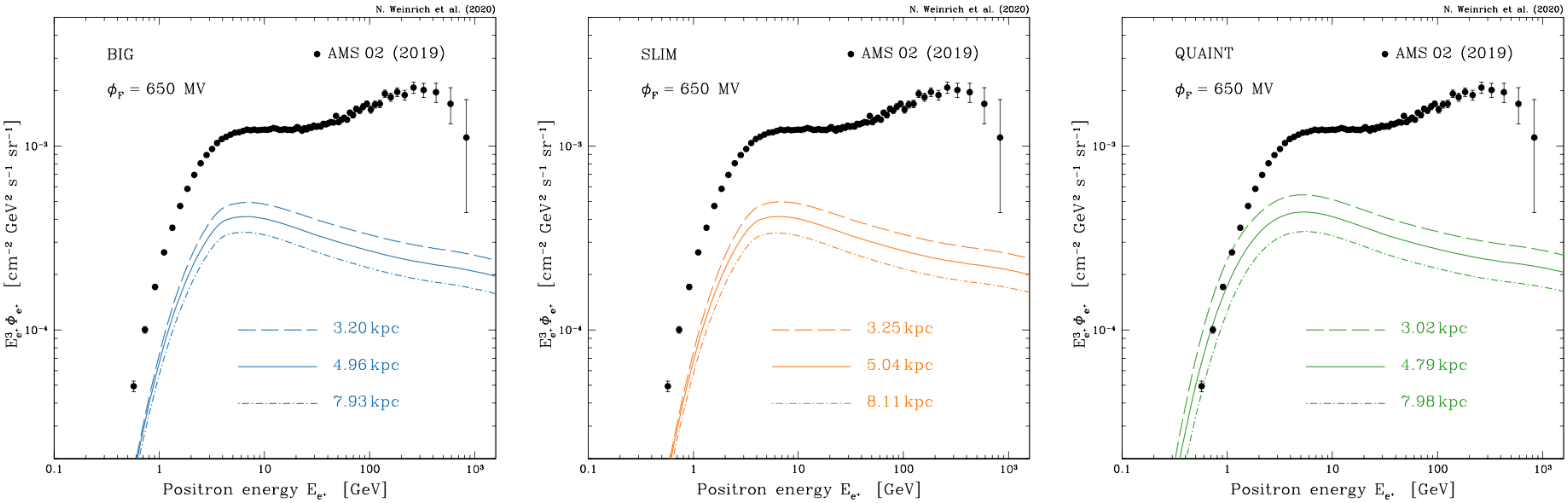

https://arxiv.org/abs/2004.00441

State of the art before our paper

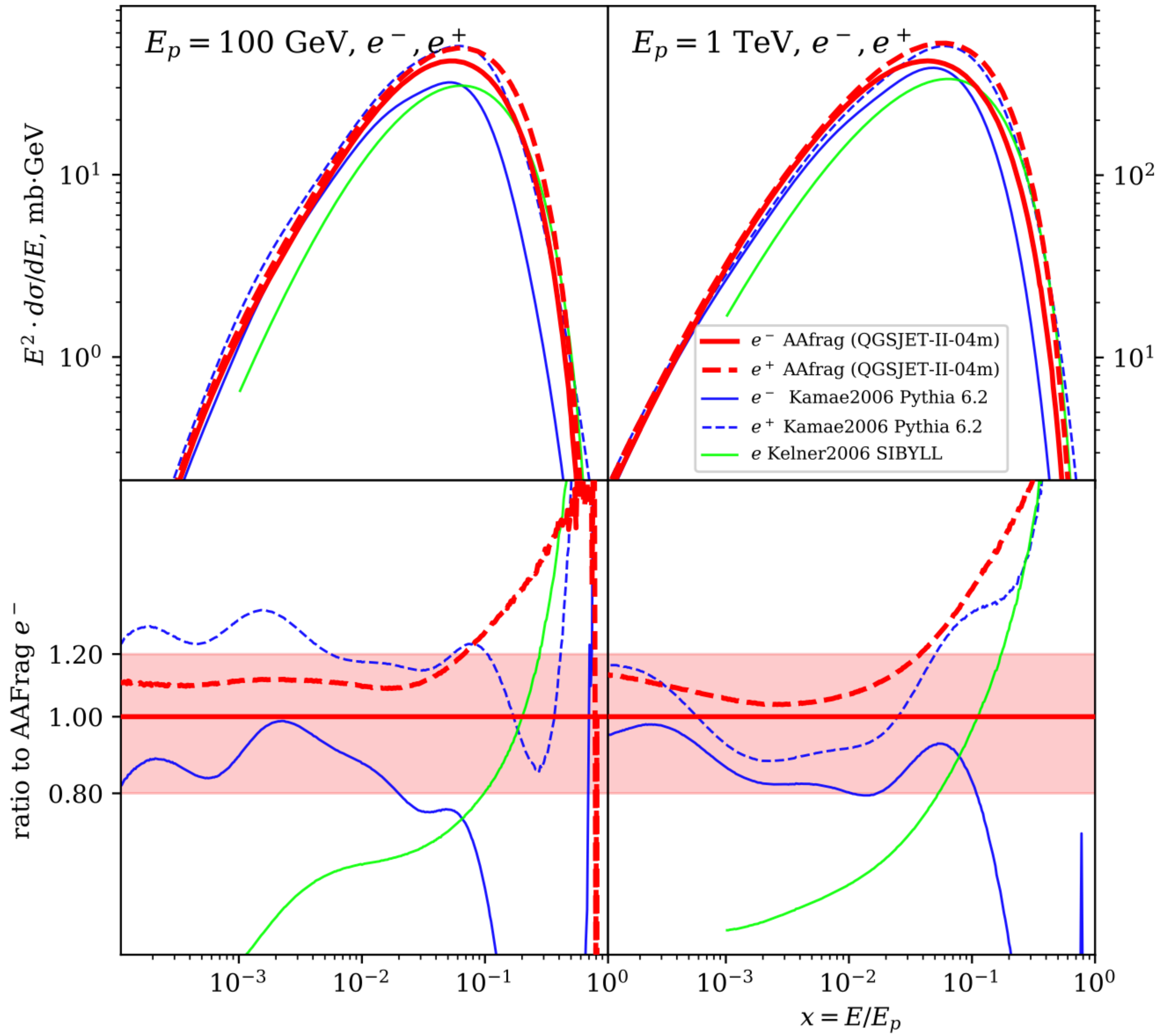

- There is at least 20-30% uncertainty on the theoretical models.

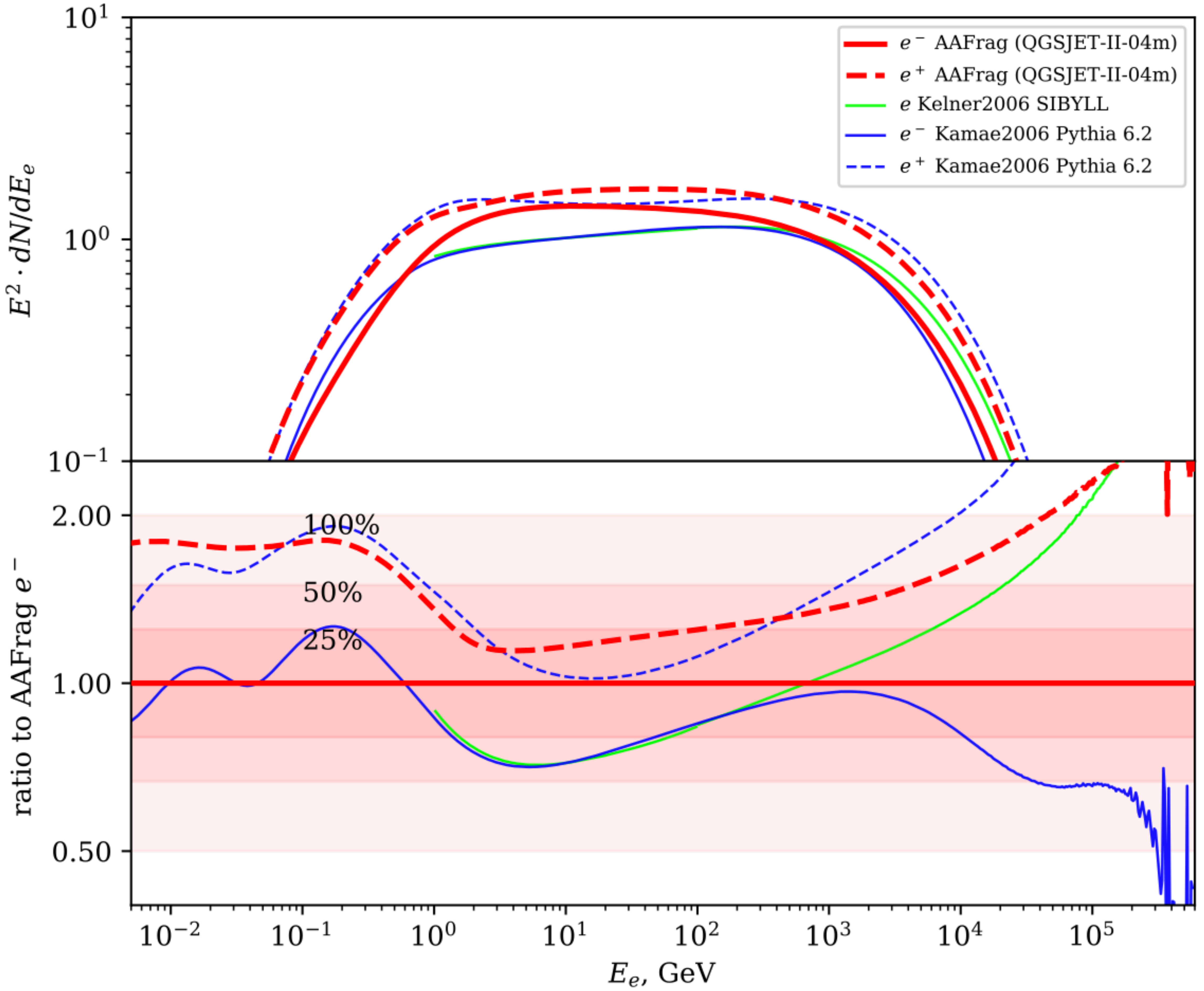

https://arxiv.org/pdf/2110.00496.pdf

Production cross section of electrons and positrons

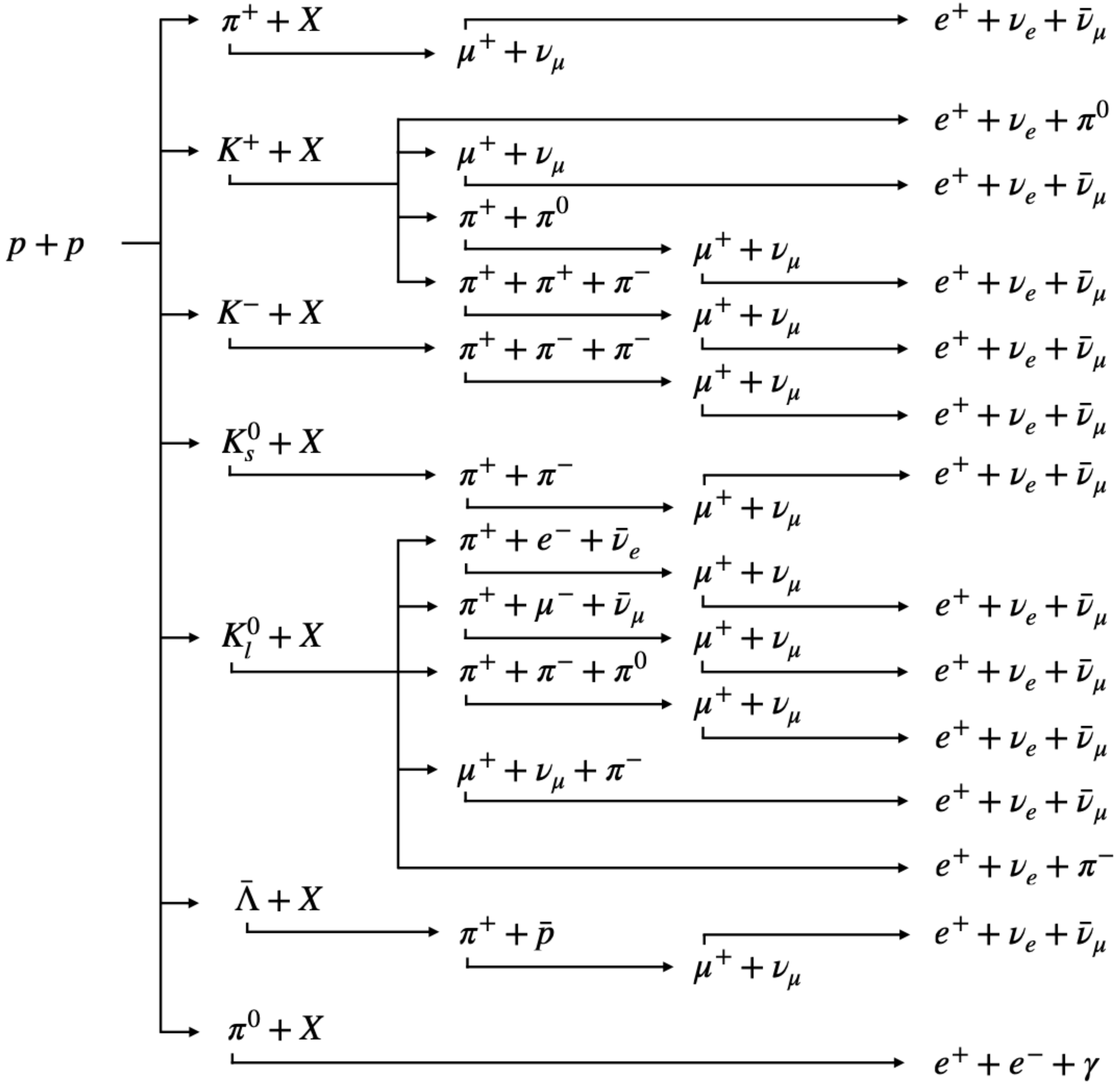

$$q(T_{e^\pm}) = \sum_{i,j} 4\pi\, n_{\mathrm{ISM},j} \int dT_i\, \phi_i(T_i) \frac{d\sigma_{ij}}{dT_{e^\pm}}(T_i, T_{e^\pm})$$

$$\frac{d\sigma_{ij}}{dT_{e^\pm}}(T_i, T_{e^\pm}) = \int dT_{\pi^\pm} \frac{d\sigma_{ij}}{dT_{\pi^\pm}}(T_i, T_{\pi^\pm})\, P(T_{\pi^\pm}, T_{e^\pm})$$

- In addition to these channel we have resonances: Δ and ρ.
- Resonance production cannot be separated from the prompt because of very short scale decay.

https://arxiv.org/abs/2203.13143

Cross section data

Experiment	$\sqrt{s}$ [GeV]		σ_{inv}	n	Ref.
NA49	17.3	$(\pi^{\pm}, K^{\pm})$	✓	-	[67, 76]
ALICE	900	$(\pi^{+}, K^{\pm})$	✓	-	[77]
CMS	900, 2760, 7000, 13000	$(\pi^{\pm}, K^{\pm})$	✓	-	[72, 78]
Antinucci	3.0, 3.5, 4.9, 5.0, 6.1, 6.8	$(\pi^{\pm})$	-	✓	[79]
	2.8, 3.0,3.2, 5.3, 6.1, 6.8	(K^{+})	-	✓	[79]
	4.9, 5.0, 6.1, 6.8	(K^{-})	-	✓	[79]
NA61/SHINE	6.3, 7.7, 8.8, 12.3, 17.3	$(\pi^{\pm}, K^{\pm})$	-	✓	[68]

$$\sigma_{\text{inv}} = \sigma_0(s)\, c_1 \left[F_p(s, p_T, x_R) + F_r(p_T, x_R) \right] A(s)$$

https://arxiv.org/abs/2203.13143

Final uncertainty of cross section

- The final uncertainty for the positrons and electrons production cross sections is at the level of 5-8%.
- **We improved significantly wrt to previous models!**
- These uncertainties are larger than the errors of AMS-02 data points but for the interpretation of the positron excess is not a big deal.

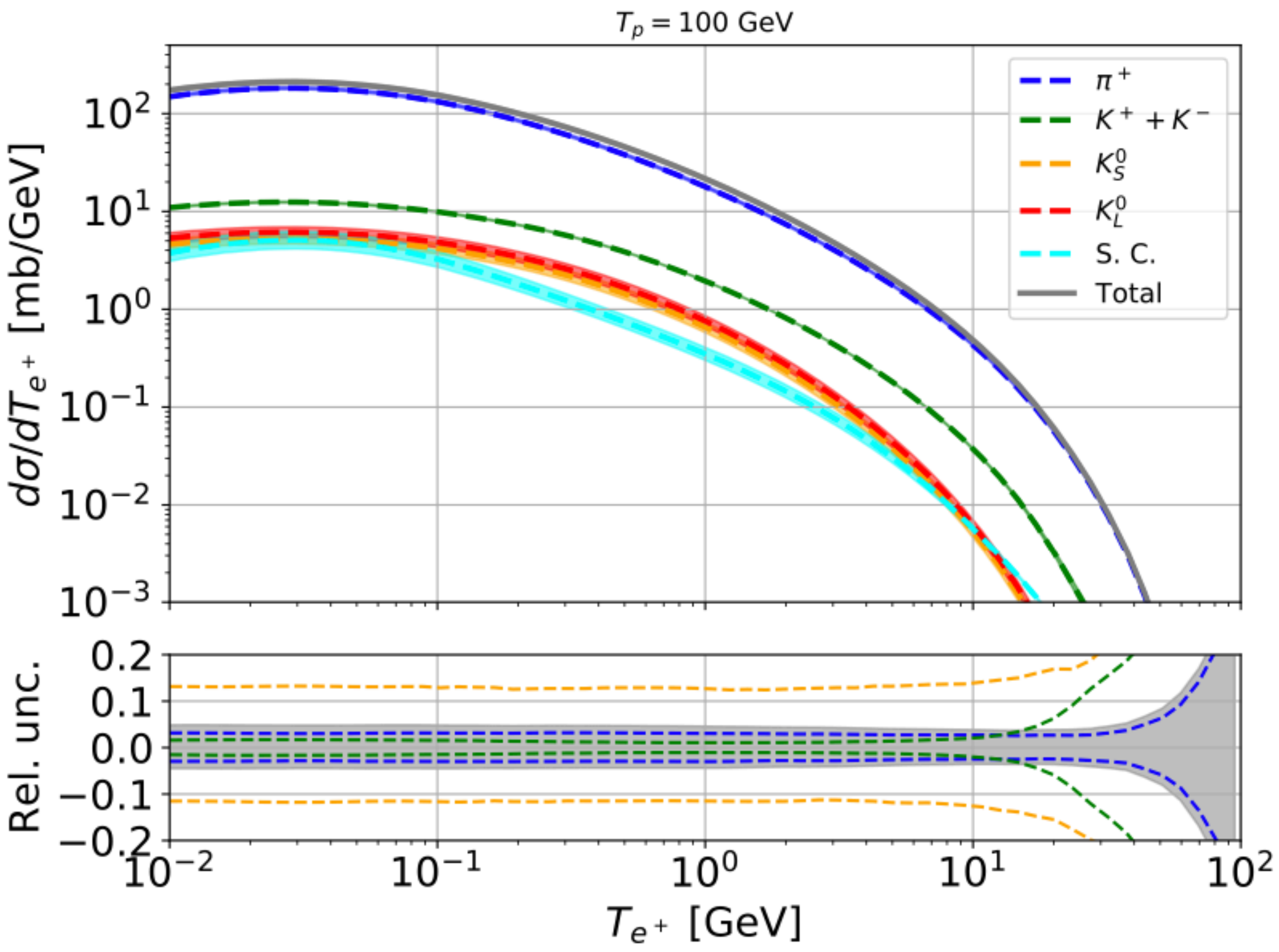

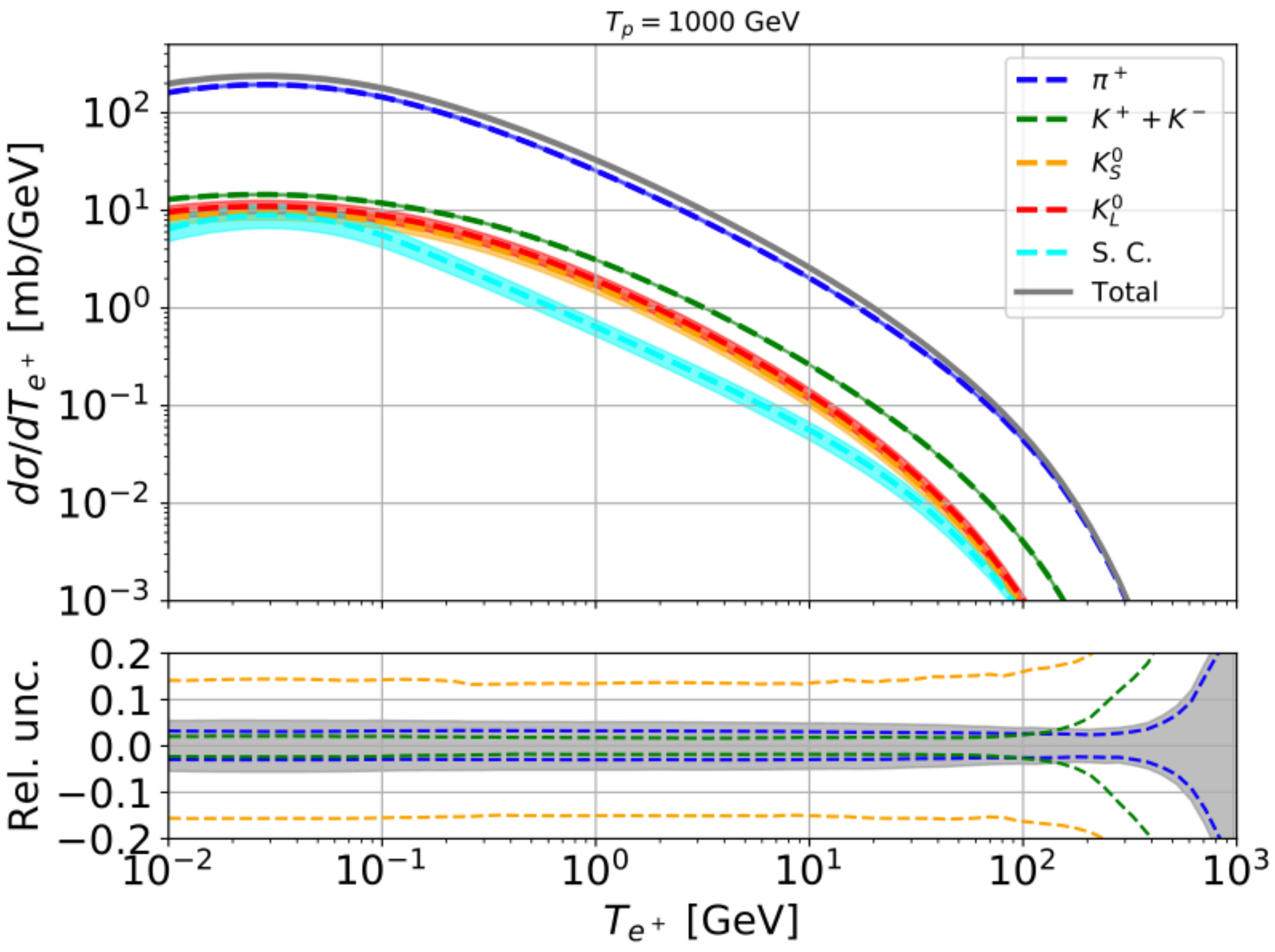

https://arxiv.org/abs/2203.13143

Nuclear part

- In the Galaxy, nuclei interactions (p + A, A + p, and A + A) give a significant contribution to the production of secondary particles.
- We used the data of NA49 for the production of π+ in p+C collisions at Ep = 158 GeV and K+ in p+C collisions at Ep = 30 GeV.

We model the inclusive Lorentz invariant cross section of the $A_1 + A_2 \to \pi^+ + X$ scattering by:

$$\sigma_{\mathrm{inv}}^{A_1 A_2}(\sqrt{s}, x_F, p_T) = f^{A_1 A_2}(A_1, A_2, x_F, D_1, D_2, D_3)\ \sigma_{\mathrm{inv}}^{pp}(\sqrt{s}, x_R, p_T), \quad (25)$$

where A_1 and A_2 are the mass numbers of the projectile and target nucleus, respectively, and D_1, D_2, and D_3 are three fit parameters. Explicitly, the factor $f^{A_1 A_2}$ is defined by:

$$f^{A_1 A_2}(x_F) = A_1^{D_1} A_2^{D_1} \left[A_1^{D_2} F_{\mathrm{pro}}(x_F) + A_2^{D_2} F_{\mathrm{tar}}(x_F) \right], \quad (26)$$

with $F_{\mathrm{pro}}(x_F)$ and $F_{\mathrm{tar}}(x_F)$ given by

$$F_{\mathrm{pro/tar}}(x_F) = \frac{1 \pm \tanh(D_3 x_F)}{2}. \quad (27)$$

In the above equations, the kinetic variables x_F and $\sqrt{s}$ refer to the nucleon-nucleon CM frame. We do not claim

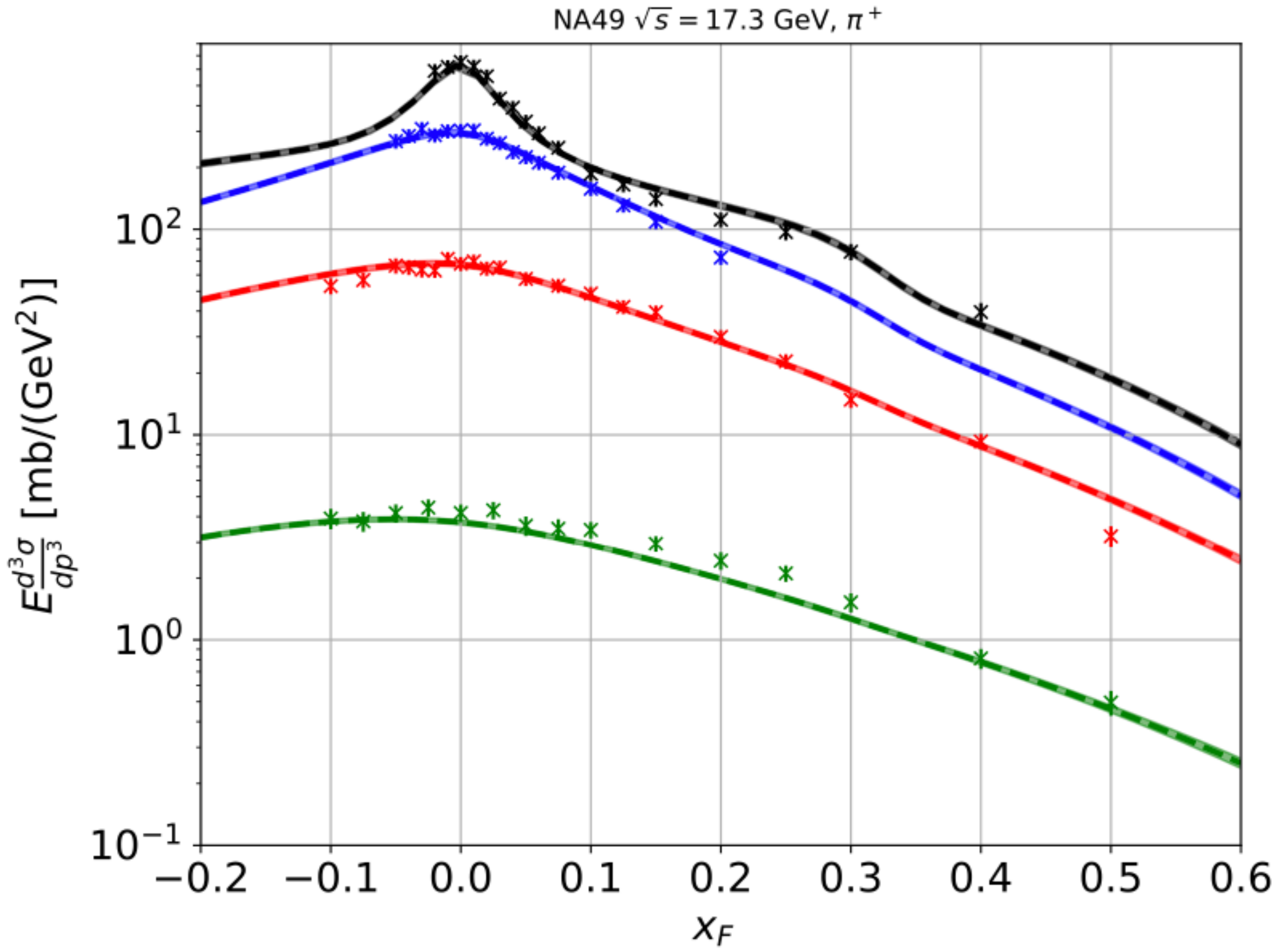

FIG. 11. Results of the fit on the NA49 data [89] invariant cross section for the inclusive π^+ production in p+C collisions. We show the NA49 data together with our fit results as a function of x_F for some representative values of p_T. Shaded bands show the 1σ uncertainty band.

https://arxiv.org/abs/2203.13143

Conclusions about positron CRs

- As for positron CRs the uncertainties on the cross sections are relatively small.
- Other uncertainties, for example regarding the size of the diffusive halo and other propagation parameters, are much more relevant.
- The science case needed for these particles are pion data with Helium.
  - **Probably data already available from the previous run of LHCb for pHe —>pions?**

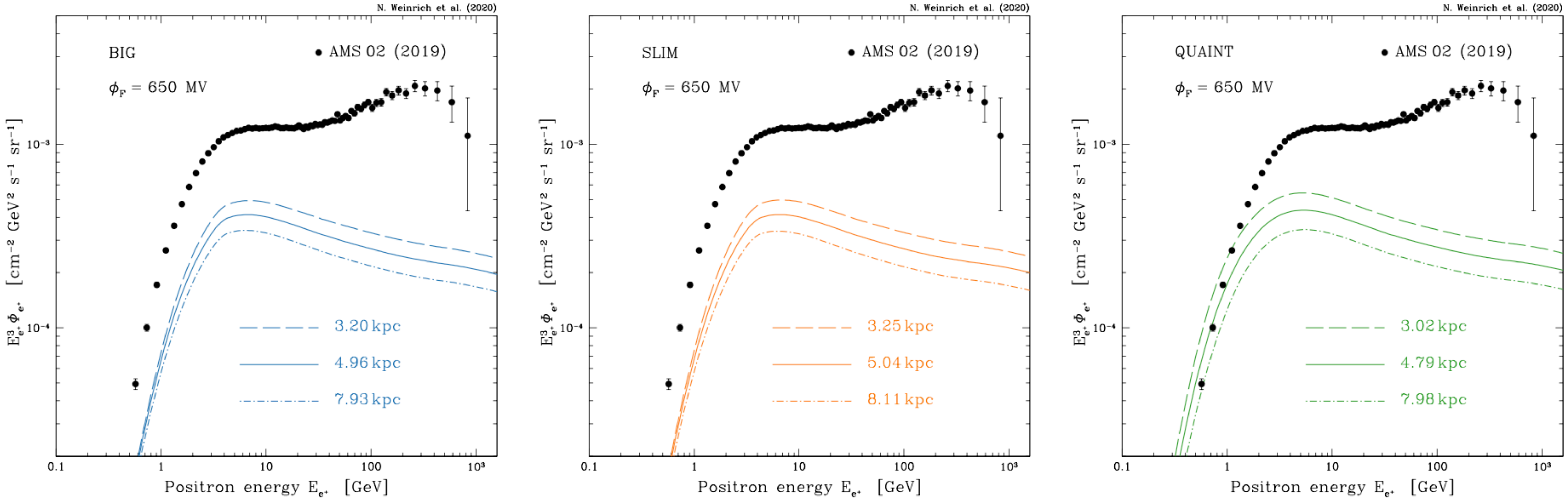

https://arxiv.org/abs/2004.00441

Gamma-ray (and neutrino) production CS

Standard picture for the gamma-ray sky

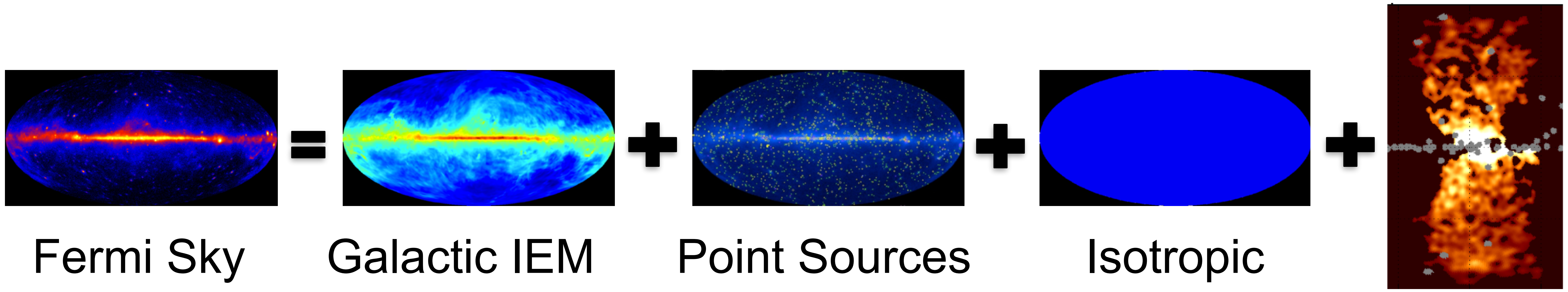

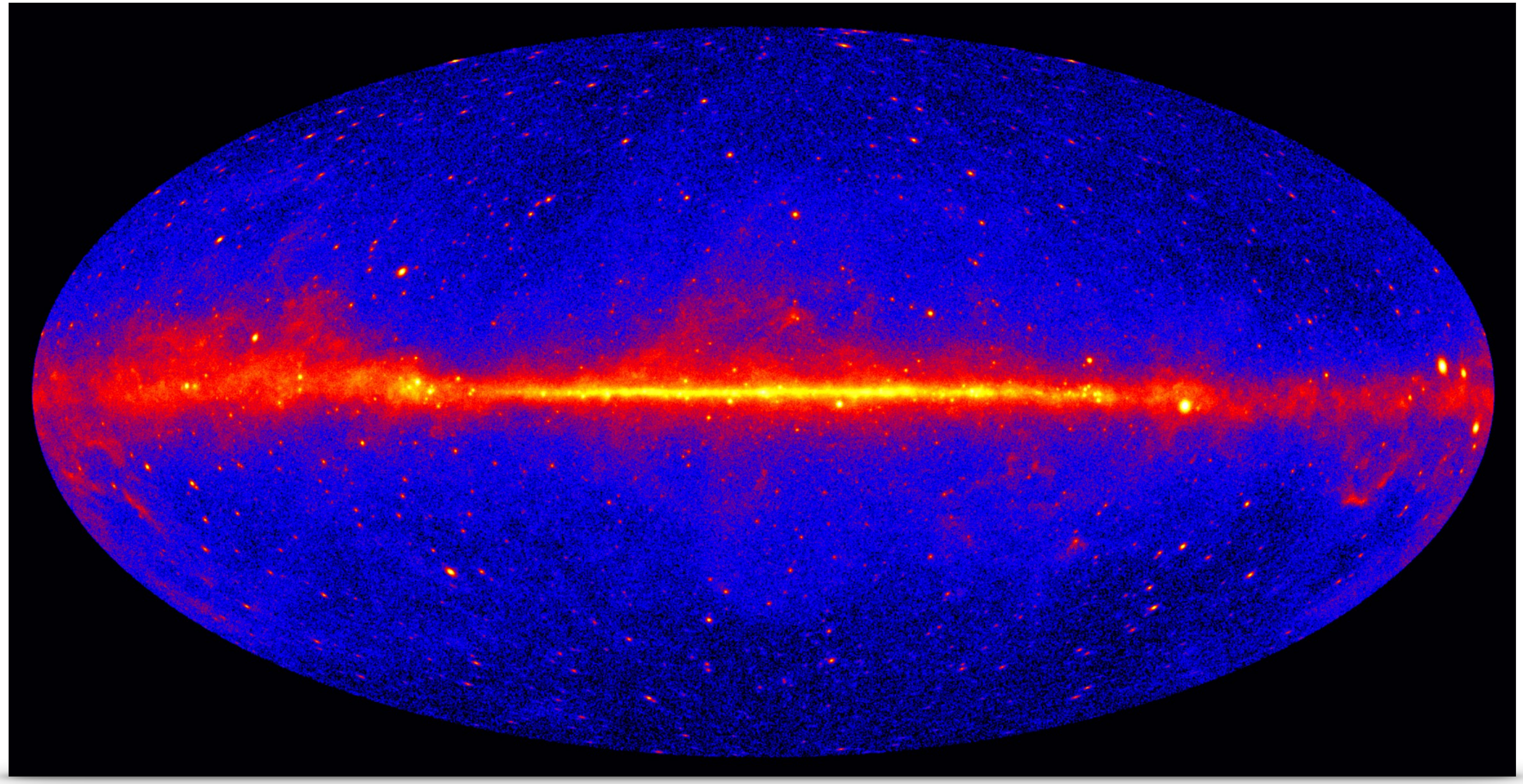

The Galactic interstellar emission

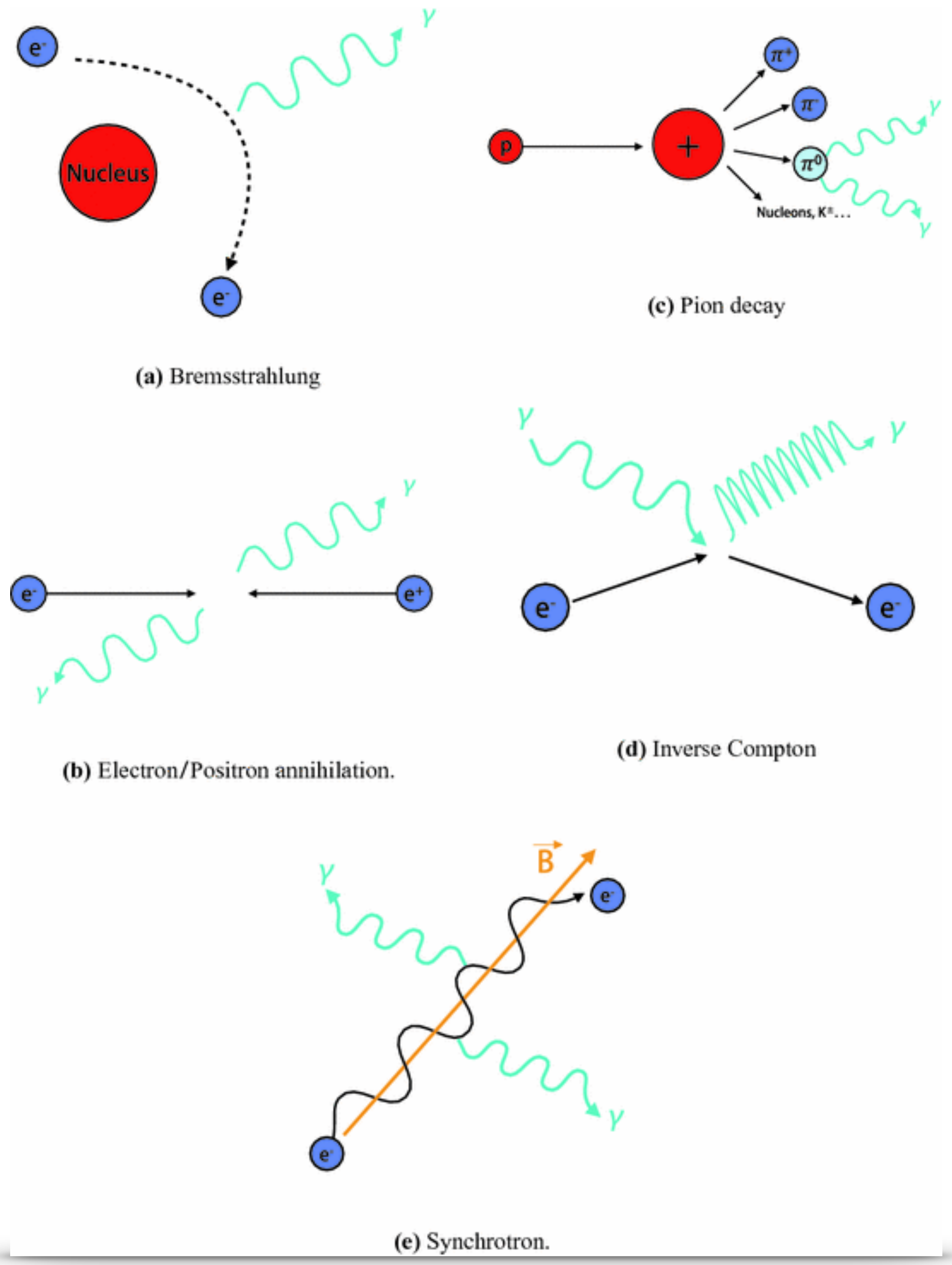

- The models usually used are divided into:
  - Bremsstrahlung, π^0, ICS, isotropic component, Sun/Moon/Loop I and the Fermi bubbles.
- The residuals are roughly at the level of 10-20% of the data depending on the region in the sky.

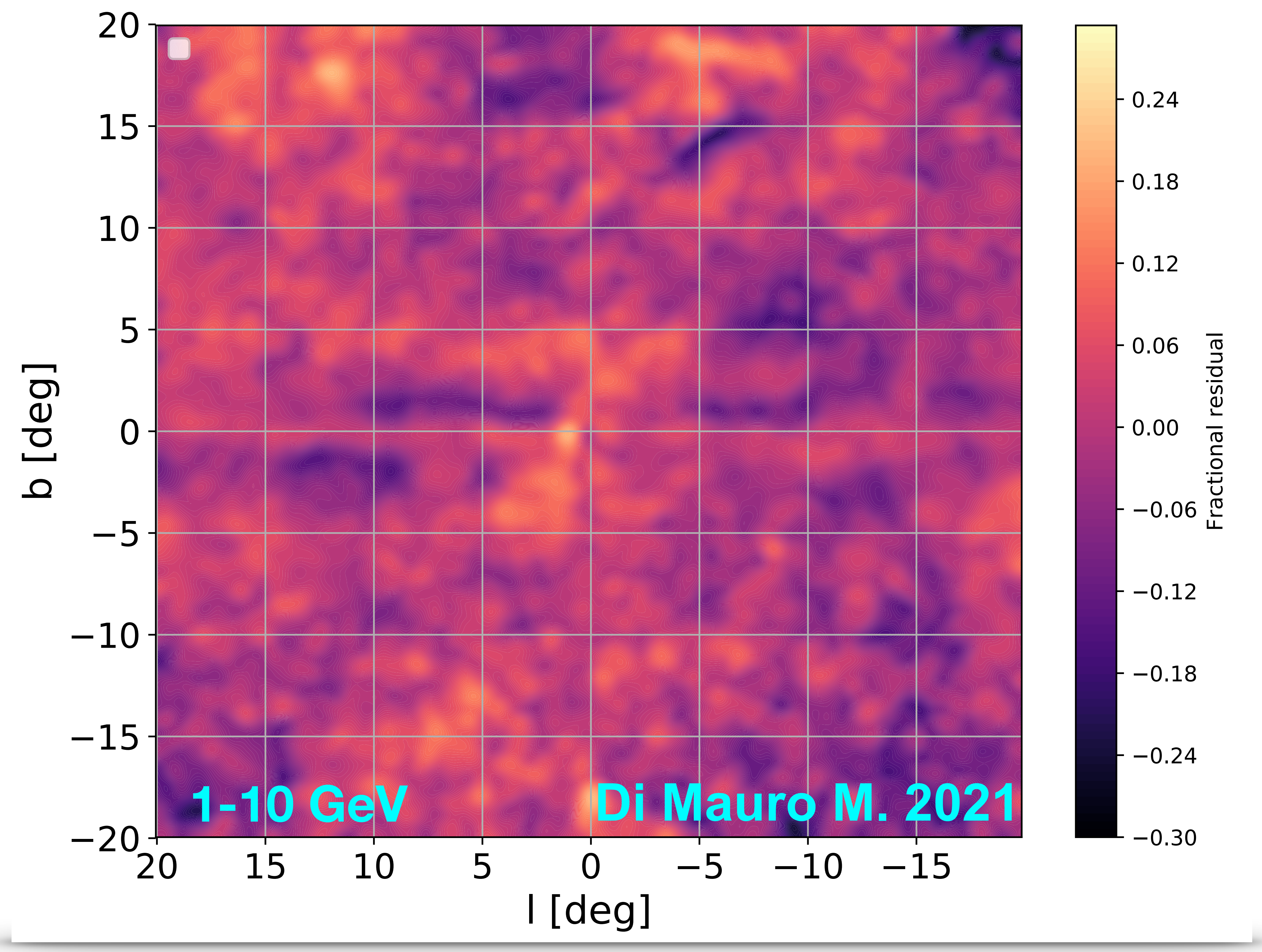

Calculation of gamma-ray flux

$$q(\vec{x}, T_\gamma) = \sum_{i,j} 4\pi \, n_{\mathrm{ISM},j}(\vec{x}) \int dT_i \, \phi_i(\vec{x}, T_i) \frac{d\sigma_{ij}}{dT_\gamma}(T_i, T_\gamma)$$

ISM density
As f function of Galactic position

CR flux
As f function of Galactic position

Pi0 production CS

$$\frac{d\sigma_{ij}}{dT_\gamma}(T_i, T_\gamma) = \int dT_{\pi^0} \, \frac{d\sigma_{ij}}{dT_{\pi^0}}(T_i, T_{\pi^0}) \; P(T_{\pi^0}, T_\gamma)$$

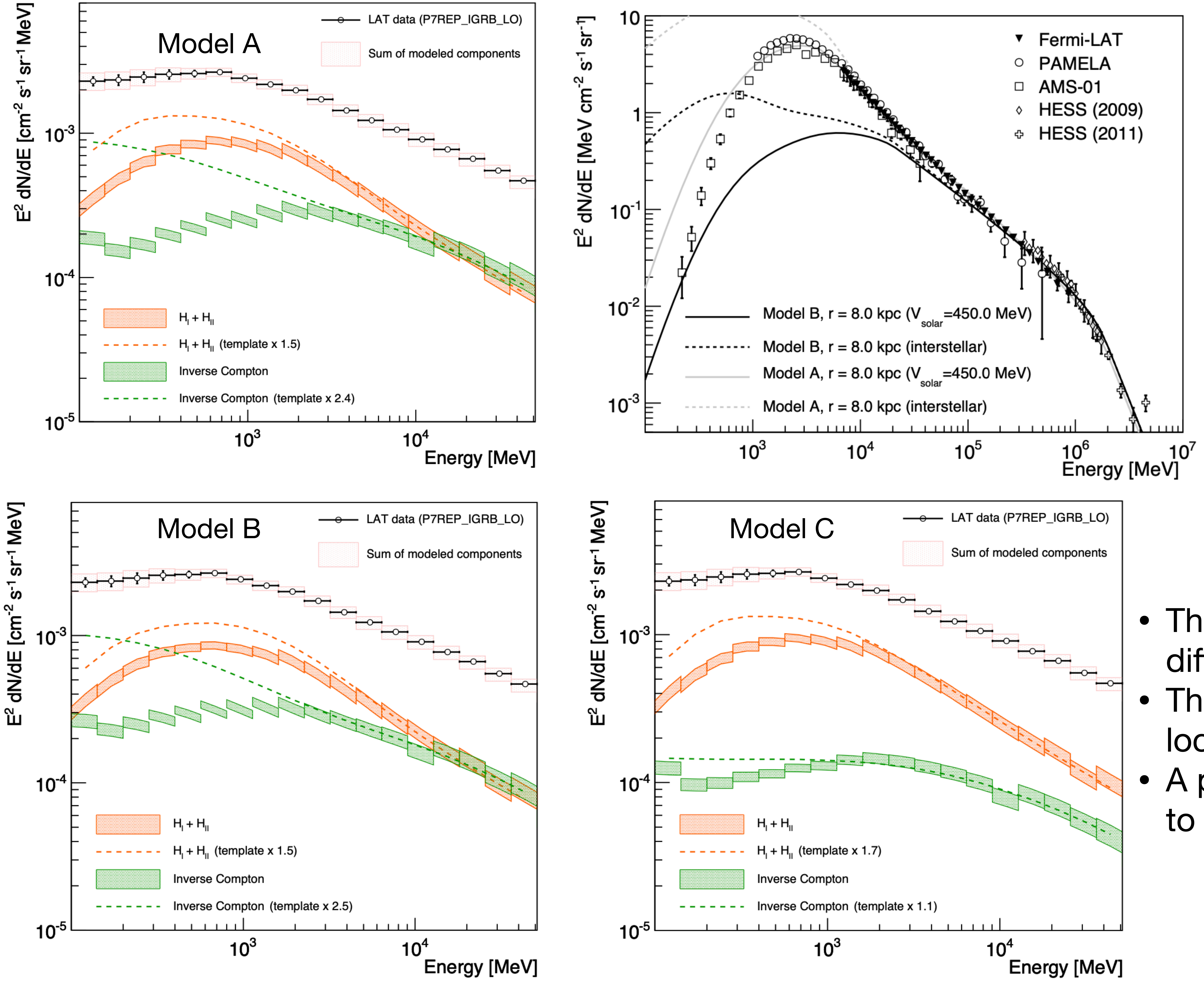

- The initial and fitted models are very different
- The models usually do not fit well the local CR fluxes.
- A part of this uncertainties is surely due to pi0 production cross sections

State of the art for the pi0 cs

- Current systematics on the CS are at the levels of 30-40%.
- Most of current analysis are based on Kamae (Pythia 6)

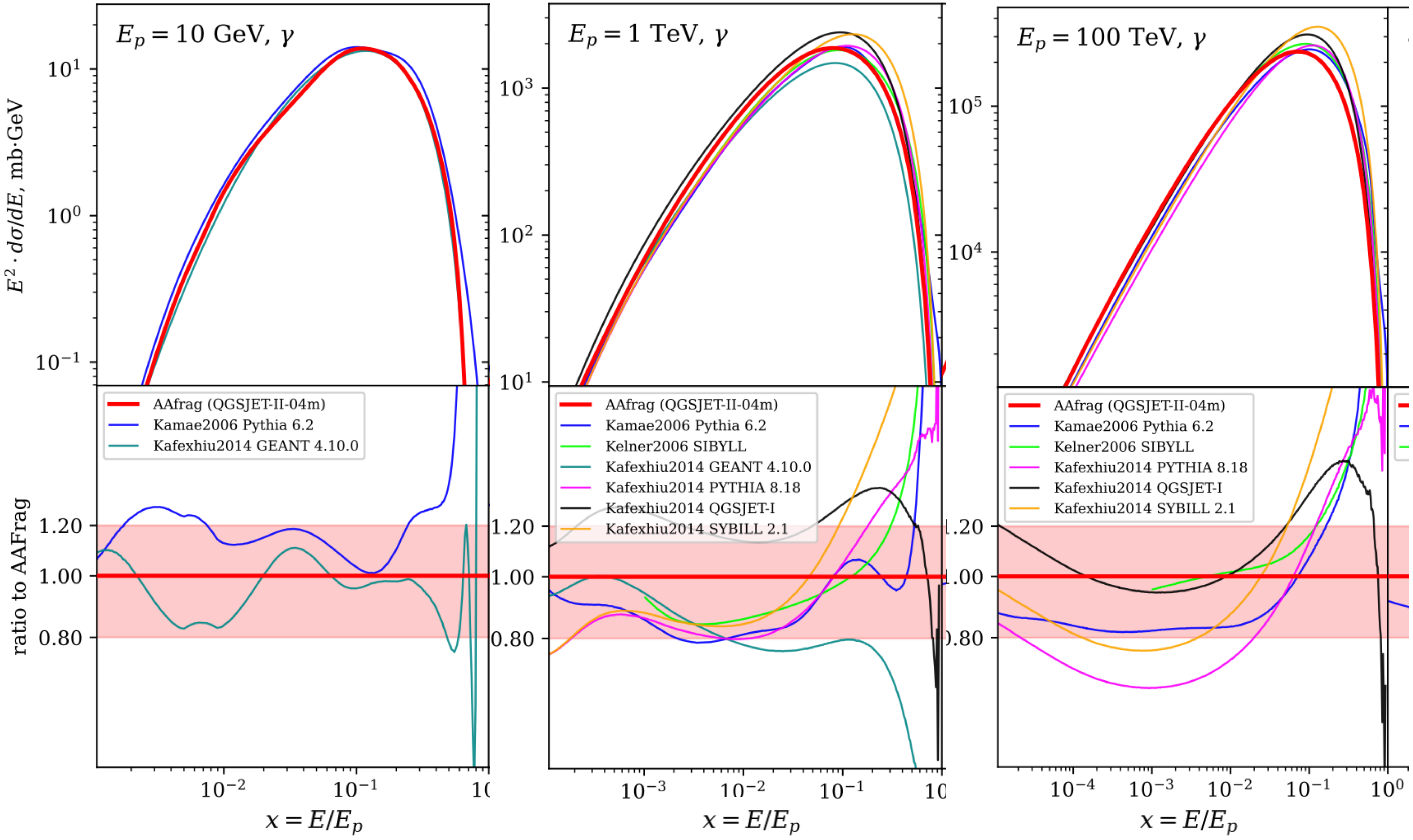

https://arxiv.org/pdf/2110.00496.pdf

Theoretical uncertainties in the flux

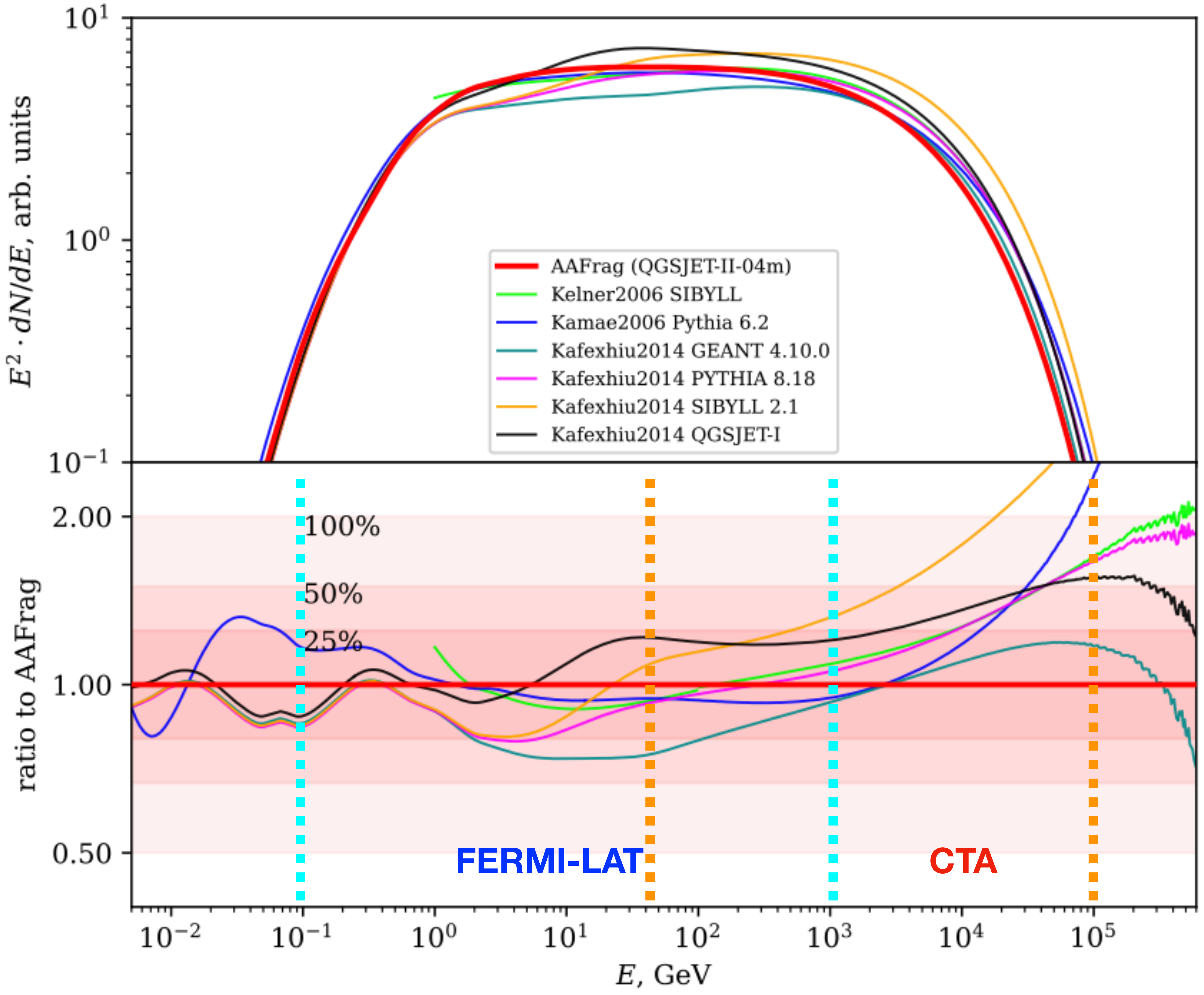

$$I_a(E) = \int_0^\infty \mathrm{d}l\, n_{\mathrm{gas}} \int_E^\infty \mathrm{d}E' \, \frac{\mathrm{d}\sigma_a}{\mathrm{d}E}(E', E) I_p(E'),$$

The systematics on the flux are at the level of 25-50%. In the CTA range could be even larger

https://arxiv.org/pdf/2110.00496.pdf

Science case

- Data for the double differential cross sections are not available.
  - The only available data are for the multiplicity of pi0 and cross section data at mid-rapidity (ALICE and PHENIX).
- We would need data for sqrt(s) between 10-100 GeV (incoming proton energy should be around 50-10000 GeV).
- A better model for the CS is very important for CTA science.

https://arxiv.org/pdf/2110.00496.pdf

Neutrinos

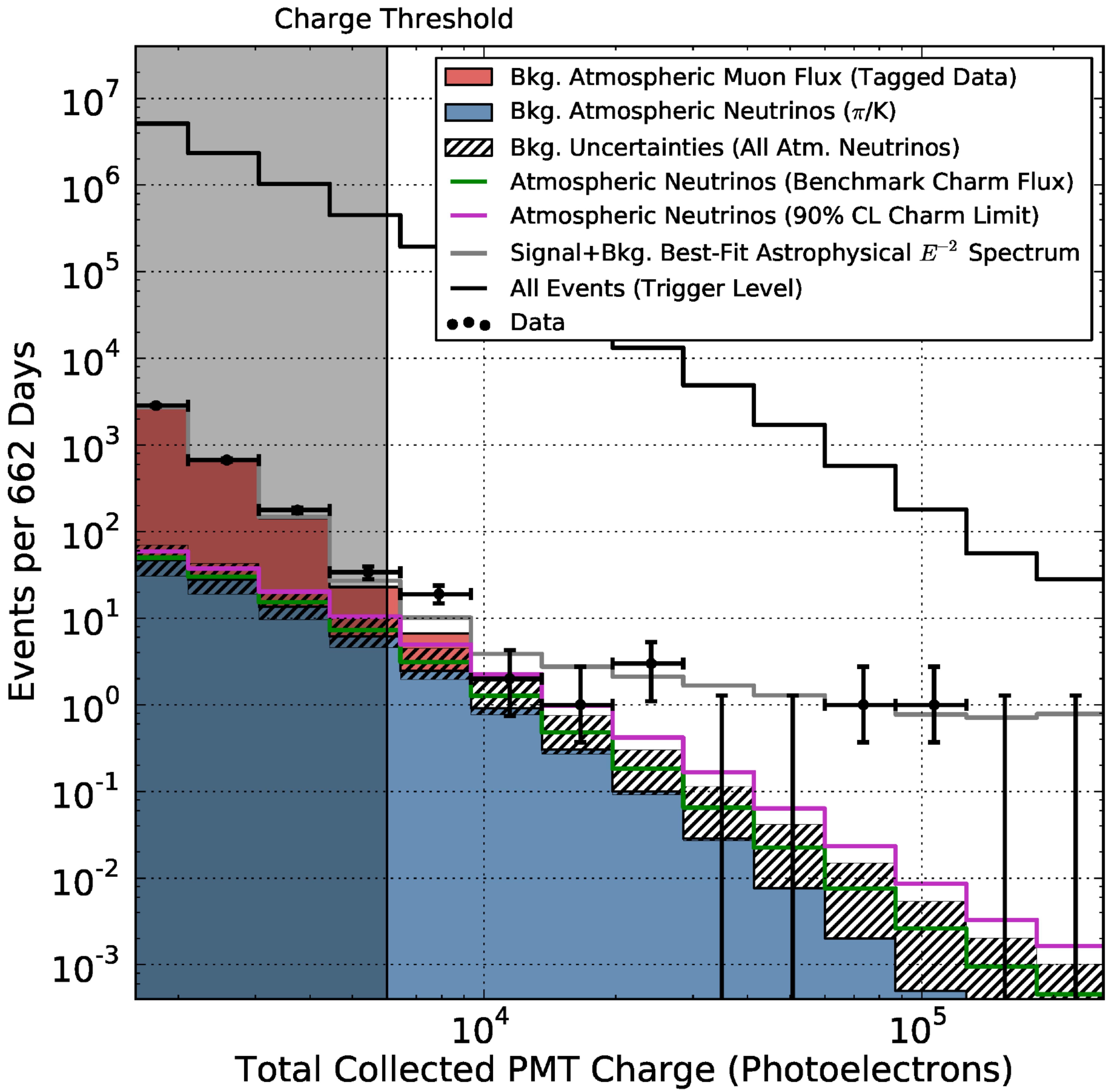

https://icecube.wisc.edu/gallery/astrophysical-neutrino-flux-with-starting-track-events/

Backup slides

MIN/MED/MAX

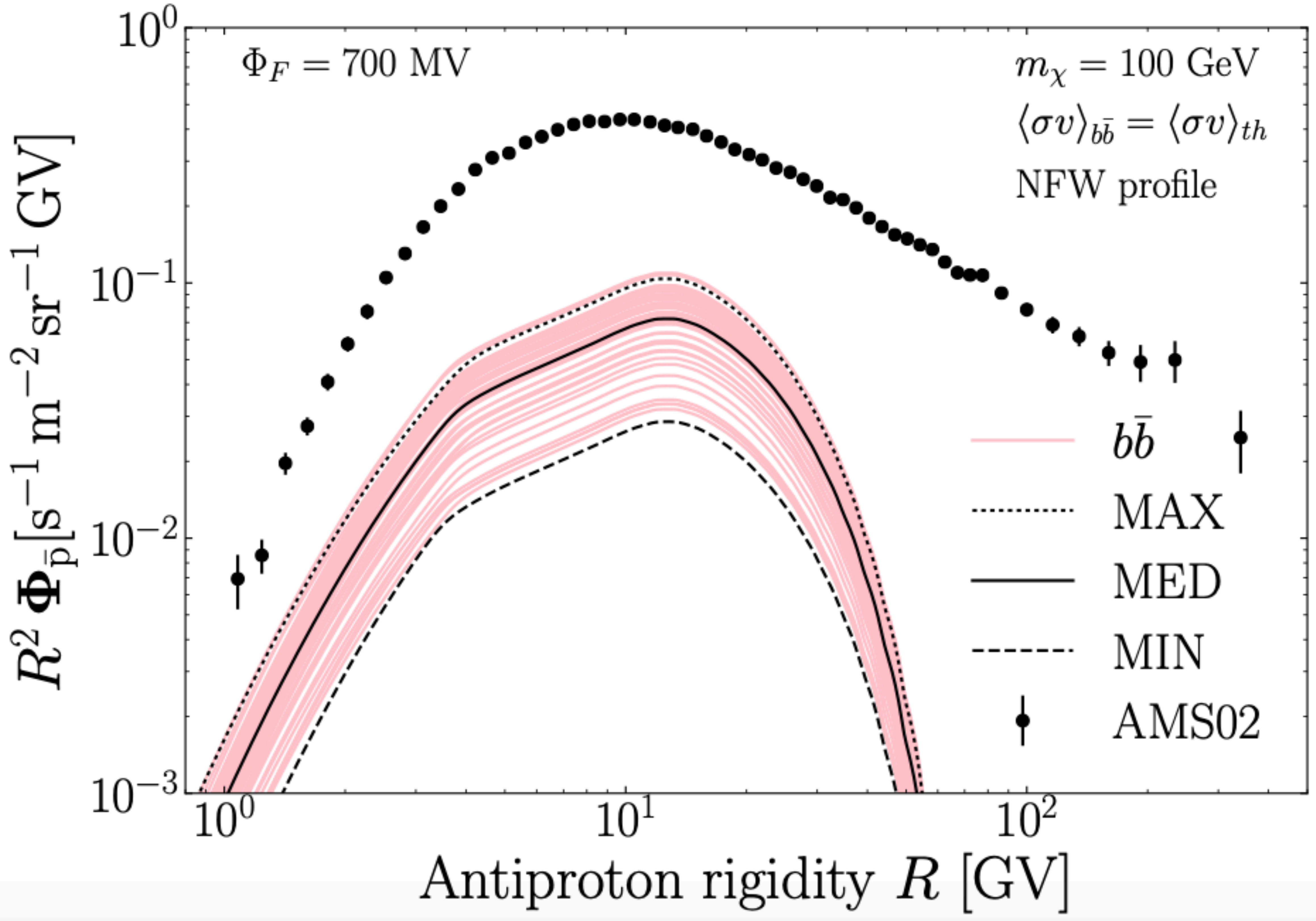

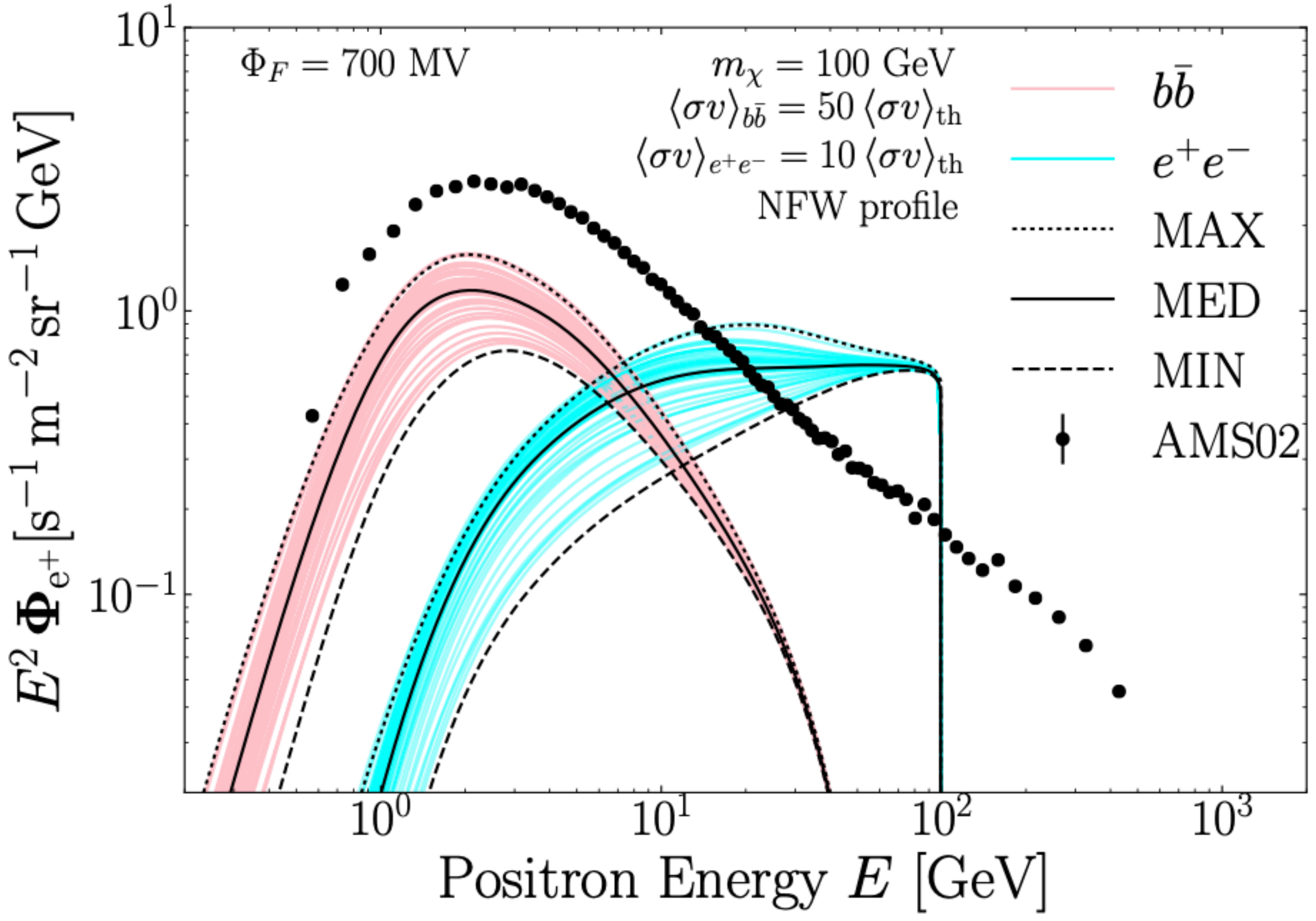

https://arxiv.org/pdf/2103.04108.pdf

Dark Matter searches

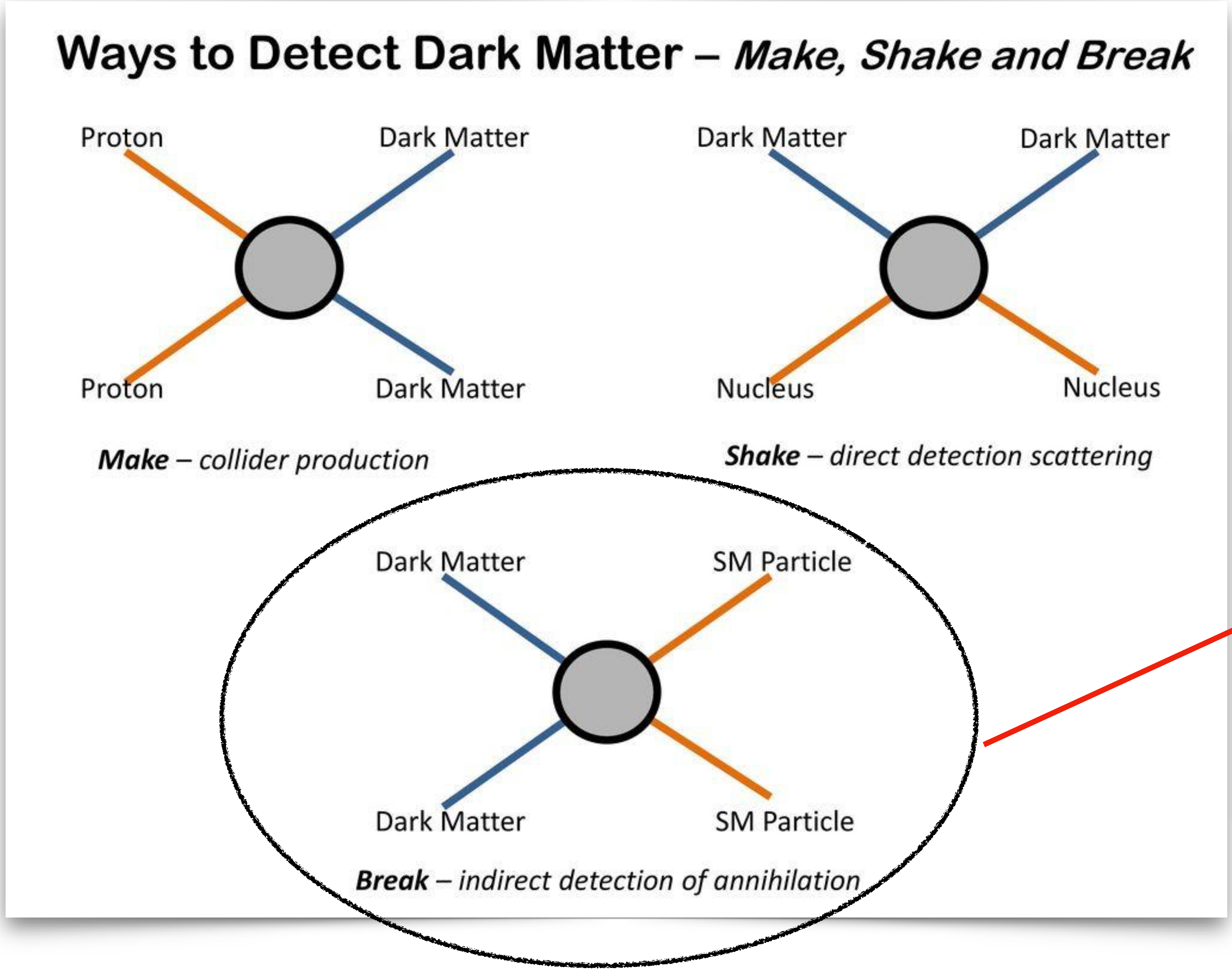

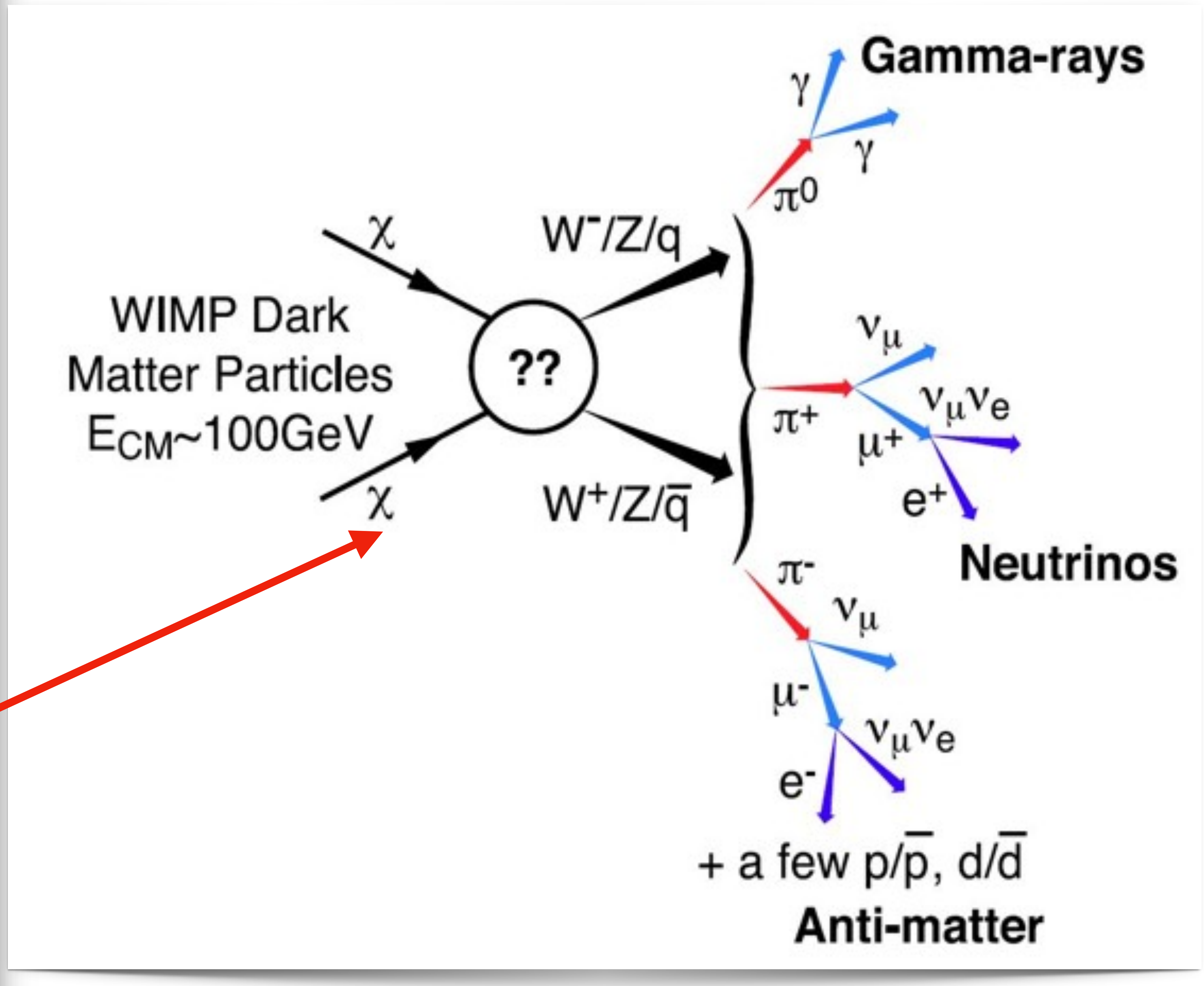

Cosmic-ray particles

- Among all cosmic rays, secondaries are the most interesting for DM searches.
- In particular antiprotons, positrons, gamma rays and neutrinos are the most studied.
- Antinuclei are also considered because the DM production should exceed the secondary one at low energy.

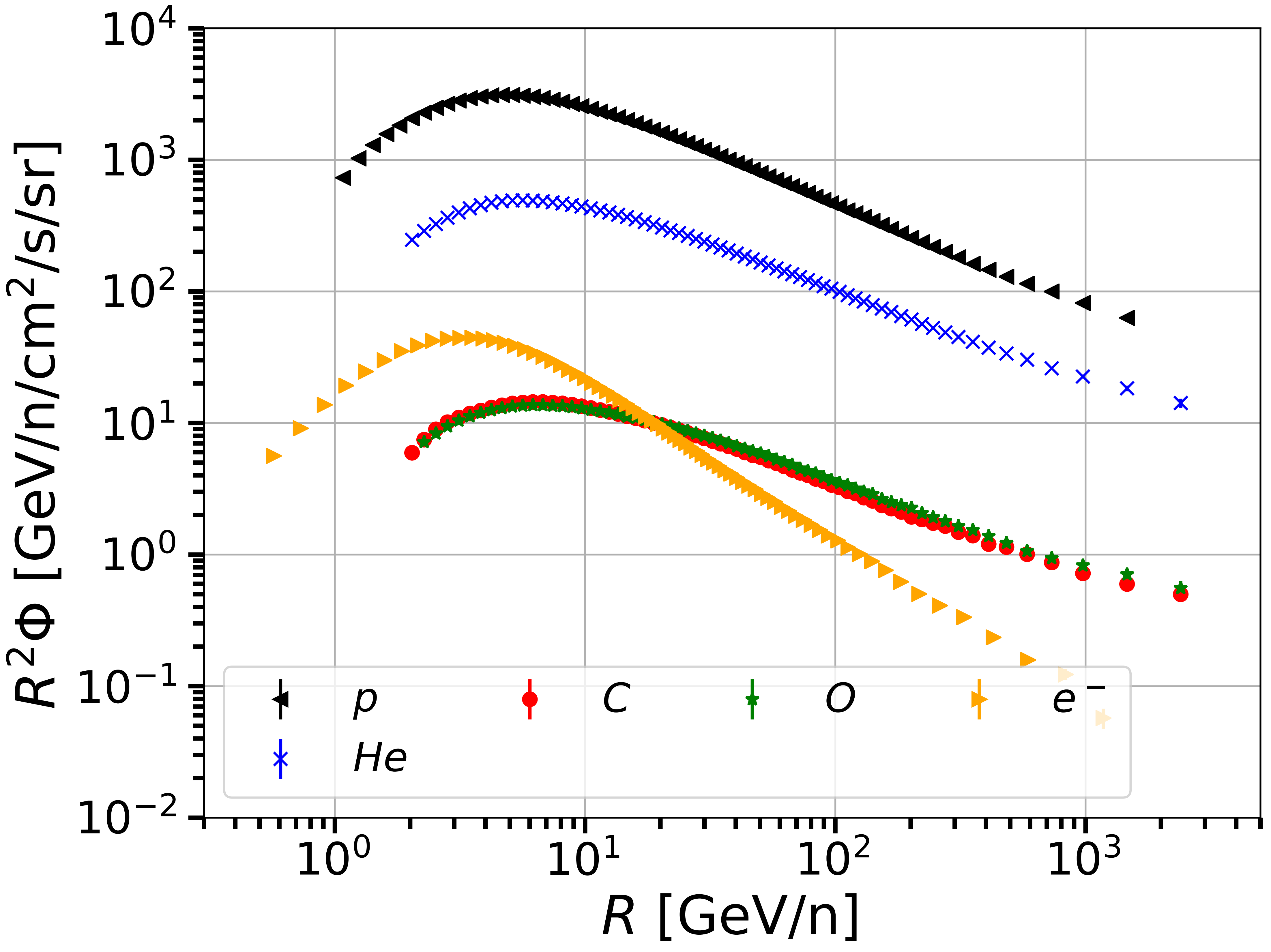

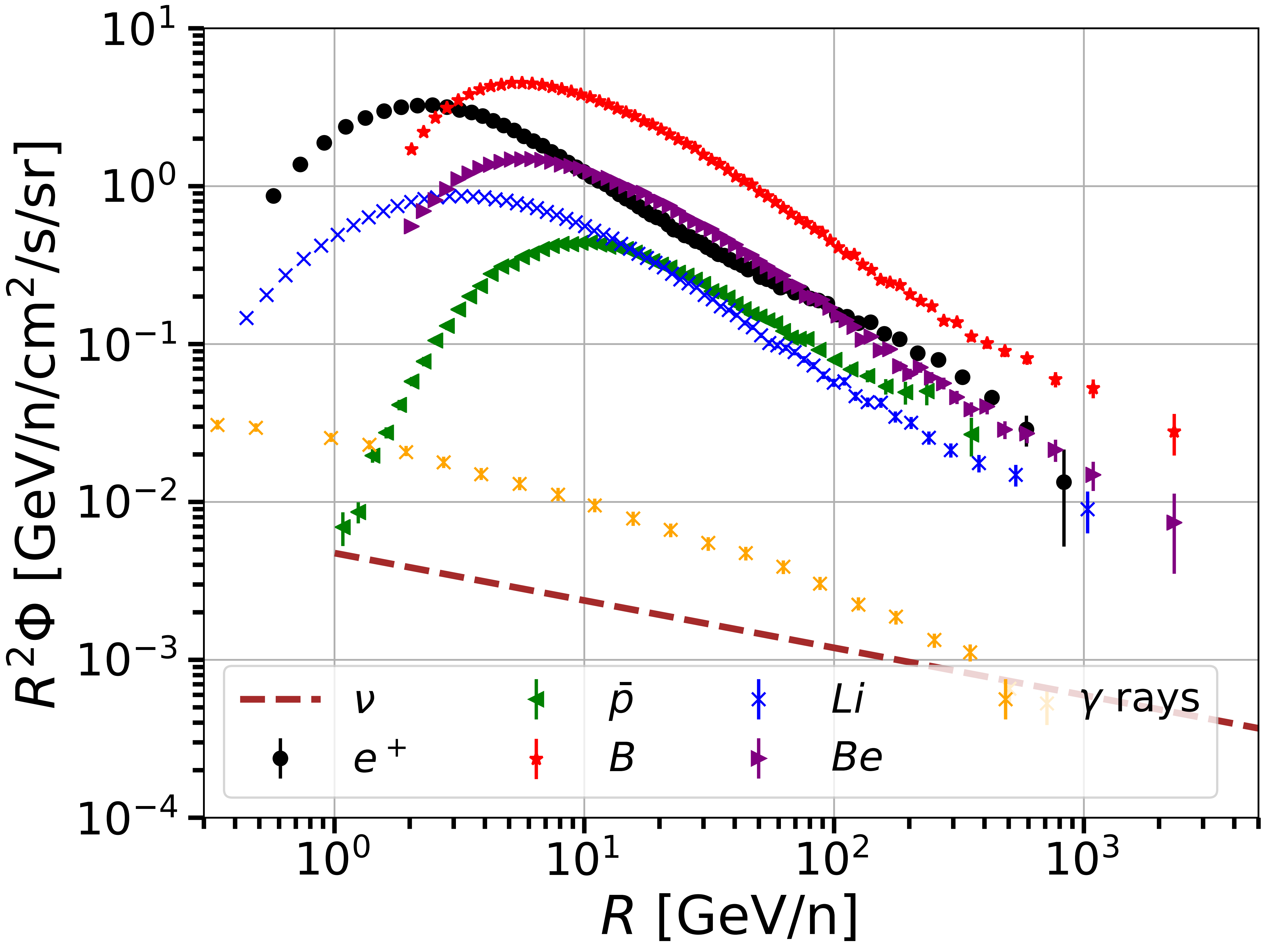

Possible excesses in cosmic-ray data

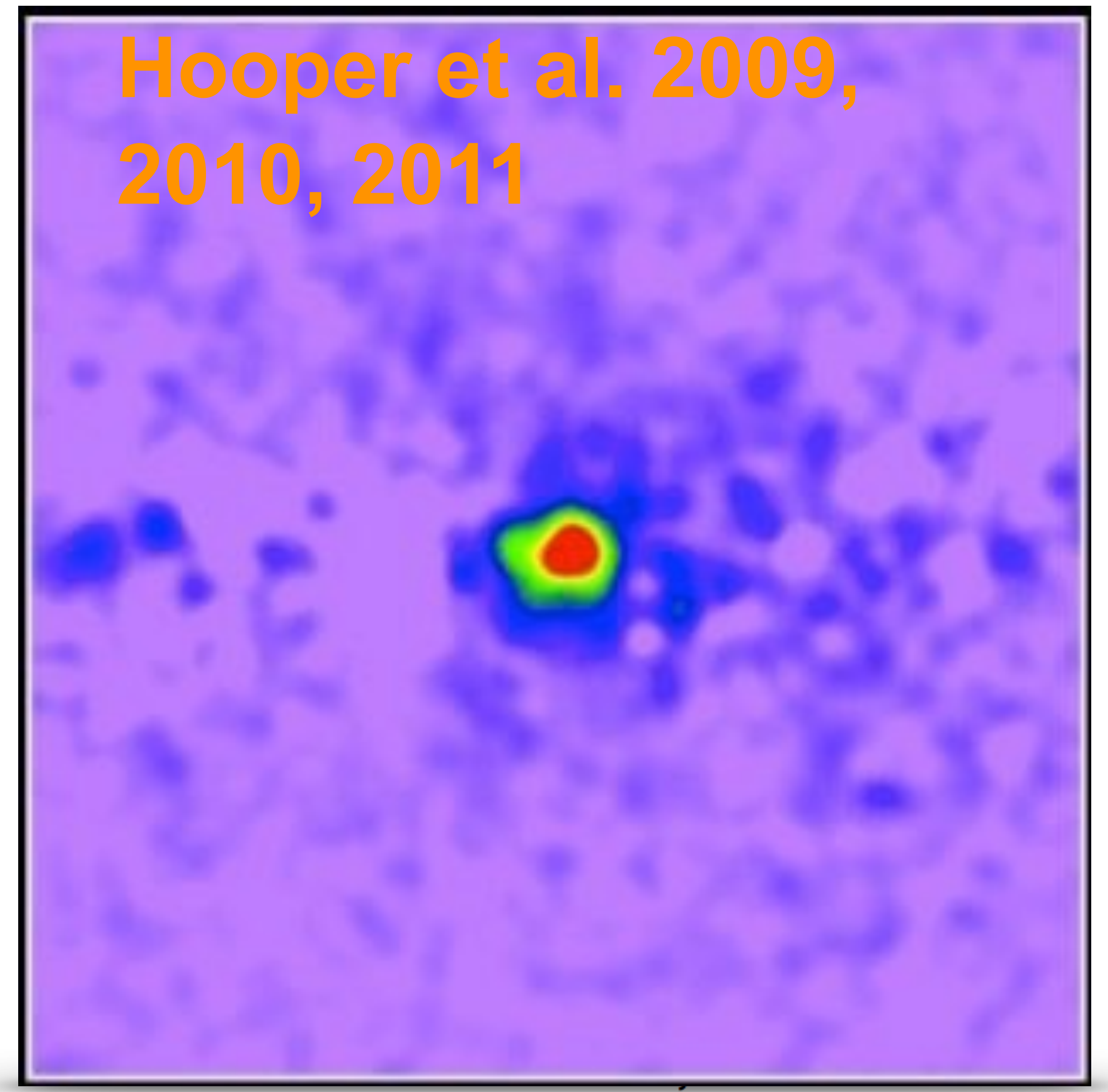

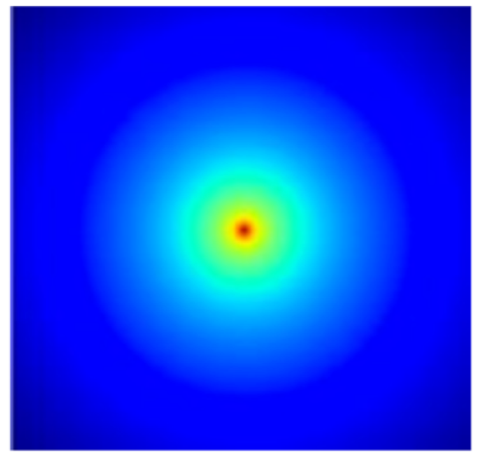

The GeV Galactic center excess

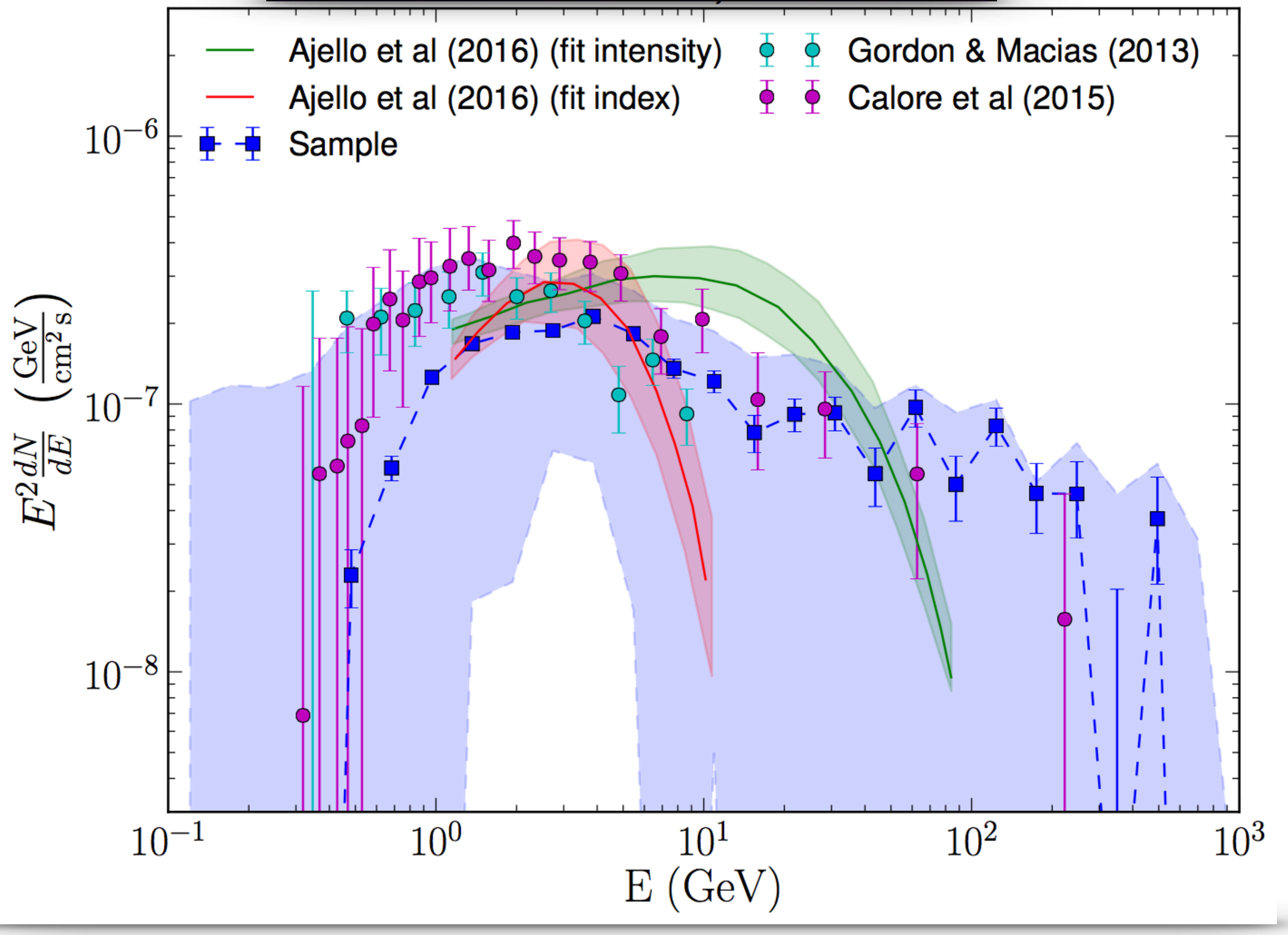

The AMS-02 antiproton excess

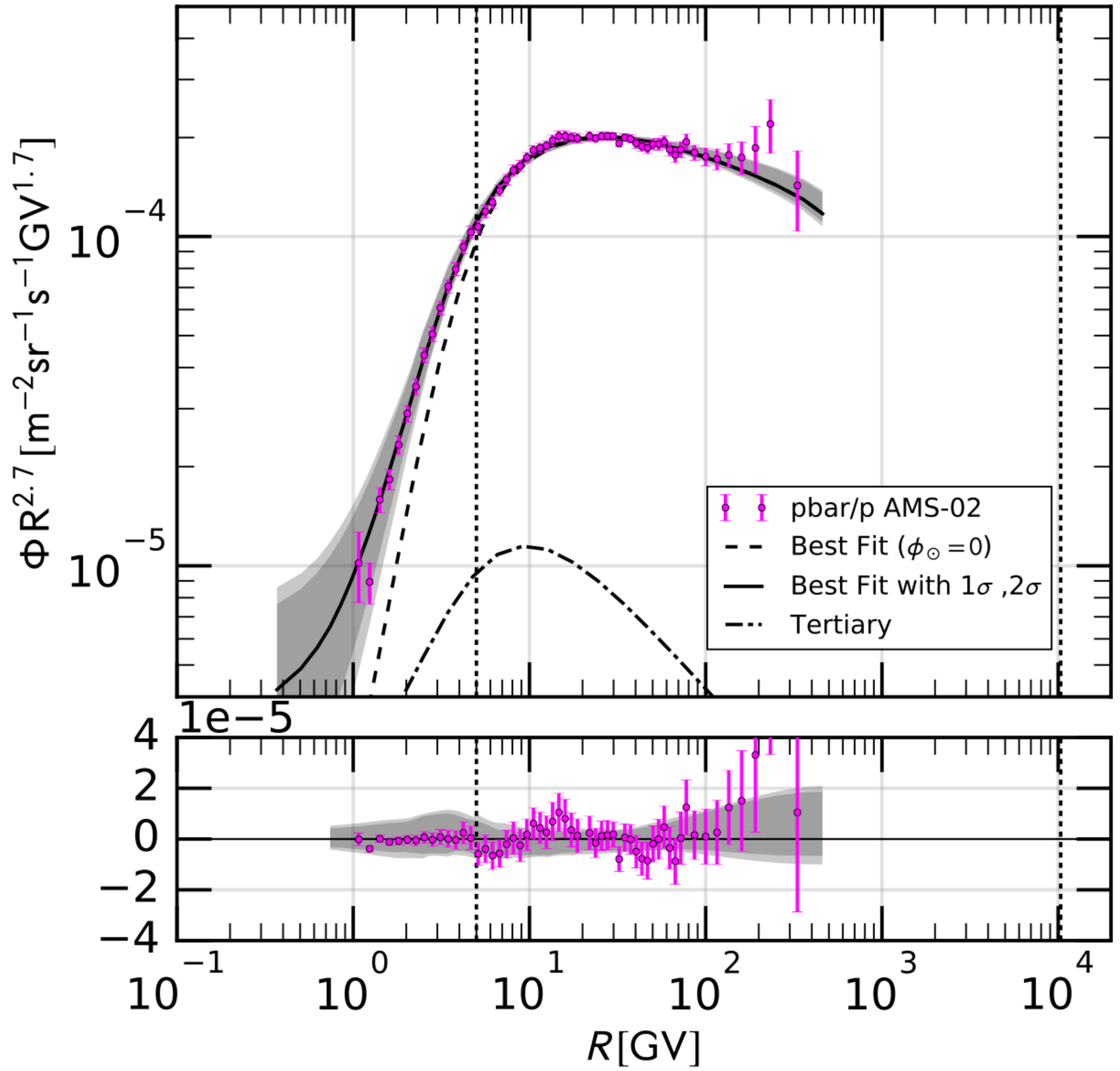

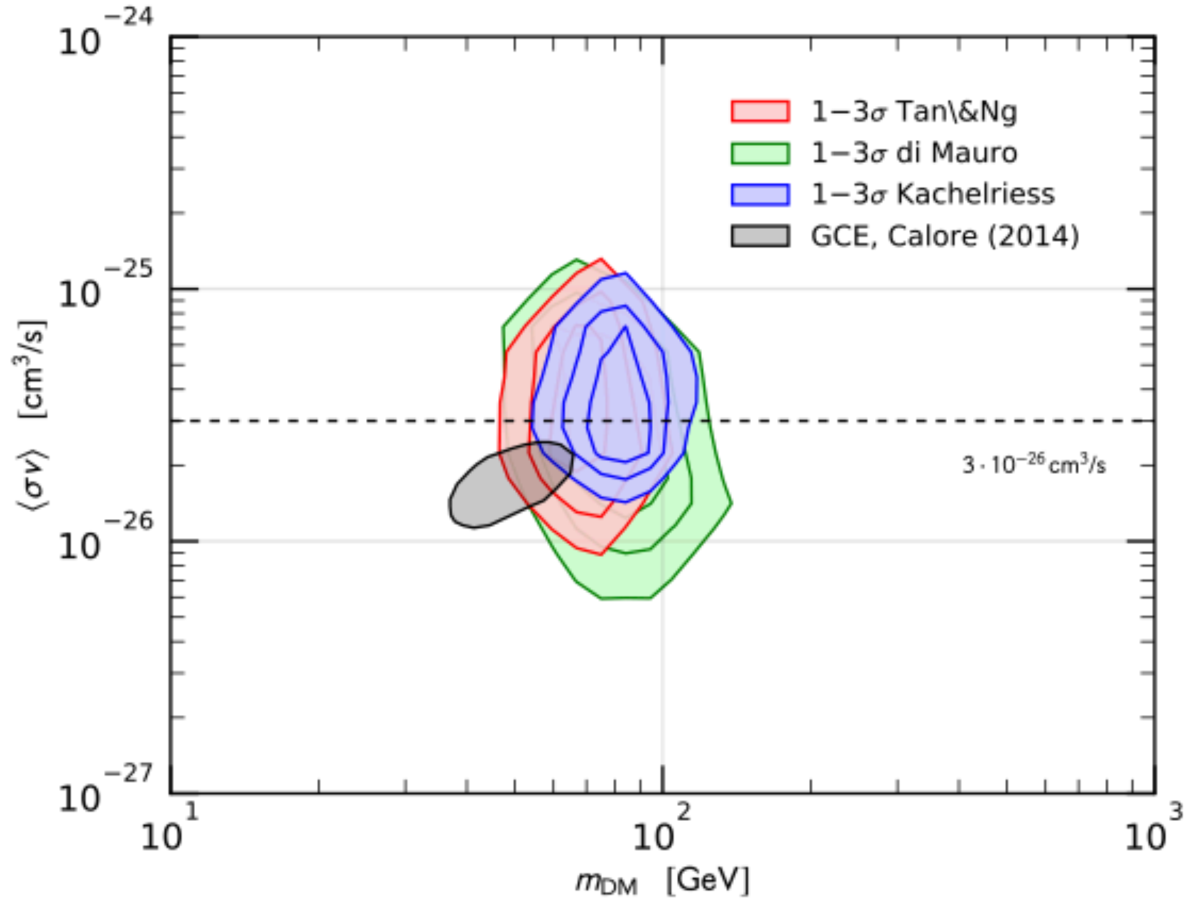

The two excesses can be both a signal from DM…

Cross section are a limiting factor

Secondary antiprotons

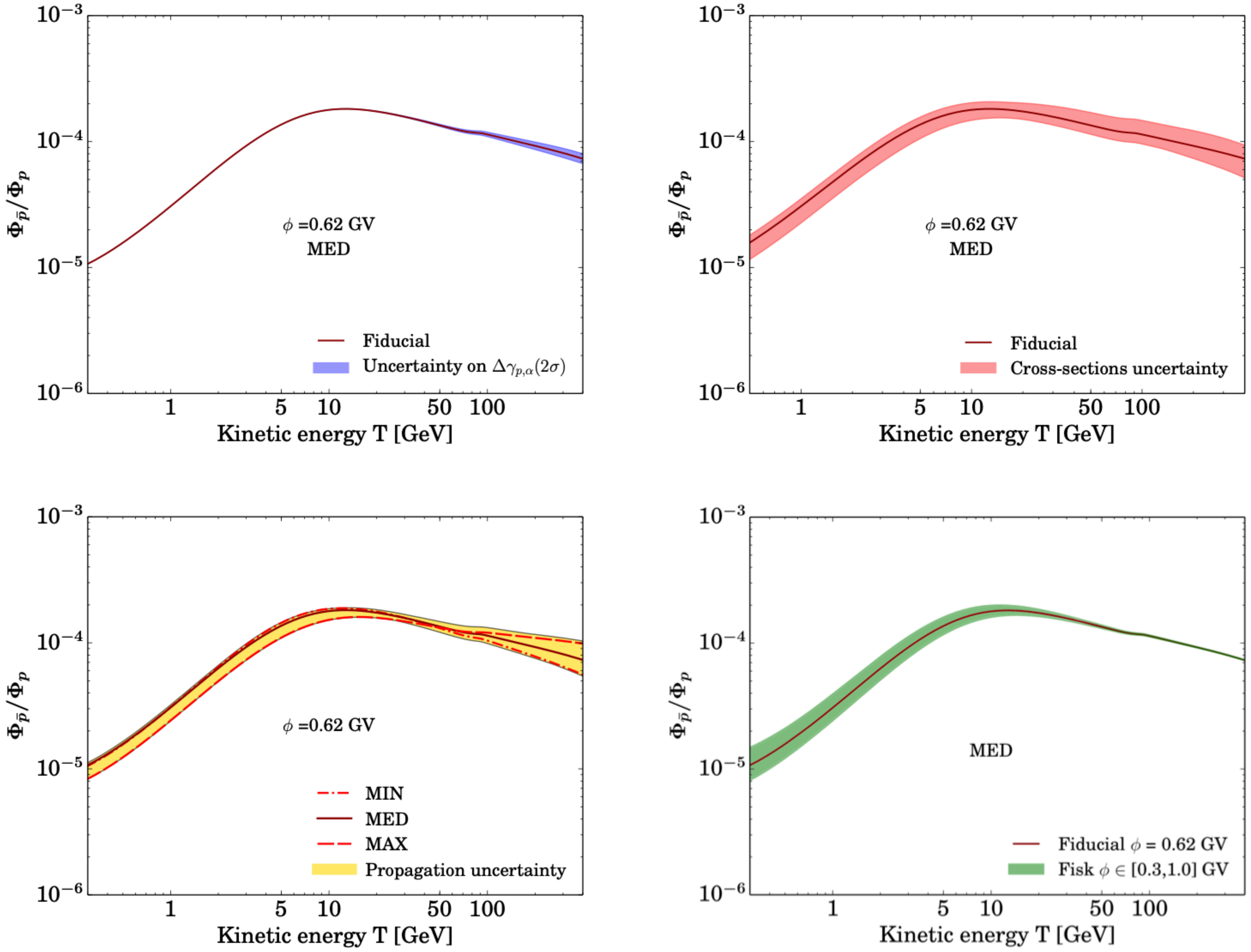

GCE flux

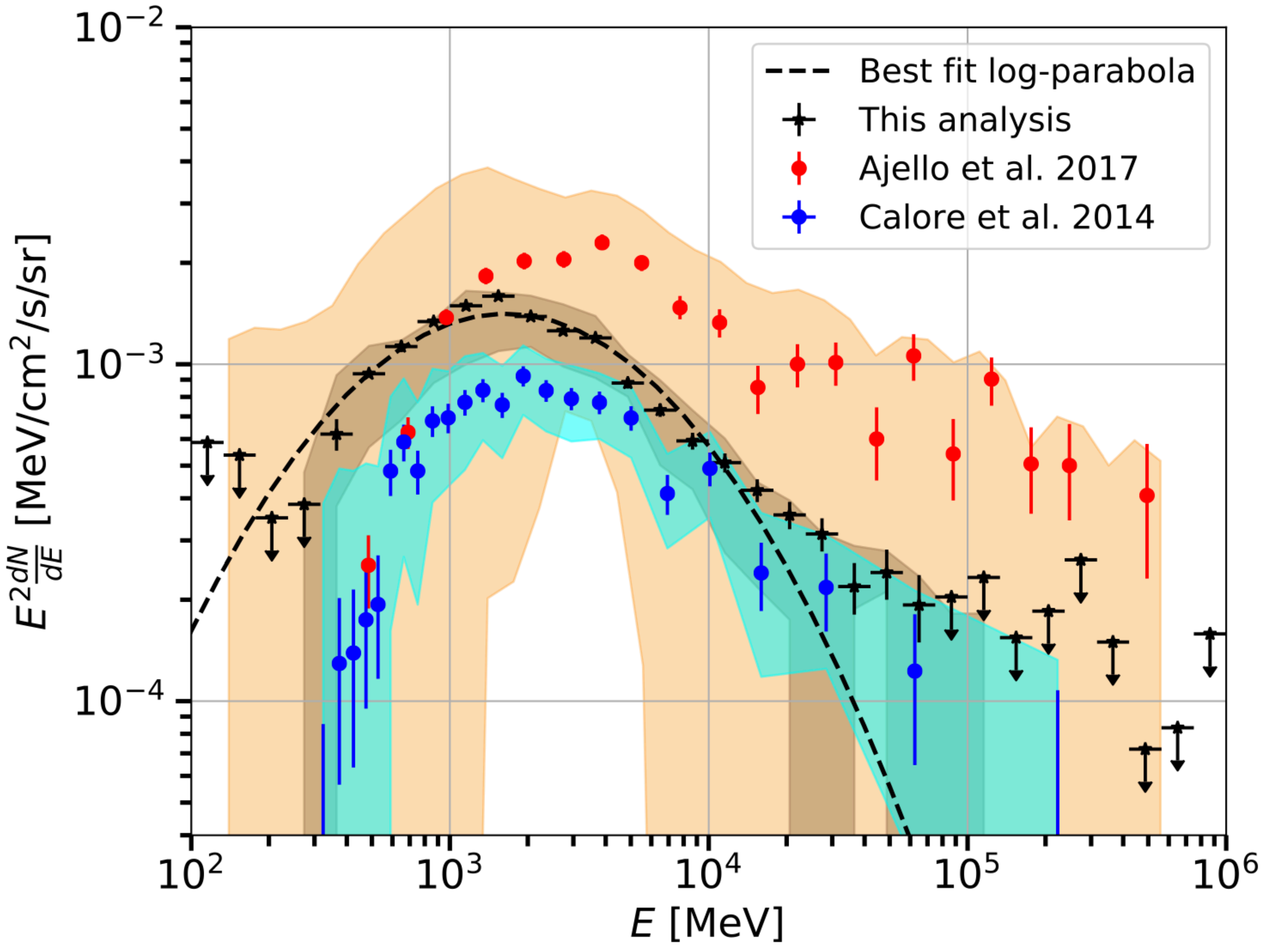

https://arxiv.org/pdf/1504.04276.pdf

https://arxiv.org/pdf/2101.04694.pdf

Nuclear Cross sections and propagation

$$\nabla \cdot (\vec{J}_i - \vec{v}_w N_i) + \frac{\partial}{\partial p}\left[p^2 D_{pp}\frac{\partial}{\partial p}\left(\frac{N_i}{p^2}\right)\right] - \frac{\partial}{\partial p}\left[\dot{p}N_i - \frac{p}{3}\left(\vec{\nabla}\cdot\vec{v}_w\right)N_i\right] = Q_{\rm source} - \frac{N_i}{\tau_i^{\rm f}} + \sum_j \Gamma^{\rm s}_{j\to i}(N_j) - \frac{N_i}{\tau_i^{\rm r}} + \sum_j \frac{N_j}{\tau^{\rm r}_{j\to i}}$$

The fragmentation timescale, $\tau_i^{\rm f}$, is associated with the total inelastic scattering of a nucleus i with the interstellar gas targets, while $\Gamma^{\rm s}_{j\to i}$ describes the source term of a secondary nucleus i by spallation of a heavier species j. The summations in equation (2.1) are over all CR species heavier than i.

In their most general form, $\tau_i^{\rm f}$ and $\Gamma^{\rm s}_{j\to i}$ can be defined as:

$$\frac{1}{\tau_i^{\rm f}(T)} = \beta(T) c n_{\rm H}\left[\sigma_{\rm H,i}(T) + f_{\rm He}\,\sigma_{\rm He,i}(T)\right] \tag{2.2}$$

and

$$\Gamma^{\rm s}_{j\to i}(T) = c n_{\rm H}\int dT'\beta(T')N_j(T')\left[\frac{d\sigma_{\rm H,j\to i}}{dT}(T,T') + f_{\rm He}\frac{d\sigma_{\rm He,j\to i}}{dT}(T,T')\right] \tag{2.3}$$

where T' is the kinetic energy per nucleon of the parent particle, $n_{\rm H} = n_{\rm HI} + 2n_{\rm H2} + n_{\rm HII}$ is the interstellar hydrogen density and $f_{\rm He} \equiv n_{\rm He}/n_{\rm H} = 0.11$ is the helium fraction (by number).

https://arxiv.org/pdf/1711.09616.pdf

Most relevant nuclear CS

Reaction $a + b \to c$	Flux impact f_{abc} [%]			σ [mb]	Data
	min	**mean**	max	range	
$\sigma(^{12}\mathrm{C} + \mathrm{H} \to {}^{6}\mathrm{Li})$	11.0	**13.6**	16.0	14.0	✓
$\sigma(^{16}\mathrm{O} + \mathrm{H} \to {}^{6}\mathrm{Li})$	11.0	**13.5**	16.0	13.0	✓
$\sigma(^{12}\mathrm{C} + \mathrm{H} \to {}^{7}\mathrm{Li})$	10.0	**11.9**	14.0	12.6	✓
$\sigma(^{16}\mathrm{O} + \mathrm{H} \to {}^{7}\mathrm{Li})$	9.6	**11.3**	13.0	11.2	✓
$\sigma(^{11}\mathrm{B} + \mathrm{H} \to {}^{7}\mathrm{Li})$	3.00	**3.52**	4.00	21.5	✓
$\sigma(^{13}\mathrm{C} + \mathrm{H} \to {}^{7}\mathrm{Li})$	2.00	**2.39**	2.80	22.1	
$\sigma(^{16}\mathrm{O} + \mathrm{He} \to {}^{6}\mathrm{Li})$	2.00	**2.38**	2.80	20.6	
$\sigma(^{7}\mathrm{Li} + \mathrm{H} \to {}^{6}\mathrm{Li})$	2.30	**2.35**	2.40	31.5	✓
$\sigma(^{12}\mathrm{C} + \mathrm{He} \to {}^{6}\mathrm{Li})$	1.90	**2.33**	2.70	21.6	
$\sigma(^{15}\mathrm{N} + \mathrm{H} \to {}^{7}\mathrm{Li})$	1.90	**2.27**	2.60	18.6	✓
$\sigma(^{12}\mathrm{C} + \mathrm{He} \to {}^{7}\mathrm{Li})$	1.70	**2.04**	2.40	19.4	

Reaction $a + b \to c$	Flux impact f_{abc} [%]			σ [mb]	Data
	min	**mean**	max	range	
$\sigma(^{12}\mathrm{C} + \mathrm{H} \to {}^{11}\mathrm{B})$	18.0	**18.1**	19.0	30.0	✓
$\boldsymbol{\sigma(^{12}\mathrm{C} + \mathrm{H} \to {}^{11}\mathrm{C})}$	16.0	**16.2**	17.0	26.9	✓
$\sigma(^{16}\mathrm{O} + \mathrm{H} \to {}^{11}\mathrm{B})$	11.3	**11.8**	12.0	18.2	✓
$\sigma(^{12}\mathrm{C} + \mathrm{H} \to {}^{10}\mathrm{B})$	7.20	**7.41**	7.60	12.3	✓
$\sigma(^{16}\mathrm{O} + \mathrm{H} \to {}^{10}\mathrm{B})$	6.82	**7.03**	7.21	10.9	✓
$\boldsymbol{\sigma(^{16}\mathrm{O} + \mathrm{H} \to {}^{11}\mathrm{C})}$	5.67	**5.89**	6.00	9.1	
$\sigma(^{11}\mathrm{B} + \mathrm{H} \to {}^{10}\mathrm{B})$	4.00	**4.07**	4.20	38.9	✓
$\sigma(^{12}\mathrm{C} + \mathrm{He} \to {}^{11}\mathrm{B})$	2.50	**2.59**	2.70	38.6	
$\boldsymbol{\sigma(^{12}\mathrm{C} + \mathrm{He} \to {}^{11}\mathrm{C})}$	2.10	**2.14**	2.20	32.0	
$\sigma(^{15}\mathrm{N} + \mathrm{H} \to {}^{11}\mathrm{B})$	2.00	**2.03**	2.10	26.1	✓

Reaction $a + b \to c$	Flux impact f_{abc} [%]			σ [mb]	Data
	min	**mean**	max	range	
$\sigma(^{16}\mathrm{O} + \mathrm{H} \to {}^{7}\mathrm{Be})$	17.0	**17.6**	19.0	10.0	✓
$\sigma(^{12}\mathrm{C} + \mathrm{H} \to {}^{7}\mathrm{Be})$	15.0	**15.9**	17.0	9.7	✓
$\sigma(^{12}\mathrm{C} + \mathrm{H} \to {}^{9}\mathrm{Be})$	8.80	**9.27**	9.80	6.8	✓
$\sigma(^{16}\mathrm{O} + \mathrm{H} \to {}^{9}\mathrm{Be})$	5.00	**5.34**	5.60	3.7	✓
$\sigma(^{16}\mathrm{O} + \mathrm{He} \to {}^{7}\mathrm{Be})$	2.70	**2.87**	3.00	14.7	
$\sigma(^{28}\mathrm{Si} + \mathrm{H} \to {}^{7}\mathrm{Be})$	2.60	**2.77**	2.90	10.8	
$\sigma(^{24}\mathrm{Mg} + \mathrm{H} \to {}^{7}\mathrm{Be})$	2.50	**2.65**	2.80	10.0	
$\sigma(^{12}\mathrm{C} + \mathrm{He} \to {}^{7}\mathrm{Be})$	2.30	**2.48**	2.60	13.7	
$\sigma(^{11}\mathrm{B} + \mathrm{H} \to {}^{9}\mathrm{Be})$	2.30	**2.36**	2.50	10.0	✓
$\sigma(^{12}\mathrm{C} + \mathrm{H} \to {}^{10}\mathrm{Be})$	2.00	**2.16**	2.30	4.0	✓
$\sigma(^{14}\mathrm{N} + \mathrm{H} \to {}^{7}\mathrm{Be})$	2.00	**2.12**	2.20	10.1	✓

Reaction $a + b \to c$	Flux impact f_{abc} [%]			σ [mb]	Data
	min	**mean**	max	range	
$\sigma(^{16}\mathrm{O} + \mathrm{H} \to {}^{15}\mathrm{N})$	26.0	**26.3**	27.0	34.3	✓
$\boldsymbol{\sigma(^{16}\mathrm{O} + \mathrm{H} \to {}^{15}\mathrm{O})}$	23.0	**23.4**	24.0	30.5	✓
$\sigma(^{16}\mathrm{O} + \mathrm{H} \to {}^{14}\mathrm{N})$	18.0	**20.0**	22.0	[23.0, 29.0]	✓
$\sigma(^{16}\mathrm{O} + \mathrm{He} \to {}^{15}\mathrm{N})$	3.30	**3.34**	3.40	39.3	
$\boldsymbol{\sigma(^{16}\mathrm{O} + \mathrm{He} \to {}^{15}\mathrm{O})}$	2.70	**2.79**	2.90	32.8	
$\sigma(^{16}\mathrm{O} + \mathrm{He} \to {}^{14}\mathrm{N})$	2.30	**2.55**	2.80	[26.0, 33.0]	
$\sigma(^{15}\mathrm{N} + \mathrm{H} \to {}^{14}\mathrm{N})$	2.10	**2.18**	2.20	24.3	✓
$\sigma(^{20}\mathrm{Ne} + \mathrm{H} \to {}^{14}\mathrm{N})$		**2.18**		[23.0, 24.0]	✓
$\sigma(^{20}\mathrm{Ne} + \mathrm{H} \to {}^{15}\mathrm{N})$		**2.09**		[22.0, 23.0]	✓

Nuclear Cross sections

- Cross section data uncertainties are typically at ~ 5 – 10% level for inelastic cross sections, and 15 – 25% level for production cross sections (Genolini et al. 2018).
- However, because the data are sometimes scarce, old, not always consistent with one another, and sometimes even missing for some reactions, several parametrisation of the whole network of reactions exist.

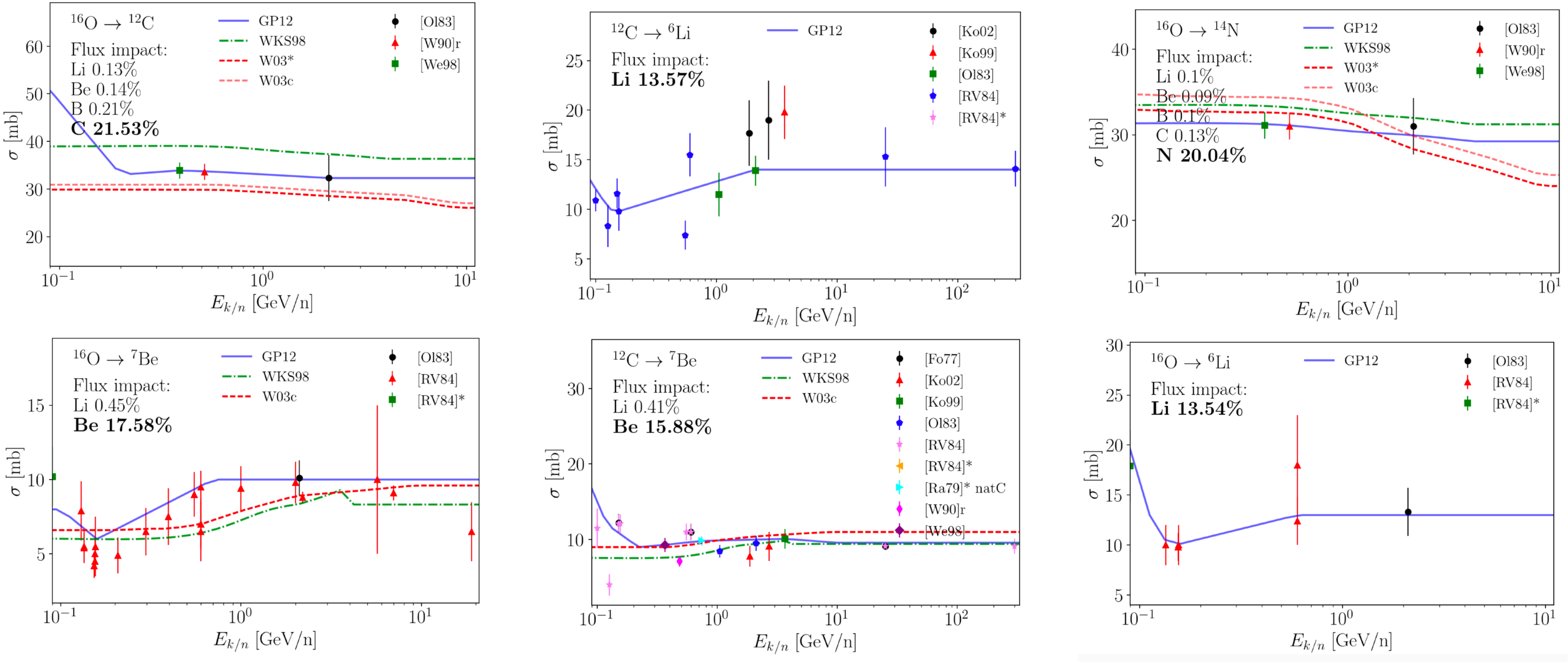

Uncertainties on nuclear CS

Uncertainties on the CS are at the level of 10-25%

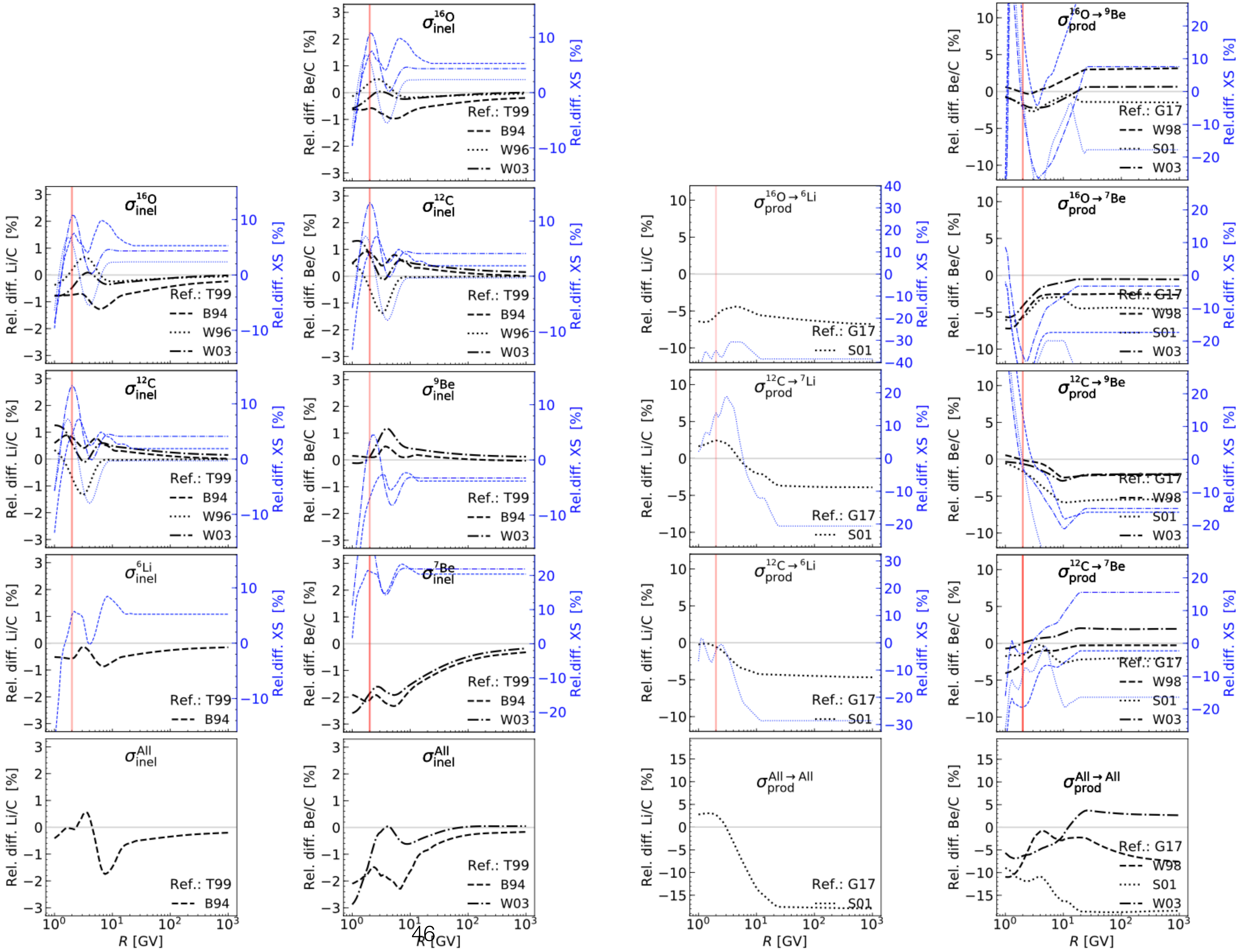

https://arxiv.org/abs/2002.11406

Reaction	Impact $(\frac{\Delta\sigma}{\sigma})^{XS}$ on flux	Norm. $\mu\,|\,\sigma$	Scale $\mu\,|\,\sigma$	Slope $\mu\,|\,\sigma$
	^{3}He			
^{3}He+H	(1.8%)	1.00 | 0.15	1.2 | 0.5	n/a
^{4}He+H	**(5.0%)**	1.00 | 0.10	1.0 | 0.25	n/a
^{16}O+H→^{3}He [5%]	(2.1%)	1.10 | 0.30	n/a	0.10 | 0.10
^{12}C+H→^{3}He [5%]	(1.5%)	1.10 | 0.30	n/a	0.05 | 0.15
^{4}He+H→^{3}He [80%]	**(7.3%)**	1.00 | 0.10	n/a	0.00 | 0.025
	Li			
^{16}O+H	(1.2%)	1.03 | 0.04	0.7 | 0.5	n/a
^{12}C+H	**(1.3%)**	1.01 | 0.04	0.8 | 0.5	n/a
^{6}Li+H	(0.8%)	1.02 | 0.04	0.7 | 0.4	n/a
^{12}C+H→^{7}Li [12%]	(3.9%)	0.90 | 0.12	n/a	0.03 | 0.15
^{12}C+H→^{6}Li [14%]	(4.7%)	0.87 | 0.15	n/a	0.00 | 0.15
^{16}O+H→^{6}Li [14%]	**(6.8%)**	0.89 | 0.28	n/a	0.00 | 0.15
	Be			
^{16}O+H	(0.9%)	1.03 | 0.04	0.7 | 0.5	n/a
^{12}C+H	(1.4%)	1.01 | 0.04	0.8 | 0.5	n/a
^{9}Be+H	(1.1%)	0.95 | 0.06	0.7 | 0.4	n/a
^{7}Be+H	**(2.7%)**	1.10 | 0.10	0.7 | 0.4	n/a
^{16}O+H→^{9}Be [5%]	(3.2%)	1.00 | 0.30	n/a	0.00 | 0.15
^{12}C+H→^{9}Be [9%]	(5.9%)	0.87 | 0.20	n/a	0.03 | 0.15
^{12}C+H→^{7}Be [16%]	(4.0%)	1.00 | 0.25	n/a	0.00 | 0.15
^{16}O+H→^{7}Be [18%]	**(7.2%)**	0.85 | 0.15	n/a	0.00 | 0.15
	B			
^{16}O+H	(0.8%)	1.03 | 0.04	0.7 | 0.5	n/a
^{12}C+H	(1.0%)	1.01 | 0.04	0.8 | 0.5	n/a
^{11}B+H	**(1.7%)**	0.98 | 0.04	0.7 | 0.4	n/a
^{12}C+H→^{10}B [7%]	(2.5%)	1.07 | 0.15	n/a	0.00 | 0.15
^{16}O+H→^{11}B [18%]	(4.0%)	0.96 | 0.18	n/a	0.00 | 0.15
^{12}C+H→^{11}B [34%]	**(7.1%)**	1.10 | 0.12	n/a	0.03 | 0.15
	N			
^{16}O+H	**(1.8%)**	1.03 | 0.04	0.70 | 0.50	n/a
^{15}N+H	(1.0%)	1.00 | 0.05	0.70 | 0.50	n/a
^{14}N+H	(1.6%)	1.02 | 0.07	0.70 | 0.50	n/a
^{16}O+H→^{14}N [20%]	(1.7%)	1.00 | 0.15	n/a	0.00 | 0.05
^{16}O+H→^{15}N [50%]	**(5.9%)**	0.90 | 0.15	n/a	0.05 | 0.10

$$\chi^2_{\rm LC-penalty} = \left(\frac{\mu_C - \sum_i C_i}{\sigma_C}\right)^2 .$$

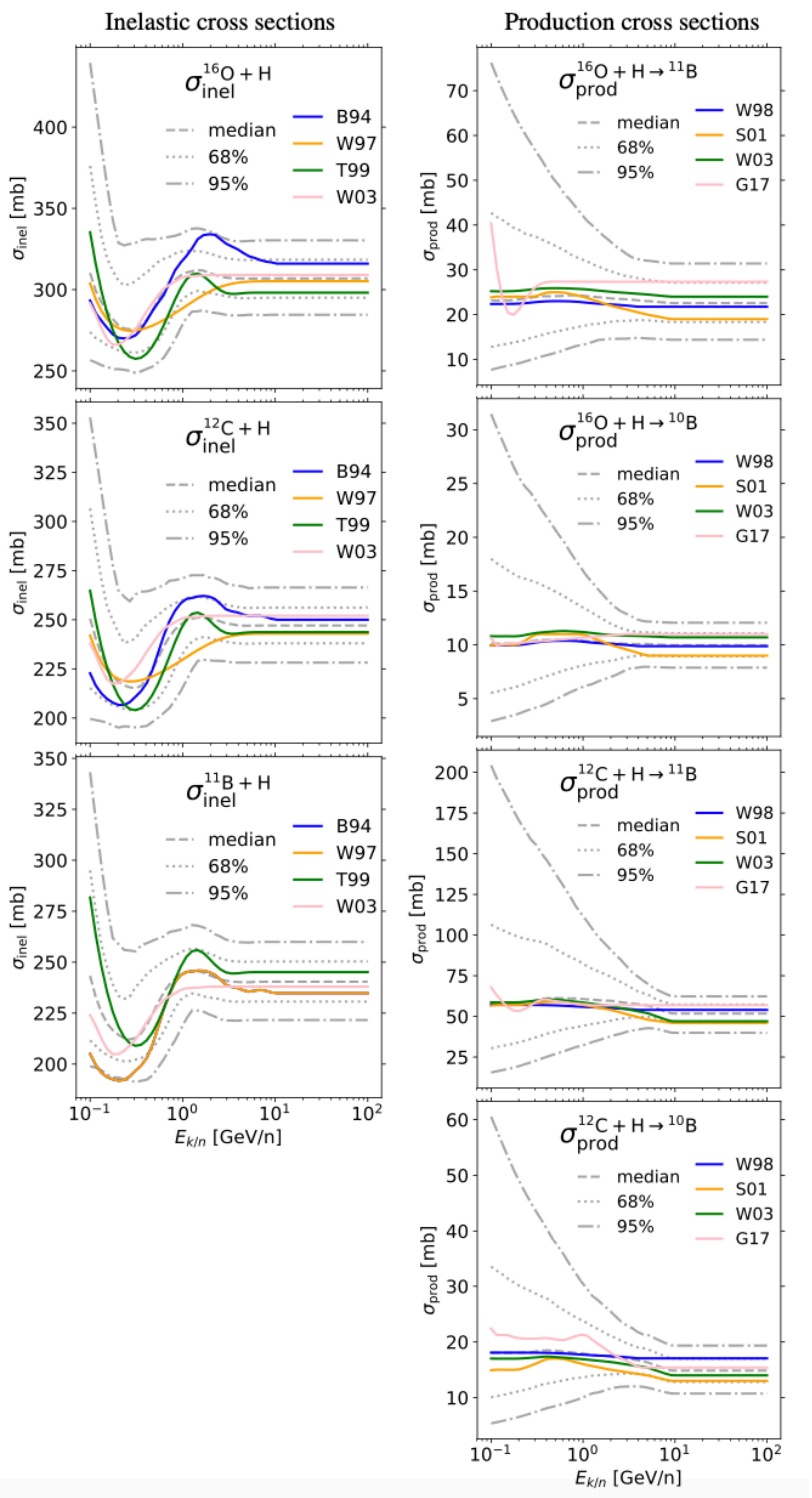

https://arxiv.org/abs/2002.11406

Nuclear CS are the dominant uncertainties in current models

- Nuclear cross sections represent the main uncertainty in the determination of the propagation parameters.
- It is relevant for the determination of the different propagation parameters.
- The size of the diffusive halo is one of the most relevant one.

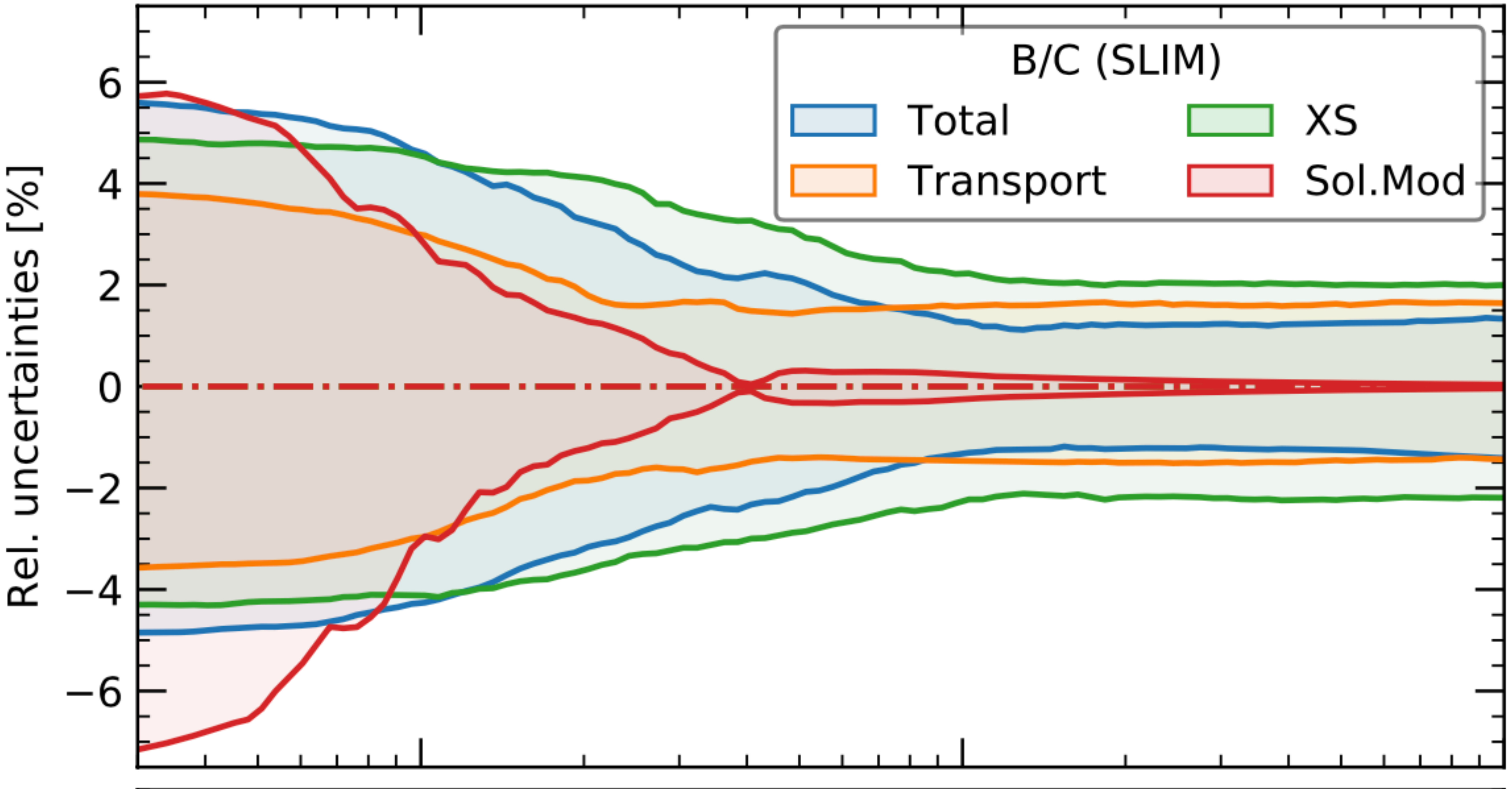

Table 1. Constraints on the halo size L and 1σ uncertainties from the combined analysis of AMS-02 Li/C, Be/B, and B/C data with USINE. We report the reduced χ^2 value for the best-fit (201 data points, 193 degrees of freedom). The different rows show the results for the original Galp-opt12 cross-section set used in our previous analysis (Weinrich et al. 2020a), and the three updated sets introduced in Maurin et al. (2022).

Fit Li/C+Be/B+B/C with USINE		
Cross-section set	L [kpc]	χ^2_r
Galp-opt12	$5.0^{+3.0}_{-1.8}$	1.20
OPT12	$5.6^{+5.6}_{-2.5}$	1.16
OPT12up22	$3.8^{+2.8}_{-1.6}$	1.13
OPT22	$4.6^{+4.0}_{-2.1}$	1.20

https://arxiv.org/abs/2002.11406